NASA Technical Memorandum 81353

CLIMATOLOGICAL CHARACTERISTICS OF HIGH ALTITUDE
WIND SHEAR AND LAPSE RATE LAYERS

L. J. Ehernberger and Nathaniel B. Guttman

February 1981

NASA

CLIMATOLOGICAL CHARACTERISTICS OF HIGH ALTITUDE

WIND SHEAR AND LAPSE RATE LAYERS

L. J. Ehernberger
Dryden Flight Research Center
Edwards, Calif.

and

Nathaniel B. Guttman
National Oceanic and Atmospheric Administration
Asheville, N.C.

NASA

National Aeronautics and
Space Administration

1981

CLIMATOLOGICAL CHARACTERISTICS OF HIGH ALTITUDE
WIND SHEAR AND LAPSE RATE LAYERS

L. J. Ehernberger
Dryden Flight Research Center
Edwards, Calif.

and

Nathaniel B. Guttman
National Oceanic and Atmospheric Administration
Asheville, N.C.

INTRODUCTION

Clear air turbulence (CAT) encountered by aircraft in the troposphere and jetstream regions extending above the tropopause has been empirically related to numerous meteorological features and synoptic patterns. Several studies (refs. 1 to 9) indicate that the principal physical features which are critical to the occurrence of CAT include vertical wind shear and atmospheric stability. As higher altitude aircraft have been developed and have encountered turbulence in the stratosphere (refs. 10 to 14), the examination of meteorological conditions has also come to include vertical wind shear and static atmospheric stability (refs. 15 to 20). The data available for the study of high altitude turbulence (HAT) inherently include localized microscale and mesoscale wind shear and lapse rate features for which no adequate climatology has been established. Moreover, a suitable climatology cannot be based on meteorological data acquired to date, since HAT projects have typically been limited to a few case studies and the meteorological elements of interest have varied with the concerns of each investigator. In addition, data for some case studies resulted from deliberate attempts to encounter HAT. Thus, without an adequate climatology, any interpretation of the statistical relationship between meteorological features and HAT must be guarded. For example, one must inquire whether the threshold levels for individual variables more accurately specify turbu-

lence, nonturbulence, or both. Further, it is not clear whether the association between individual meteorological variables and HAT is due to physical cause-effect relationships or simply to coincidental seasonal patterns. This problem is of greater significance to the practitioner who wishes to apply the results of individual research studies to operational forecasting procedures than it is to the scientist who wishes to identify the physical processes that generated a particular turbulence event.

The study discussed herein was initiated to obtain preliminary indications of the climatology of selected variables that were expected to be associated with the occurrence or nonoccurrence of high altitude turbulence. Both theoretical considerations and empirical evidence show that certain combinations of vertical wind shear and temperature lapse rate are associated with turbulence. The classical concept of Richardson number (Ri), the ratio of thermal stability to the square of the vertical wind shear, indicates that turbulence will prevail or propagate when Ri is less than 1; that is, when the kinetic energy available from wind shear exceeds the energy needed to overcome the static stability or buoyancy forces in the atmosphere. In addition, when dynamic conditions favor Kelvin-Helmholtz instability, gravity wave motion can amplify and subsequently break into turbulence. The critical value of Ri for this process has been shown to be less than 0.25 (refs. 2 and 21). This process has been observed to result in strong turbulence when wind shear increases to large magnitudes in the presence of high static stability (refs. 3, 7, and 15). The primary variables chosen for the present study are the strongest positive lapse rates, negative lapse rates, vertical wind shear, and wind shear windspeed product (vertical gradient of kinetic energy) that occur within separate layers of the upper troposphere and lower stratosphere. Wind shear in the troposphere and windspeed at selected mandatory levels are also included. This paper reports some of the initial frequency distributions and data problems. Examples of the application of the climatological data are discussed, and recommendations for further study are made.

SYMBOLS AND ABBREVIATIONS

CAT   clear air turbulence

HAT   high altitude turbulence

HICAT   high altitude clear air turbulence

n   number of observations in a statistical sample

$P(\ )$	probability of an event ( ); the conditional probability of event y based on knowing that event x does occur is designated $P(y/x)$
Ri	Richardson number, the ratio of the energy needed to overcome atmospheric buoyancy to the kinetic energy available from vertical wind shear
s^2	variance of an observed variable
$T_0,\ T_1,\ T_2$	turbulence intensity categories used in reference 17, nominally characterized as negligible, light, and moderate, respectively
V	wind velocity in the horizontal plane
$\dfrac{\Delta V}{\Delta Z}$	vertical wind shear, the rate of change of the horizontal wind velocity with altitude
x	dummy variable
Z	vertical Cartesian coordinate, also designation for hours (and minutes) in Greenwich mean time
z	normal distribution standardized variable equal to $\dfrac{x - \mu_x}{\sigma_x}$
α	measure of uncertainty; the confidence level equals $1 - \alpha$
γ	lapse rate for a layer of low static stability (rate of ambient temperature decrease with altitude), °C/km
$-\gamma$	temperature inversion rate for a layer of high static stability, °C/km
Δ	incremental operator
μ	mean value
σ^2	true variance of the population from which the variable is sampled
χ^2	chi-square distribution variable

Subscripts:

flt   flight level

low   low altitude

max   maximum

100   100 millibar level

300   300 millibar level

Seasons:

W   winter (Dec. to Feb.)

SP   spring (Mar. to May)

SU   summer (June to Aug.)

F   fall (Sept. to Nov.)

A   annual (all seasons combined)

Turbulence events:

NF   not forecast

NR   not encountered (not recorded)

TF   forecast

TR   encountered

DATA AND PROCEDURES

Since this was a pilot study, the data sample, class intervals, and altitude layers of interest were selected somewhat arbitrarily, with emphasis on phenomena above the troposphere. Consideration was given to the quality of the initial upper air observations, the results of turbulence studies, and the suitability of the data for automatic processing. For the period from July 1, 1970 to June 30, 1971, the 00Z and 12Z radiosonde observations were examined for 20 upper-air stations in the western United States. This period was selected because the wind and thermal upper air data taken after July 1, 1970 were consolidated into new and much improved archival formats at the National Climatic Center. In addition, more rigorous quality control procedures were implemented at

this time. The 20 stations selected were San Diego, Oakland, and Vandenberg Air Force Base, Calif.; Yucca Flat, Ely, and Winnemucca, Nev.; Denver and Grand Junction, Colo.; Albuquerque, N. Mex.; Tucson and Winslow, Ariz.; Lander, Wyo.; Salt Lake City, Utah; Boise, Idaho; Great Falls and Glasgow, Mont.; Spokane and Quillayute, Wash.; and Medford and Salem, Oreg. The height, temperature, and both zonal and meridional wind components were recorded for each mandatory and significant pressure level from 700 millibars to the termination of the sounding.

Table 1 lists the class intervals and restrictions for the variables examined. The maximum values of each variable within the indicated layer were summarized seasonally and annually after the data for both observation times for all stations were combined. Univariate percent frequencies and cumulative percent frequencies were computed for all variables for all layers. Bivariate percent frequencies were also computed for selected elements and layers.

The computational procedures involved the partitioning of the layers given in table 1 into sublayers defined by mandatory and significant levels in the radiosonde observations. Meteorological variables were computed for overlapping sublayers after insuring that the restrictions and threshold values in table 1 were met. The maximum value of the variable in the given layer was extracted and retained for later analysis. It is important to note that for this maximum value, the values of other variables that occurred simultaneously were not retained. For example, if the maximum wind shear was observed in the sublayer between 135 and 150 millibars, the corresponding values in this sublayer of lapse rate and the wind shear windspeed product were not retained in the data base unless they also met their respective threshold criteria. This deficiency presented serious problems in the subsequent determination of multivariate relationships.

The values of the tabulated univariate frequency data for the parameters listed in table 1 were plotted against cumulative percent frequencies on normal probability versus logarithmic scales. Both annual and seasonal data for each layer were graphed for most of the variables; the graphs are presented in figures 1 through 67, which are discussed in the next section. The lines of fit are manual fairings that are intended to show gross features of the distributions and not lines of best fit based on least squares or other theory. The threshold values given in table 2 are represented by thin vertical lines on the graphs. A logarithmic scale was chosen because the lower magnitude class intervals contained most of the observations, thus skewing the frequency distributions. Using this scale, a straight line fit would indicate a log-normal probability density function.

The authors recognize that probability plotting and manual fairing is subjective in that the validity of any assumed statistical model is based on visual examination. The advantages of the technique are that the method is simple, the data are pictorially represented, the reasonableness of an assumed model is easily evaluated, and the parameters and percentiles of the distribution can be estimated. The main disadvantages are the lack of both objectivity and of a probabilistic framework that could be provided by statistical calculations and tests for the distribution functions.

RESULTS

Univariate Distributions

Results are presented for each variable in the sequence of annual and then seasonal frequency distributions. Data for wind shear and lapse rate are given first for combined layers and then for the individual layers in the lower stratosphere. The distributions of windspeed with altitude are shown in figures 1 to 5 for the data sample used in this study. The 300 millibar level shows the highest windspeeds and is consistent with the midlatitude jetstream that occurs just below the tropopause. Speeds generally decrease up to about 50 millibars and then increase slightly. The increase in windspeeds above 50 millibars (70 mb in summer) is associated with the change in circulation patterns between the troposphere and stratosphere. Tropospheric midlatitude winds are predominantly westerly throughout the year, while lower stratospheric winds are predominantly westerly in winter and easterly in summer. This stratospheric wind reversal is strongly reflected in the seasonal windspeed distributions at 50 and 30 millibars. At each level through 70 millibars (figs. 6 to 9) the windspeeds are highest in winter, lowest in summer, and slightly higher in spring than in fall. At 50 millibars (fig. 10) the winds are strongest in winter and about the same through the other three seasons. At 30 millibars the influence of the shift from westerlies to easterlies causes the summer windspeeds to exceed those in winter to the 75 percentile frequency of occurrence (fig. 11).

On either an annual or seasonal basis, the distributions for maximum wind shear within the lower troposphere, 700 to 350 millibars, and the lower stratosphere, 175 to 20 millibars, are similar (figs. 12 to 16). Stronger values of the maximum wind shear, 0.014 to 0.03 per second, occur relatively more often in the upper troposphere, 350 to 175 millibars. The distributions for these three broad atmospheric layers merge and change shape between shear values of 0.03 and 0.05 per second. This change in the distribution near the 99.9 percentile

6

suggests the presence of measurement errors in the data. Seasonally, strong wind shears are most frequent during winter and least frequent during summer in each of these three layers (figs. 17 to 20).

The frequency of strong wind shears in the individual layers above 175 millibars shows a consistent decrease with altitude from the 175 to 125 millibar layer to 40 to 20 millibar layer during each of the seasons as well as on an annual basis (figs. 21 to 25). As shown in figures 26 to 30, each of these layers also contains strong wind shears most frequently in winter and least frequently in summer. This seasonal pattern is most pronounced in the upper layers, in spite of the tendency for the windspeeds at these levels to be lowest in the spring rather than in the summer. The relative absence of strong wind shears in summer even though windspeeds are not at a minimum suggests a decreased occurrence of dynamic perturbations at 50 millibars and 30 millibars in summer.

Distributions for the product of wind shear and windspeed (figs. 31 to 35) show decreasing magnitudes as altitude increases. A typical seasonal behavior, with small magnitudes most prevalent in summer and large magnitudes most prevalent in winter, is observed in all layers except for the 40 to 20 millibar layer (figs. 36 to 41). In this layer, large magnitudes occur least frequently in the spring, when windspeeds are lowest, and in summer, when wind shears are minimal.

The annual maximum positive lapse rate observed within a layer decreases in magnitude with increasing layer altitude, as shown in figure 42. This decrease with altitude is also characteristic of the individual seasons (figs. 43 to 46) except for the 175 to 125 millibar and 125 to 80 millibar layers. In winter and spring the magnitudes of the lapse rates do not decrease noticeably with altitude from the 175 to 125 millibar layer to the 125 to 80 millibar layer but remain approximately the same. During these seasons the layers above 175 millibars are usually in the lower stratosphere, where conditions are controlled by the intense midlatitude cyclonic activity in the troposphere and by the energy and momentum transfer through the tropopause. In general the seasonal patterns (figs. 47 to 54) show higher positive lapse rates in winter in the stratosphere and in summer in the troposphere. These patterns are a reflection of an increase of dynamic perturbations in the winter stratosphere and increased heating of the earth and convective activity in the troposphere during the summer.

Above 125 millibars, strong inversions occur less frequently as altitude increases (figs. 55 to 59). In the lower layers strong inversions are more prevalent between 350 and 175 millibars than between 700 and 350 millibars. The 175 to 125 millibar

layer is similar to the 350 to 175 millibar curves in the summer and fall and to the 125 to 80 millibar curves in winter and spring. The correlation of the 175 to 125 millibar layer with tropospheric conditions in the summer or with stratospheric conditions in the winter is directly dependent upon the seasonal shift in the height of the tropopause.

The seasonal patterns within layers (figs. 60 to 67) are variable. Between 700 and 350 millibars and between 80 and 40 millibars, strong inversions occur least often in summer and with similar frequency in the other three seasons. Between 350 and 125 millibars they occur more often in winter and spring and less often in summer and fall. Virtually no seasonal pattern exists in the 125 to 80 millibar layer. In the 40 to 20 millibar layer inversions are strongest in winter, weakest in summer, and about the same magnitude in spring and fall. The maximum inversions in the lower stratosphere as a whole (tropopause to 20 mb) are strongest in winter, weakest in summer, and stronger in spring than fall.

Bivariate Distributions

The joint occurrence of two variables with values of sufficient magnitude for both to affect the development of turbulence is of particular significance to operational fore-casting procedures. If they frequently occur together, for example, and are highly correlated, then only one need be included in an objective scheme. On the other hand, if both variables affect the development of turbulence but are not correlated with each other, both should be included.

Therefore, bivariate contingency tables were prepared to examine the dependence of positive and negative lapse rates and high altitude wind shears on the other variables, as well as on each other. No attempt was made to arrive at distribution assumptions. The bivariate tables were reduced to four-cell contingency tables by arbitrarily assigning threshold values to each variable above which noticeable high altitude turbulence might be expected. These values are shown in table 2. The technique estimates those variables that could be important in an objective forecasting scheme such as a multivariate linear regression model.

A difficulty in the use of the present data set was experienced when an objective chi-square test was applied to the annual four-cell contingency tables. The procedure tested the null hypothesis that the two dichotomous variables are independent in the statistical sense, that is, that the proba-bility of an observed value of one variable is not affected by an observed value of the second variable. Using a 0.95 confidence level, the null hypothesis of independence was not rejected

8

for five of the contingency tables: negative lapse rate
(125 to 80 mb) versus wind shear (350 to 175 mb); negative
lapse rate (80 to 60 mb) versus wind shear (350 to 175 mb);
positive lapse rate (175 to 125 mb) versus wind shear
(700 to 350 mb); positive lapse rate (175 to 125 mb) versus
wind shear (350 to 175 mb); and positive lapse rate (175 to 125 mb)
versus windspeed (300 mb). The computed chi-square values for
most of the other contingency tables were statistically unreason-
ably high so that the validity of the use of this test for all
contingency tables was questioned.

The chi-square test is based on the assumption that the
individual observations of a variable are randomly selected
from the total population of possible independent observations.
The construction of the present data set negates the assumption
of independence and thus invalidates the chi-square test.
Time and space correlations are inherent in the data base,
since 12-hour sequential observations taken at several stations
over areas which tend to share homogeneous terrain features
and synoptic patterns are combined into one set. It is well
known that dynamic regimes in the stratosphere tend to change
slowly. Thus, several sequential radiosonde observations over
a homogeneous horizontal area can actually reflect the same
atmospheric regime. This correlation between observations
means that the contingency tables contain multiple counts of
essentially the same observation. These multiple counts lead
to the faulty chi-square test conclusion that a high degree of
dependence exists between variables. A similar problem was
previously addressed in reference 22, which presents a method
for estimating the number of independent observations contained
in the total sample population. Another deficiency of applying
the chi-square test to annual data samples is the possibility
that the variables tested may be positively correlated in one
season but negatively correlated in another. The data set
used for this pilot study was not designed for such evalua-
tion; however, the empirical results are relatively informative
in spite of the lack of rigorously established statistical
validity.

Seasonal percent frequencies of the joint occurrence of
positive and negative lapse rates and high altitude wind
shears with the other variables meeting the criteria listed in
table 2 are presented in tables 3, 4, and 5. These tables
summarize the values obtained from one cell in each contingency
table that contains the joint occurrence of strong values for
both variables. Table 3 lists the joint empirical percent
frequencies of the simultaneous occurrence of positive lapse
rates equal to or greater than 4° C per kilometer with each of
the other wind variables listed in table 2. Table 4 is similar
except that a negative lapse rate (inversion) of less than or
equal to -5° C per kilometer is the main variable. Table 5
presents the percent frequencies of the joint occurrence of

high wind shears in separate layers and also with high windspeeds at several levels. Several other joint combinations of variables and layers are possible; the ones depicted herein were subjectively chosen as being of most interest to high altitude turbulence situations affecting supersonic cruise aircraft operating over the western United States.

It should be noted that the use of the term "joint occurrence" in this report does not refer to the simultaneous occurrence of variables within a given sublayer. The term refers only to the simultaneous occurrence of values within the main layers. For example, a radiosonde observation could yield a maximum wind shear between 130 and 120 millibars and a maximum positive lapse rate between 105 and 90 millibars. The contingency table would contain a count for the joint occurrence of wind shear and positive lapse rate within the 125 to 80 millibar main layer even though the individual variable values did not occur simultaneously within the same sublayer.

The joint occurrence of stratospheric strong positive lapse rate or reduced buoyant stability and high wind shear is associated with low Richardson number and therefore suggests an increased probability of turbulence. From table 3 it is apparent that this condition is often observed in the summer (61 percent of the soundings) in the 175 to 125 millibar layer and in more than a third of the soundings in the 125 to 80 millibar layer. It also occurs almost half the time in winter in the 175 to 125 millibar and 125 to 80 millibar layers. Note that the wind shear and lapse rate threshold values, 0.005 per second and 4° C per kilometer, respectively, are equivalent to a Richardson number threshold which is an order of magnitude less stringent than the theoretical criteria.

The joint occurrence of positive lapse rate with high values of the wind shear windspeed product does not appear to be as strong through 80 millibars. Above 80 millibars, the statistics for wind shear and the wind shear windspeed product are approximately equivalent. Table 3 also shows that about a third of the time positive lapse rates from 175 to 80 millibars in winter are coincident with high windspeeds at 700 and 300 millibars. As altitude increases above 80 millibars in winter, the joint occurrence of high lapse rates with the other variables decreases. In summer, the joint frequencies are nil.

Joint percent frequencies for negative lapse rates or inversions with other variables are shown in table 4. The highest value, 44 percent, occurs in summer for the lapse rate wind shear combination in the 125 to 80 millibar layer. This combination also occurs in the 80 to 60 millibar layer with approximately equal frequency throughout the year. During the winter, the joint occurrence of strong inversions and high values of each of the other variables, except low altitude

10

wind shears, is observed about 20 percent of the time. In summer, most of the variables are jointly observed infrequently.

Table 5 shows the percent frequencies of high altitude wind shears occurring with low altitude shears and high windspeeds at the selected levels. The frequencies are low in all cases in summer. The winter correlations are strongest for wind shears in the layers between 175 and 60 millibars and windspeeds at 700, 300, and 100 millibars. High 70 millibar windspeeds in winter are observed almost half the time that strong shears in the 80 to 60 millibar layer occur. At all six levels high speeds appear to be observed more often with strong wind shears than with either positive lapse rates or inversions.

Further comparisons were also made between the bivariate frequencies observed and those calculated on the assumption of independence. Strong dependence was not exhibited below 80 millibars. For the layers above 80 millibars, wind shear showed some dependence on the windspeed at altitudes of 100 millibars and higher in all seasons. For example, the joint occurrence of wind shear in the 60 to 40 millibar layer and strong 100 millibar windspeeds in the spring season was 17 percent, in contrast to less than 11 percent calculated on the assumption of independence. Positive lapse rates in the layers above 80 millibars indicated some statistical dependence, but not as uniformly as wind shear. All joint variables showed higher frequencies than calculated (on the assumption of independence) by a factor of one-third or more, for at least one season in the layers above 80 millibars. Similar dependence was not shown for negative lapse rate except in the 60 to 40 millibar and 40 to 20 millibar layers, where they tend to be associated with strong wind shears and windspeeds. As an example, the observed joint frequency of negative lapse rates and strong wind shears in the 40 to 20 millibar layer was approximately twice as great as calculated for all seasons.

The dependence found between joint variables may be sensitive to the nearness of the selected thresholds to physically critical values for the layers of interest.

DISCUSSION

Application of Climatology to Turbulence Studies

Climatological information, when available, can benefit turbulence forecast studies in three separate areas. First, it can allow the investigator to evaluate the meteorological parameters which appear to be associated with specific data samples. Second, climatology for the appropriate meteorological parameters provides a means for estimating seasonal variations

in the occurrence of turbulence on the basis of limited amounts
of experimental data. Finally, when predictors are obtained
from a limited amount of observational data, their performance
can be evaluated on an annual and seasonal basis by the use of
climatological information. These applications are discussed
in the paragraphs below.

   Meteorological parameter association with turbulence.—The
meteorological conditions observed in association with turbulence
are usually summarized in terms of the observed frequencies
within each turbulence intensity category which fulfill specified
criteria for the magnitude of the meteorological variable.
The average value of the meteorological variable within each
turbulence category is also used to expose variables which
influence the turbulence intensity. Comparisons of the results
from studies of high altitude turbulence (HAT) with statistics
obtained in the present study are presented below.

   High altitude turbulence results reported in reference 16
are presented in table 6 in terms of the frequencies of samples
in each intensity category which exceeded specified meteoro-
logical criteria. Corresponding frequencies from the present
sample of upper air data for the western United States are
also shown on an annual and seasonal basis. For the area of
the reference 16 HAT sample, the frequency of maximum wind
observations exceeding 36 meters per second is believed to be
closely approximated by the frequency of 300 millibar winds
exceeding 30 meters per second. On this basis, the maximum
wind values for the turbulence samples exceed the threshold
criteria for 36 and 37 percent of the cases in the T_0 and T_1
intensity categories and appear to be representative of the annual
wind background. However, the maximum wind values for the T_2
intensity samples exceed the threshold criteria in 69 percent
of the cases; therefore, the frequency for the T_2 category
differs significantly from the frequency for the other categories
and the annual background. For this reason, the stronger
turbulence is believed to be associated with higher speeds in
the upper troposphere. It is further inferred that it is more
prevalent in the winter season and rare in summer. The frequen-
cies for the 100 millibar windspeed exceeding 21 meters per second
exhibit even more contrast. The T_0 and T_1 category frequencies
are significantly lower than the annual frequency, but the
frequency for the T_2 intensity category is significantly greater
than the winter frequency as well as the annual frequency.

   Unlike the present data, which were separated into 700 to
350 millibar and 350 to 175 millibar layers, the lower altitude
wind shear frequencies for the reference 16 HAT data were not
separated into layers. For comparison the present data are

12

shown for each of these layers, and the frequency for the combined layers is taken to be less than or equal to their sum. The frequencies of strong lower altitude wind shear for the T_0 and T_1 categories are near the winter season frequencies indicated by the present data. However, for the T_2 category, the frequency of high wind shear is also significantly greater than either the annual or seasonal frequencies.

Wind shear, lapse, and inversion rate data for the reference 16 HAT samples were the maximum values measured within 610 meters of the flight altitude in turbulence. Most of these turbulence samples were obtained from flight altitudes between 12.2 and 21.0 kilometers, which may be represented by the present data for layers between 175 millibars and 40 millibars. These layers for the present data are thicker than the ±610 meters for the reference 16 HAT samples, and therefore their frequencies are somewhat higher than they would have been had the samples been taken from thinner layers. In addition, the annual statistics and the seasonal patterns for the maximum wind shears, lapse rates, and inversion rates change significantly with altitude. Therefore the table contains data for layers which represent the range of frequencies and seasonal patterns as well as an overall annual average value.

Wind shears and lapse rates near the HAT altitude equal or exceed the specified values at increasingly greater frequencies for the T_0, T_1, and T_2 intensity categories. The frequency for strong inversion rates is least for the T_1 category. The frequency for the T_2 category is significantly greater than the background frequency indicated by the present data. In consideration of the relatively shallow layers used with the HAT data, the frequency of strong inversions for the T_0 samples is assumed to be at least as great as the background frequency. An overall observation of the table 6 data is that the specified ranges for all the variables are associated with T_2 intensity HAT. Weaker values of the variables typify background conditions except for the 100 millibar windspeed, V_{100}, and the flight altitude wind shear, $\left(\frac{\Delta V}{\Delta Z}\right)_{flt}$, which also appear skillful in designating very light turbulence or nonturbulent conditions.

Another study (ref. 19) reported results for similar meteorological variables associated with samples obtained by the USAF high altitude clear air turbulence (HICAT) program. Data from reference 19 and corresponding frequency data from the present sample are presented in table 7. The specified ranges used in reference 19 are slightly different from the ranges specified in reference 16, and a larger altitude interval (±2000 meters above and below the flight level) was used to obtain data for

the strongest lapse and inversion layers. One effect of this procedural difference is a tendency for the frequencies in the three HICAT turbulence intensity categories to be more closely grouped near the frequency for all data in the study. Also, the frequencies of strong inversions are significantly greater in the HICAT sample than in the present data.

Average values in each intensity category were also determined for some of the meteorological variables in the HAT and HICAT samples. As shown in tables 8 and 9, the average values of the variables generally increase with turbulence intensity. Different procedures were used in the two studies, so direct comparison of all variables is not feasible. It may be noted that the maximum windspeed shows less variation with intensity for the HICAT sample. This may be due to the wide variation in geographical areas and weather circulation patterns from which the HICAT data were obtained. Regional differences in the statistics of the meteorological variables may impact the experimental results as much as different experimental procedures.

Both the average values of the meteorological parameters for the turbulence intensity categories and the frequencies at which they exceed selected values allow the investigator to interpret the circumstances attending the data samples. For example, the average value of a variable for the nonturbulent and/or light turbulence categories may be near the climatological mean but significantly less than the mean for the more intense category. In this case it would be assumed that high values of the variable would be associated with an increased probability of strong turbulence. On the other hand, low values of the variable may not appreciably increase the probability of weak or nonturbulent conditions. Thus, the availability of the appropriate climatology for the meteorological variables would enable investigators to judge whether specific variable ranges can discriminate conditions for intense turbulence, nonturbulence, or both.

Turbulence occurrence climatology.—Another application of climatological data is the interpetation of results from limited turbulence sampling data to more general rates or probabilities on a seasonal or annual basis. Such rates can be either turbulence occurrence rates or turbulence forecast verification rates. Both turbulence occurrence rates and the meteorological variables in the experimental sample may be influenced by weather pattern anomalies existing during the data collection period. To translate the results from such data into rates typical of the seasonal or annual periods, the data are first examined to determine the variables and the magnitudes which most strongly discriminate between the turbulence categories of interest. This may be accomplished in terms of either conditional probabilities or multiple regression techniques. Climatology for the variables of interest should then be acquired to determine the probability distributions for the magnitude ranges used and to identify

14

dependence between variables. Finally, the turbulence occurrence rates for the experimental sample are converted to rates for the individual seasons by using climatological frequencies for the meteorological variables with the derived regression relation-ships or conditional probabilities.

Estimating forecast verification rates.—Bias in experimental samples due to size and mission management often precludes the direct use of the sample statistics for estimating the forecast performance of individual predictors as well as for estimating turbulence climatology. The estimation of operational verification rates can be accomplished on the basis of the probability that turbulence will be encountered in the seasons and regions of interest. Their probability values may be obtained from either the methods described in the preceding section or from other available sources. The probability of turbulence encounter, $P(TR)$, is used with estimates for the probabilities that turbulence will be fore-cast for cases when it is encountered, $P(TF/TR)$, and for cases when it is not encountered, $P(TF/NR)$. It is assumed that the experimental data frequencies for the selected predictors provide adequate statistical estimates of these conditional probabilities. Verification estimates are desired in terms of the probability that turbulence will be: (1) encountered when forecast, $P(TR/TF)$; (2) encountered but not forecast, $P(TR/NF)$; (3) not encountered even though it has been forecast, $P(NR/TF)$; and (4) neither encountered nor forecast, $P(NR/NF)$. For convenience of expres-sion, we can also define the probability that turbulence is not encountered as

$$P(NR) = 1 - P(TR)$$

the probability that turbulence was not forecast even though it was encountered as

$$P(NF/TR) = 1 - P(TF/TR)$$

and the probability that turbulence was not forecast when it was not encountered as

$$P(NF/NR) = 1 - P(TF/NR)$$

Estimates for the verification rates desired are then given by:

$$P(TR/TF) = \frac{P(TF/TR)\ P(TR)}{P(TF/TR)\ P(TR)\ +\ P(TF/NR)\ P(NR)}$$

$$P(TR/NF) = \frac{P(NF/TR)\ P(TR)}{P(NF/TR)\ P(TR)\ +\ P(NF/NR)\ P(NR)}$$

$$P(NR/TF) = 1 - P(TR/TF)$$

$$P(NR/NF) = 1 - P(TR/NF)$$

Sample Size Considerations

The primary purpose of the climatology studies discussed herein is to establish the statistics for selected meteorological variables which are related to the occurrence of clear air turbulence. Univariate frequency distributions, conditional distributions, bivariate contingencies, conditional probabilities, and correlation properties are all applicable to the interpretation of the meteorological data associated with turbulence. The importance of sample size for the determination of the distribution functions and statistical confidence levels can be appreciated by inspection of the empirical curves and by evaluation of statistical criteria.

Several of the curves obtained for the present sample exhibit a lack of stability in their distribution functions. This is particularly evident at the tail of the distributions, where a limited number of observations are available and individual points can greatly modify the shape of the distribution curve. The lack of a straight line or a consistent simple curvature pattern in the central part of the distribution is another indication of insufficient statistical stability. Thus, the foremost drawback in this initial study is the small size of the sample used. Although the present results only give a gross approximation of the statistics, they do provide helpful indications of the relative frequencies for the threshold magnitudes and seasons of interest.

The sample size required for the desired degree of statistical confidence can be estimated on the assumption that the observations are independent and that the distribution is known. Convenient expressions of statistical confidence are commonly available for the mean value and variance of Gaussian distributed variables. To illustrate the effect of sample size it will be assumed that the measured variables are either Gaussian or have been transformed into variables with a Gaussian distribution. Let us specify that it is desired to know the variance, σ^2, to within ±10 percent and with a certainty of 95 percent. In other words, the ratio of the measured variance, s^2, to the true variance, σ^2, must be between 0.9 and 1.1. To attain 95 percent confidence that the results are within this interval, the probability that the ratio s^2/σ^2 is less than 0.9 must be limited to 0.025, and at the same time the probability that the ratio is not greater than 1.1 must be at least 0.975. The number of independent observations needed is found from the inequality

$$\frac{\chi^2_{\alpha/2}}{n-1} \leq \frac{s^2}{\sigma^2} \leq \frac{\chi^2_{1-\alpha/2}}{n-1}$$

where χ^2 is the chi-square parameter, α is given by 1 minus the confidence level desired, and n is the number of observations. The values of the ratios

$$\frac{\chi^2_{0.025}}{n-1} \leq 0.9$$

and

$$\frac{\chi^2_{0.975}}{n-1} \geq 1.1$$

are available in reference 23 and indicate sample size requirements of 740 and 800 independent observations, respectively. Observation requirements increase rapidly with the accuracy desired. For example, 3200 observations would be needed if it were desired for the observed variance (s^2) to be within ±5 percent of the true variance (σ^2) instead of within ±10 percent.

Sample size requirements for nearness of the sampled mean value, $\overline{x}$, to the mean value of the population, μ_x, at specified confidence levels are found similarly for Gaussian variables. The t-distribution is used to relate the desired tolerance on the mean value estimate, $\overline{x} - \mu_x$, to the sample variance for specified confidence levels where

$$\frac{t}{\sqrt{n}} = \frac{\overline{x} - \mu_x}{s}$$

The desired sample size, n, is found by use of the inequality

$$\frac{t_{1-\alpha/2}}{\sqrt{n}} \leq \frac{\overline{x} - \mu_x}{s} \leq \frac{t_{\alpha/2}}{\sqrt{n}}$$

When n exceeds 120, t becomes constant for given levels of confidence and the evaluation is analogous to the case of sampling a population with known variance where the standardized normal distribution variable, z, is used,

$$\frac{z_{1-\alpha}}{\sqrt{n}} < \frac{\overline{x} - \mu_x}{\sigma_x} \leq \frac{z_{\alpha/2}}{\sqrt{n}}$$

For a confidence level specified at 95 percent certainty, the number of observations required to assure that the sample mean value is accurate to within approximately 0.1 standardized unit is 384. If the sample size of 800 observations found for the variance criteria is used, it would provide 95 percent certainty that the sample mean value is accurate to within approximately 0.07 standardized unit.

We can consider the number of stations and the period of record required to provide the 95 percent confidence levels discussed above. If we assume that each given observation location will yield an independent observation each 10 days, we require at least 10 years of record from more than 20 stations spaced sufficently to yield the necessary degree of statistical independence and stability. These sample size estimates are not given as study requirements but only to be descriptive of the technical considerations necessary to achieve stable results.

Recommendations

The present results can be improved by the analysis of data for a significantly longer period of record. The benefits of an expanded study would be to more accurately establish the distributions for the small scale vertical temperature gradients, wind shear, and so forth, and to determine their dependence on wind conditions observed at the standard synoptic levels. Other properties, such as their joint occurrence as a function of threshold, persistence, periodic seasonal oscillation, and interannual variation could be examined but were beyond the scope of the present study. As noted in the previous section, the statistical confidence obtained is determined by the number of independent samples used or the degrees of freedom in the data set. Several previous studies provide results which are indicative of temporal and spatial correlation in the wind components. However, considerably less is known about the degree of correlation between observations for other variables, such as vertical wind shear or temperature gradient. Therefore, the first task recommended is to assess the single station univariate temporal correlations for the variables of interest. Applicable time series analysis methods include autocorrelation, spectra, and Markov chain techniques (ref. 24).

Spatial dependence can be determined by the same methods as temporal dependence if distance between observations is substituted for time. Spatial results for autocorrelation and Markov chain techniques would be in terms of lag distance instead of lag time. For spectra in the spatial domain, results would be in terms of wavelength instead of frequency

units (for example, cycles per year). Analysis of both temporal and spatial correlation should be accomplished for each season as well as on an annual basis.

Once the univariate correlation characteristics in time and space have been established, an appropriate data set can be created for multivariate analysis. Either of two approaches may be indicated by the results at this point. First, the data set may be formed by including only observations which are separated sufficiently to insure adequate independence. If this is not feasible, more frequent observations may be used, but the number of observations will need to be adjusted to reflect the actual number of degrees of freedom (ref. 22) for evaluation of statistical confidence in the results.

Deterministic periodic oscillations which significantly contribute to the total variance may be identified by the spectral analyses for some of the variables. Such components are usually related to the known periodicities of physical phenomena and can be eliminated from the original data to yield a new time series comprised mainly of sampling variations and noncyclic persistence.

The thickness of the layers defined in the present study was not uniform. Layers were selected for convenience in correlating winds reported at the mandatory meteorological analysis levels with wind shears and temperature gradients at nearby altitudes. The pressures separating the layers in the present study were spaced equally between the mandatory levels. In the stratosphere, the geometrical layer thickness ranged from 1824 meters for the layer between 80 millibars and 60 millibars to 4481 meters for the layer between 40 millibars and 20 millibars. Since a uniform layer thickness was not used, the empirical probabilities for each layer are biased by thickness. Therefore it is recommended that a uniform layer thickness be defined and incorporated in future studies.

CONCLUDING REMARKS

A pilot study was performed to characterize the statistical behavior of the maximum vertical wind shears and temperature gradients occurring in specified altitude layers. The study used data from 20 upper air stations in the western United States for a 1 year period of record and emphasized layers in the lower stratosphere. In general, strong wind shears, lapse rates, and inversions were observed less frequently as altitude increased from 175 millibars to 20 millibars. On a seasonal basis, the shears and gradients were stronger in winter and weaker in summer, but minor deviations to the pattern were noted in association with increased tropopause altitude in

summer and with the stratospheric wind reversal in the spring and fall.

The empirical probability distribution curves tended to follow a log-normal distribution curve. Because of the limited sample size, the distribution curves showed indications of instability, but even so, they provide a coarse estimation of the percentile frequencies for the higher magnitudes of interest.

The joint occurrence of variables exceeding specified magnitudes was examined with bivariate contingency tables. The contrast between univariate probability and conditional probability for several pairs of variables indicated weak dependence. However, these cases of dependence were essentially limited to altitudes and seasons when the frequencies of the strong magnitudes were relatively low. For most of the contingency tables the computed chi-square values were unreasonably high. This is believed to be due to serial correlation between samples for each of the variables, and therefore valid conclusions on the degree of dependence between variables could not be established with the present chi-square test results.

Applications of the univariate and bivariate results to studies of turbulence encountered by aircraft were discussed. Examples presented included the translation of limited aircraft turbulence encounter experience into the amount of turbulence and the forecast verification rates which could be expected on a climatological basis.

Recommended steps for improving the present results are given below.

1. Extend the data base to a significantly longer period of record.

2. Analyze univariate temporal correlation (dependence) for geographically representative single station records.

3. Analyze univariate spatial correlation.

4. Evaluate the period of record, number of stations, and the spacing of observations needed to provide the desired statistical confidence.

5. Establish appropriate data sets and implement multiple station multivariate analyses.

Dryden Flight Research Center
  National Aeronautics and Space Administration
    Edwards, Calif. 93523, Nov. 12, 1980

REFERENCES

1. Atlas, D.:   Clear Air Turbulence Detection Methods—A Review.
   Clear Air Turbulence and Its Detection, Yih-Ho Pao and
   Arnold Goldburg, eds., Plenum Press, 1969.

2. Clark, James W.:   Laboratory Investigations of Atmospheric
   Shear Flows Using an Open Water Channel.   Aerodynamics of
   Atmospheric Shear Flows, AGARD CP No. 48, Feb. 1970,
   pp. 15-1—15-16.

3. Dutton, John A.; and Panofsky, Hans A.:   Clear Air Turbulence:
   A Mystery May Be Unfolding.   Science, vol. 167, no. 3920,
   Feb. 13, 1970, pp. 937-944.

4. Endlich, Roy. M.:   The Mesoscale Structure of Some Regions of
   Clear-Air Turbulence.   J. Appl. Meteorol., vol. 3, June 1964,
   pp. 261-276.

5. Endlich, R. M.; and McLean, G. S.:   Empirical Relationships
   Between Gust Intensity in Clear-Air Turbulence and Certain
   Meteorological Quantities.   J. Appl. Meteorol., vol. 4,
   Apr. 1965, pp. 222-227.

6. Kadlec, Paul W.: A Study of Flight Conditions Associated With
   Jet Stream Cirrus, Atmospheric Temperature Change, and Wind
   Shear Turbulence.   Final Report, Contract Cwb-10674, U.S.
   Weather Bureau (Dept. Commerce), June 1964.

7. Panofsky, Hans A., et al.:   Case Studies of the Distribution of
   CAT in the Troposphere and Stratosphere.   J. Appl. Meteorol.,
   vol. 7, June 1968, pp. 384-389.

8. Reiter, Elmar R.:   Clear Air Turbulence: Problems and Solutions.
   Clear Air Turbulence Meeting, Soc. Automot. Eng., 1966,
   pp. 5-12.

9. Wurtele, Morton G.:   Meteorological Conditions Surrounding the
   Paradise Airline Crash of 1 March 1964.   J. Appl. Meteorol.,
   vol. 9, no. 5, Oct. 1970, pp. 787-795.

10. Coleman, Thomas L.; and Steiner, Roy: Atmospheric Turbulence
    Measurements Obtained From Airplane Operations at Altitudes
    Between 20,000 and 75,000 Feet for Several Areas in the
    Northern Hemisphere.   NASA TN D-548, 1960.

11. Steiner, Roy: A Review of NASA High-Altitude Clear Air Turbu-
    lence Sampling Programs.   J. Aircraft, vol. 3, no. 1,
    Jan.-Feb. 1966, pp. 48-52.

12. Kordes, Eldon E.; and Love, Betty J.: Preliminary Evaluation of XB-70 Airplane Encounters With High-Altitude Turbulence. NASA TN D-4209, 1967.

13. Crooks, Walter M.; Hoblit, Frederic M.; Mitchell, Finis A.; et al.: Project HICAT—High Altitude Clear Air Turbulence Measurements and Meteorological Correlations. AFFDL-TR-68-127, Air Force Flight Dynamics Lab., Wright-Patterson AFB, Nov. 1968.

14. Ehernberger, L. J.; and Love, Betty J.: High Altitude Gust Acceleration Environment as Experienced by a Supersonic Airplane. NASA TN D-7868, 1975.

15. Helvey, Roger A.: Observations of Stratospheric Clear-Air Turbulence and Mountain Waves Over the Sierra Nevada Mountains. AFCRL-68-0001, Air Force Cambridge Res. Lab., Dec. 1967.

16. Ehernberger, L. J.: Atmospheric Conditions Associated With Turbulence Encountered by the XB-70 Airplane Above 40,000 Feet Altitude. NASA TN D-4768, 1968.

17. McPherson, A.; and Nicholls, J. M.: Mountain Waves in the Stratosphere Measured by an Aircraft over the Western U.S.A. during February, 1967. Aerodynamics of Atmospheric Shear Flows, AGARD CP No. 48, Feb. 1970, pp. 3-1—3-12.

18. Nicholls, J. M.: Measurements of Stratospheric Airflow and Clear Air Turbulence, up to 63000 ft, Over and Downwind of Mountainous Terrain. International Conference on Atmospheric Turbulence, Proceedings. Roy. Aeronaut. Soc., May 1971.

19. Ball, John T.: Cloud and Synoptic Parameters Associated With Clear Air Turbulence. NASA CR-111778, 1970.

20. Veazey, Don R.: A Literature Survey of Clear Air Turbulence. NASA CR-106211, 1970.

21. Drazin, P. G.: The stability of a shear layer in an unbounded heterogeneous inviscid fluid. J. Fluid Mech., vol. 4, part 2, June 1958, pp. 214-224.

22. Charles, B. N.: On Some Limitations of Upper Wind Records. J. Geophys. Res., vol. 64, no. 3, March 1959.

23. Beyer, William H., ed.: Handbook of tables for Probability and Statistics. The Chemical Rubber Co., c.1966.

24. Crutcher, Harold L.; and Guttman, Nathaniel B.: Markov Chain Techniques for Predicting the Maximum Wind in the Maximum Dynamic Pressure Region for Launching Space Vehicles. NASA CR-61258, 1969.

TABLE 1.—VARIABLES, CLASS INTERVALS, AND RESTRICTIONS

Variable	Layers or levels (mb)	Univariate class intervals	Bivariate class intervals	Restrictions
Low altitude vector wind shear	700-175, 700-350, 350-175	.000-.013, .014-.016, .017-.019, ... sec⁻¹	.000-.013, .014-.016, ..., .029-.031, $\geq$.032 sec⁻¹	$\lvert\Delta V\rvert \geq 7$ msec⁻¹ $\lvert\Delta z\rvert \geq 0.5$ km
High altitude vector wind shear	175-20, 175-125, 125-80, 80-60, 60-40, 40-20	.000-.004, .005-.006, .007-.008, ... sec⁻¹	.000-.004, .005-.006, ..., .019-.020, $\geq$.021 sec⁻¹	$\lvert\Delta V\rvert \geq 3$ msec⁻¹ $\lvert\Delta z\rvert \geq 0.5$ km
High altitude wind shear x mean layer speed	175-20, 17-125, 125-80, 80-60, 60-40, 40-20	.000-.029, .030-.039, .040-.049, ...msec⁻²	.000-.029, .030-.039, ..., .050-.059, .060-.079, .080-.099, .100-.149, ..., .200-.249, $\geq$.250 msec⁻²	$\lvert\Delta V\rvert \geq 3$ msec⁻¹ $\lvert\Delta z\rvert \geq 0.5$ km
Positive lapse rate	tropopause-20, 700-350, 350-175, 125, 125-80, 80-60, 60-40, 40-20	0.00-2.99, 3.00-3.99,....., 4.00-4.99, ...°Ckm⁻¹	0.00-2.99, 3.00-3.99, ..., 8.00-8.99, $\geq$9.00°Ckm⁻¹	$\lvert\Delta T\rvert \geq 1.5°C$
Negative lapse rate (inversion)	tropopause-20, 700-350, 350-175, 175-125, 125-80, 80-60, 60-40, 40-20	0.00-2.99, 3.00-4.99, ..., 7.00-8.99, 9.00-12.99, ..., 29.00-32.99, 33.00-40.99, ..., 57.00-64.99, $\geq$65.00°Ckm⁻¹	0.00-2.99, 3.00-4.99, ..., 7.00-8.99, 9.00-12.99, ..., 21.00-24.99, $\geq$25.00°Ckm⁻¹	$\lvert\Delta T\rvert \geq 1.5°C$
Windspeed	300	0.0-9.9,...., 40.0-49.9, $\geq$50.0 msec⁻¹	0.0-9.9, ..., 40.0-49.9, $\geq$50.0 msec⁻¹	- - - - - -
Windspeed	100	0.0-9.9, 10.0-14.9, ..., 25.0-29.9, $\geq$30.0 msec⁻¹	0.0-9.9, 10.0-14.9, ..., 25.0-29.9, $\geq$30.0 msec⁻¹	- - - - - -
Windspeed	700, 70, 50, 30	0.0-4.9, ..., 20.0-24.9, $\geq$25.0 msec⁻¹	0.0-4.9, ..., 20.0-24.9, $\geq$25.0 msec⁻¹	- - - - - -

23

TABLE 2.—ARBITRARY THRESHOLDS FOR VARIABLES EXPECTED TO CONTRIBUTE TO TURBULENCE DEVELOPMENT

Variable	Threshold
Low altitude shear (700 to 175 mb)	$\geq$.014 sec^{-1}
High altitude shear (175 to 20 mb)	$\geq$.005 sec^{-1}
Shear x speed (60 to 20 mb)	$\geq$.03 msec^{-2}
Shear x speed (80 to 60 mb)	$\geq$.05 msec^{-2}
Shear x speed (125 to 80 mb)	$\geq$.08 msec^{-2}
Shear x speed (175 to 125 mb)	$\geq$.15 msec^{-2}
Positive lapse rate (175 to 20 mb)	$\geq$4 °Ckm^{-1}
Negative lapse rate (175 to 20 mb)	$\geq$5 °Ckm^{-1}
Windspeed (300 mb)	$\geq$30 msec^{-1}
Windspeed (100 mb)	$\geq$20 msec^{-1}
Windspeed (700, 70, 50, 50 mb)	$\geq$10 msec^{-1}

TABLE 3.—SEASONAL EMPIRICAL BIVARIATE PERCENT FREQUENCIES FOR VARIABLES MEETING CRITERIA IN TABLE 2

	Positive lapse rate layer, mb																			
	175-125				125-80				80-60				60-40				40-20			
	W	SP	SU	F	W	SP	SU	F	W	SP	SU	F	W	SP	SU	F	W	SP	SU	F
Wind shear layer—																				
700-350 mb	18	11	4	12	21	12	3	10	11	7	0	5	8	5	0	3	4	2	0	2
350-175 mb	24	17	9	17	24	18	6	12	12	8	1	6	9	5	0	4	4	2	0	2
Same as column	48	41	61	50	46	41	36	37	21	17	3	13	15	9	1	7	9	2	0	3
Shear x speed layer—																				
Same as column	38	29	26	37	45	34	17	31	21	16	0	10	17	9	1	7	10	2	0	3
Windspeed level—																				
700 mb	36	25	14	29	39	27	10	24	22	14	1	12	17	9	0	7	9	3	0	3
300 mb	33	24	9	27	35	25	7	28	19	14	1	12	15	9	0	7	8	3	0	3
100 mb	27	17	0	13	28	18	0	10	16	11	0	5	12	8	0	4	7	3	0	2
70 mb	--	--	--	--	--	--	--	--	19	11	0	8	--	--	--	--	--	--	--	--
50 mb	--	--	--	--	--	--	--	--	--	--	--	--	11	3	0	3	--	--	--	--
30 mb	--	--	--	--	--	--	--	--	--	--	--	--	--	--	--	--	7	0	0	2

TABLE 4.—SEASONAL EMPIRICAL BIVARIATE PERCENT FREQUENCIES FOR VARIABLES MEETING CRITERIA IN TABLE 2

	Negative lapse rate layer, mb																			
	175-125				125-80				80-60				60-40				40-20			
	W	SP	SU	F	W	SP	SU	F	W	SP	SU	F	W	SP	SU	F	W	SP	SU	F
Wind shear layer—																				
700-350 mb	4	7	1	5	6	9	3	10	9	8	2	8	11	6	1	6	7	4	1	4
350-175 mb	13	10	2	6	12	10	5	11	11	10	4	10	11	8	2	7	9	7	2	5
Same as column	29	30	12	19	24	25	44	34	22	23	21	25	20	15	7	15	16	10	3	8
Shear x speed layer—																				
Same as column	24	20	7	15	22	21	19	28	21	21	5	17	22	15	10	14	18	10	8	9
Windspeed level—																				
700 mb	24	16	5	13	23	17	9	21	21	17	6	19	20	13	3	14	15	10	2	9
300 mb	22	14	3	11	20	16	6	20	19	16	4	18	18	13	2	13	14	9	1	8
100 mb	15	10	0	5	14	10	3	9	16	12	2	10	17	13	0	7	14	12	0	5
70 mb	--	--	--	--	--	--	--	--	20	14	2	2	--	--	--	--	--	--	--	--
50 mb	--	--	--	--	--	--	--	--	--	--	--	--	13	4	5	5	--	--	--	--
30 mb	--	--	--	--	--	--	--	--	--	--	--	--	--	--	--	--	12	2	7	5

TABLE 5.—SEASONAL EMPIRICAL BIVARIATE PERCENT FREQUENCIES
FOR VARIABLES MEETING CRITERIA IN TABLE 2

	Wind shear layer, mb																			
	175-125				125-80				80-60				60-40				40-20			
	W	SP	SU	F	W	SP	SU	F	W	SP	SU	F	W	SP	SU	F	W	SP	SU	F
Wind shear layer—																				
700-350 mb	21	15	4	14	19	14	4	13	17	18	3	10	15	8	2	7	9	5	1	5
350-175 mb	32	22	10	20	29	22	10	18	25	19	6	15	20	12	3	9	13	7	1	6
Windspeed level—																				
700 mb	48	35	18	37	45	32	17	35	40	27	11	27	32	18	5	18	23	10	2	12
300 mb	46	34	13	34	43	32	13	34	37	27	8	26	30	18	4	17	20	9	1	11
100 mb	38	26	0	17	36	27	0	18	34	26	0	15	28	17	0	10	21	9	0	16
70 mb	--	--	--	--	--	--	--	--	47	30	3	21	--	--	--	--	--	--	--	--
50 mb	--	--	--	--	--	--	--	--	--	--	--	--	24	7	6	7	--	--	--	--
30 mb	--	--	--	--	--	--	--	--	--	--	--	--	--	--	--	--	19	2	7	18

TABLE 6.—PERCENT FREQUENCY OF VARIABLES IN SPECIFIED RANGES FOR
THE REFERENCE 16 TURBULENCE INTENSITY CATEGORIES AND SEASONS

Variable	Specified range	Turbulence-intensity category (ref. 16)			A	Season, present sample			
		T_0	T_1	T_2		W	SP	SU	F
V_{max}	≥ 36 m/sec	36	37	69	25	40	28	7	26
V_{300}	≥ 30 m/sec	--	--	--	37	54	41	14	40
V_{100}	≥ 21 m/sec	4	7	56	20	38	26	0.3	15
$\left(\frac{\Delta V}{\Delta Z}\right)_{low}$	$\geq .02$ sec^{-1}	16	19	56	<10.7 (350–175 mb) (700–350 mb)	<18.3 10.3 8.0	<12.5 7.5 5.0	<2.9 2.1 .86	<9.3 5.3 4.0
$\left(\frac{\Delta V}{\Delta Z}\right)_{flt}$	$\geq .005$ sec^{-1}	16	48	69	47 (60–40 mb) (175–125 mb)	---- 35 67	---- 23.7 64.4	---- 12 63	---- 21 64.4
γ_{flt}	≥ 4.0 °C/km	12	26	56	36 (60–40 mb) (175–125 mb)	---- 23 60	---- 15 50	---- 1.7 78	---- 12.5 64
$-\gamma_{flt}$	≥ 5.0 °C/km	32	18	56	32 (60–40 mb) (125–80 mb)	---- 29 31	---- 26 32	---- 19 49	---- 28 41

TABLE 7.—PERCENT FREQUENCY OF VARIABLES IN SPECIFIED RANGES
FOR THE REFERENCE 19 TURBULENCE INTENSITY CATEGORIES

Variable	Specified range	Turbulence-intensity category (ref. 19)				Present sample annual
		< Light	Light	≥ Light to moderate	All data	
γ	>3.2 °C/km	40	55	74	47	53
	≥ 5.6 °C/km	15	30	44	26	25
$-\gamma$	>4.9 °C/km	39	55	62	51	33
	≥ 8.2 °C/km	19	29	42	25	18
$\left(\frac{\Delta V}{\Delta Z}\right)_{flt}$	$\geq .006$ sec^{-1}	38	48	46	42	44
	$\geq .008$ sec^{-1}	17	26	36	23	27
$V\left(\frac{\Delta V}{\Delta Z}\right)$	$\geq .07$ m/sec^{-2}	41	55	53	47	52
	$\geq .12$ m/sec^{-2}	20	36	41	28	34

TABLE 8.——AVERAGE VALUES OF METEOROLOGICAL VARIABLES
FOR THE REFERENCE 16 TURBULENCE INTENSITY CATEGORIES

Variable	T_0	T_1	T_2	All data
V_{max}, m/sec	34	33	47	37
V_{100}, m/sec	12	12	20	14
$\left(\frac{\Delta V}{\Delta Z}\right)_{low}$, per sec	.012	.015	.021	.015

TABLE 9.——AVERAGE VALUES OF METEOROLOGICAL VARIABLES
FOR THE REFERENCE 19 TURBULENCE INTENSITY CATEGORIES

Variable	<Light	Light	$\geq$Light to moderate	All data
V_{max}, m/sec	36	40	42	38
γ_{flt}, °C/km	2.6	3.6	5.2	3.4
$-\gamma_{flt}$, °C/km	5.2	6.2	9.5	6.3
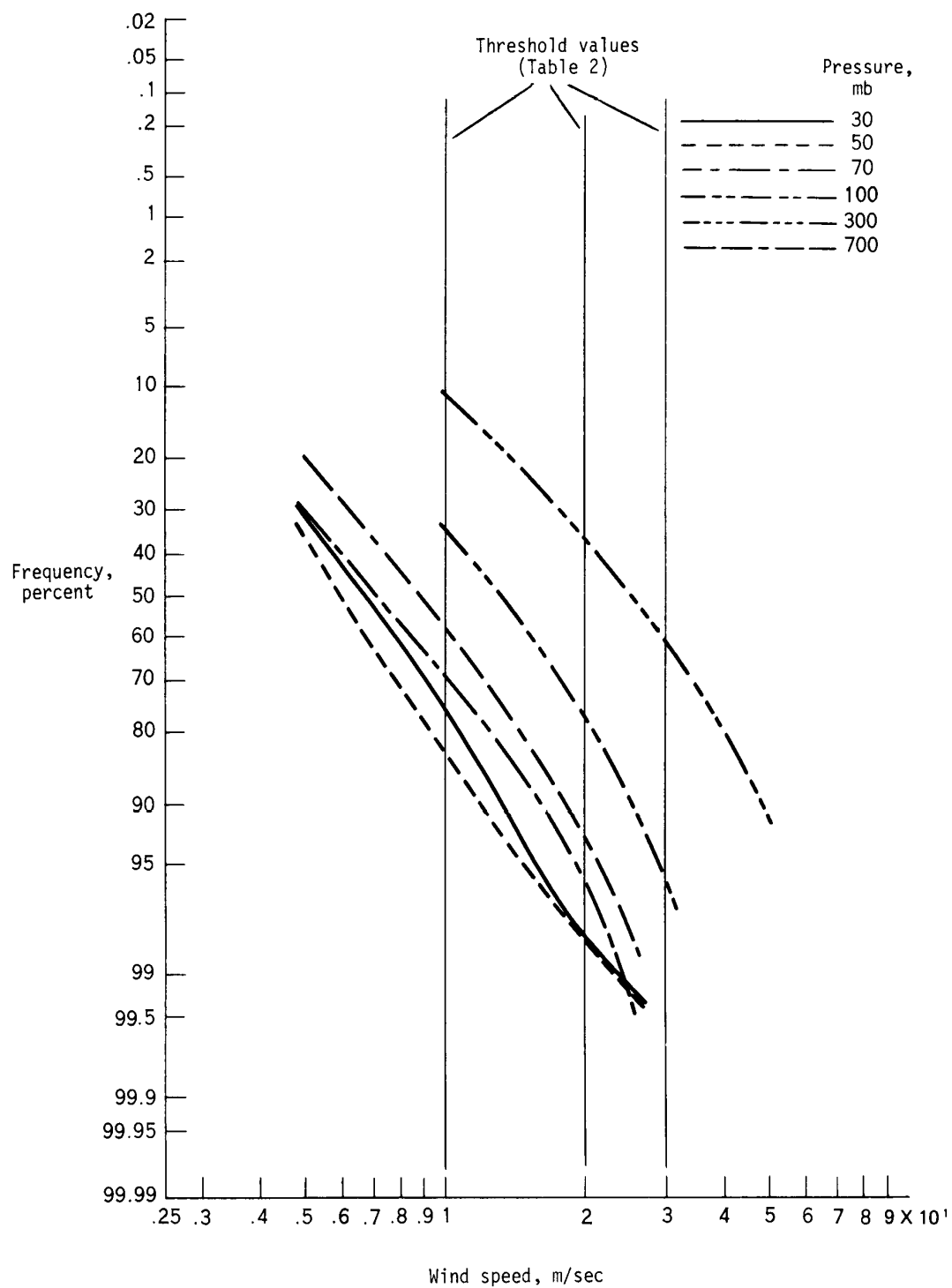
Figure 1. Annual cumulative distributions of wind speeds
for indicated pressure levels.

30
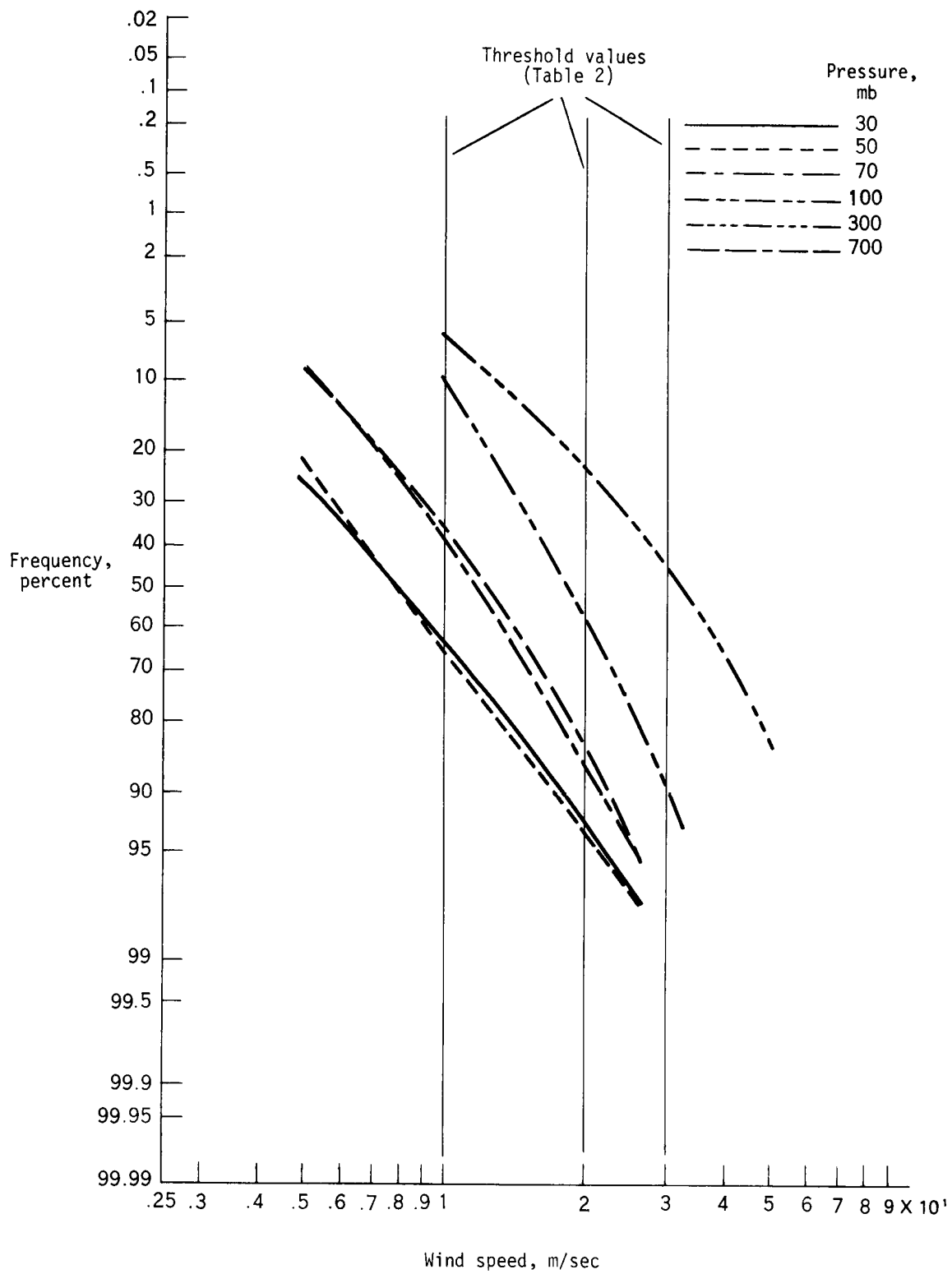
Figure 2. Winter cumulative distributions of wind speeds
for indicated pressure levels.
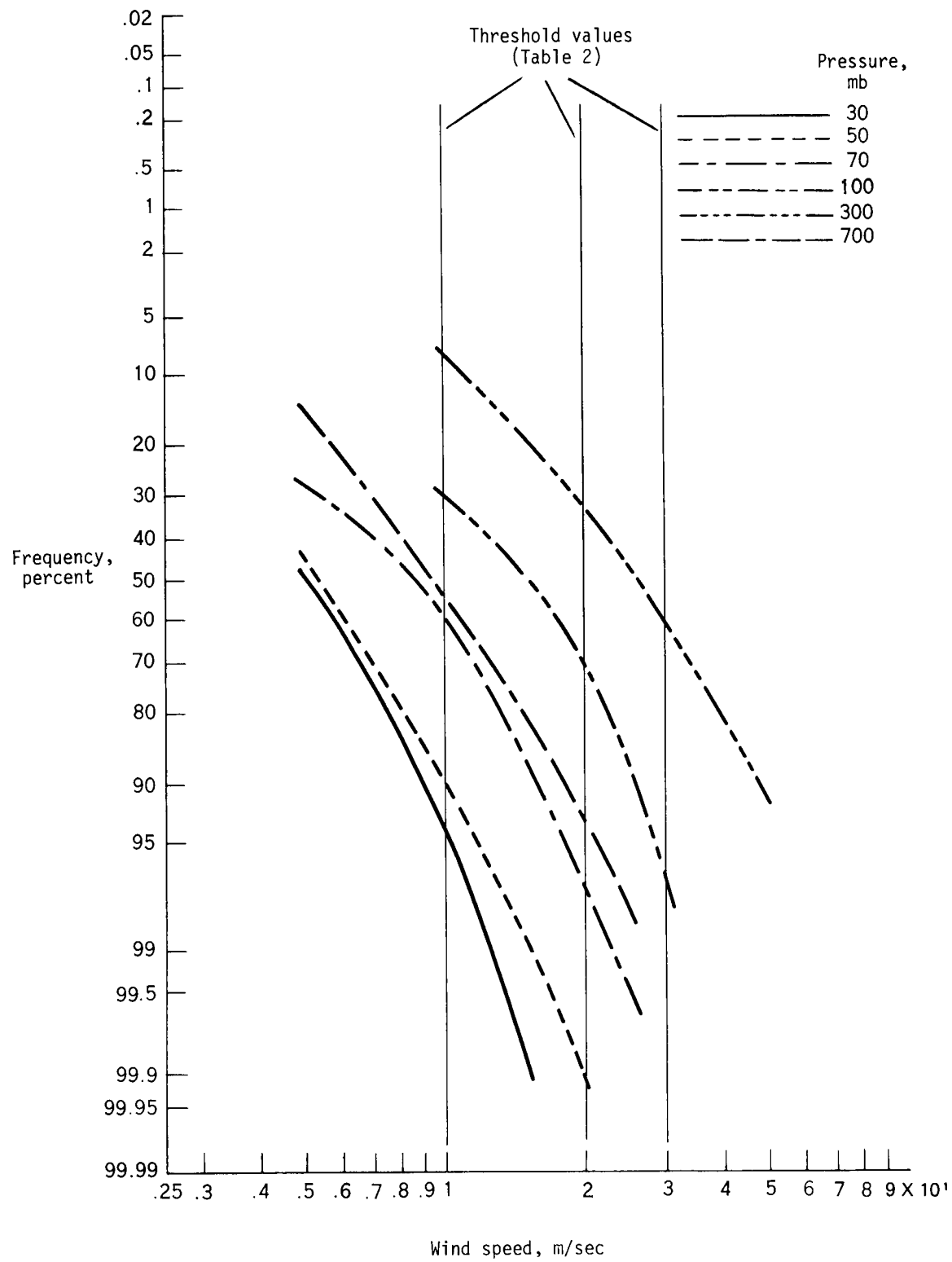
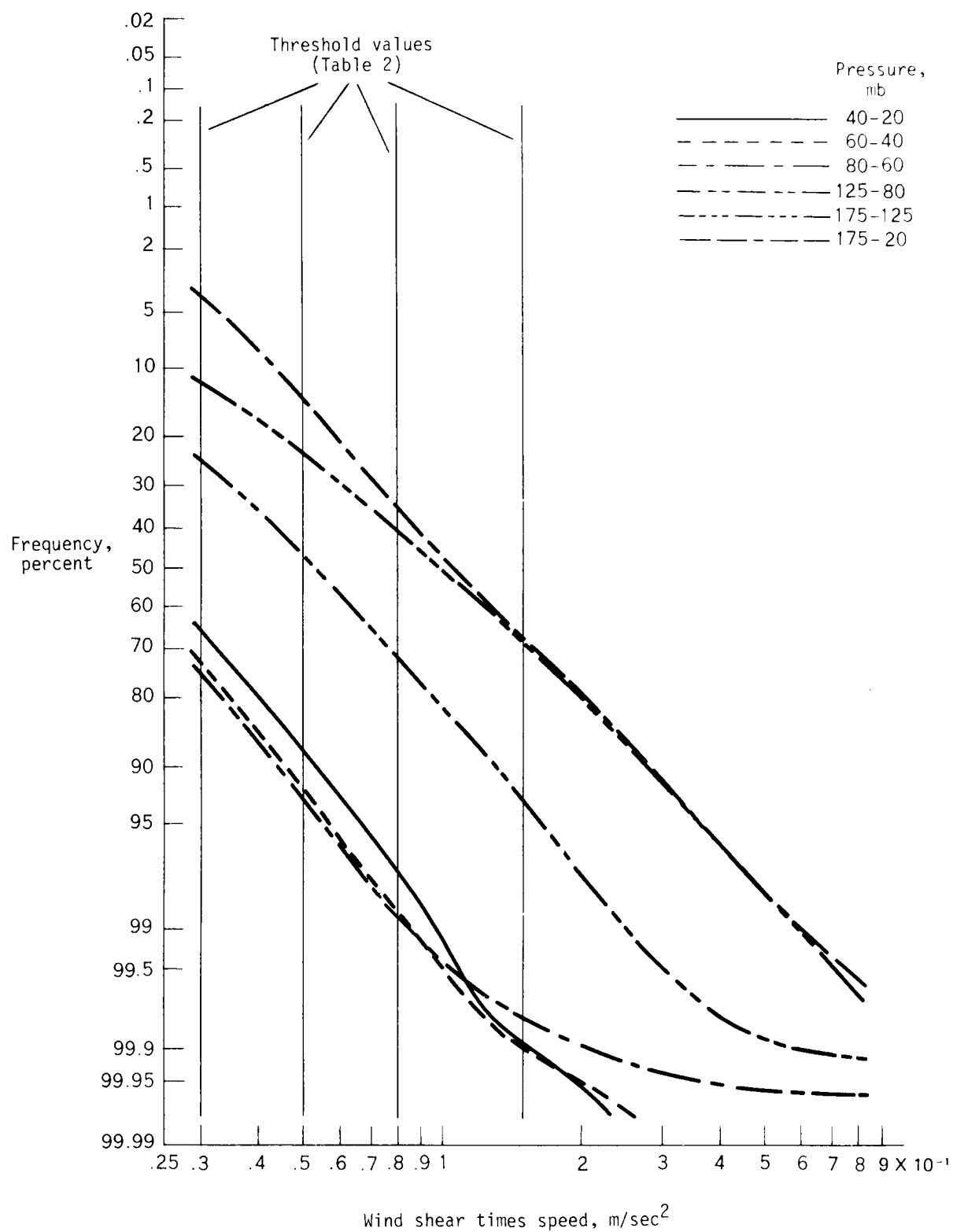Figure 3. Spring cumulative distributions of wind speeds
for indicated pressure levels.
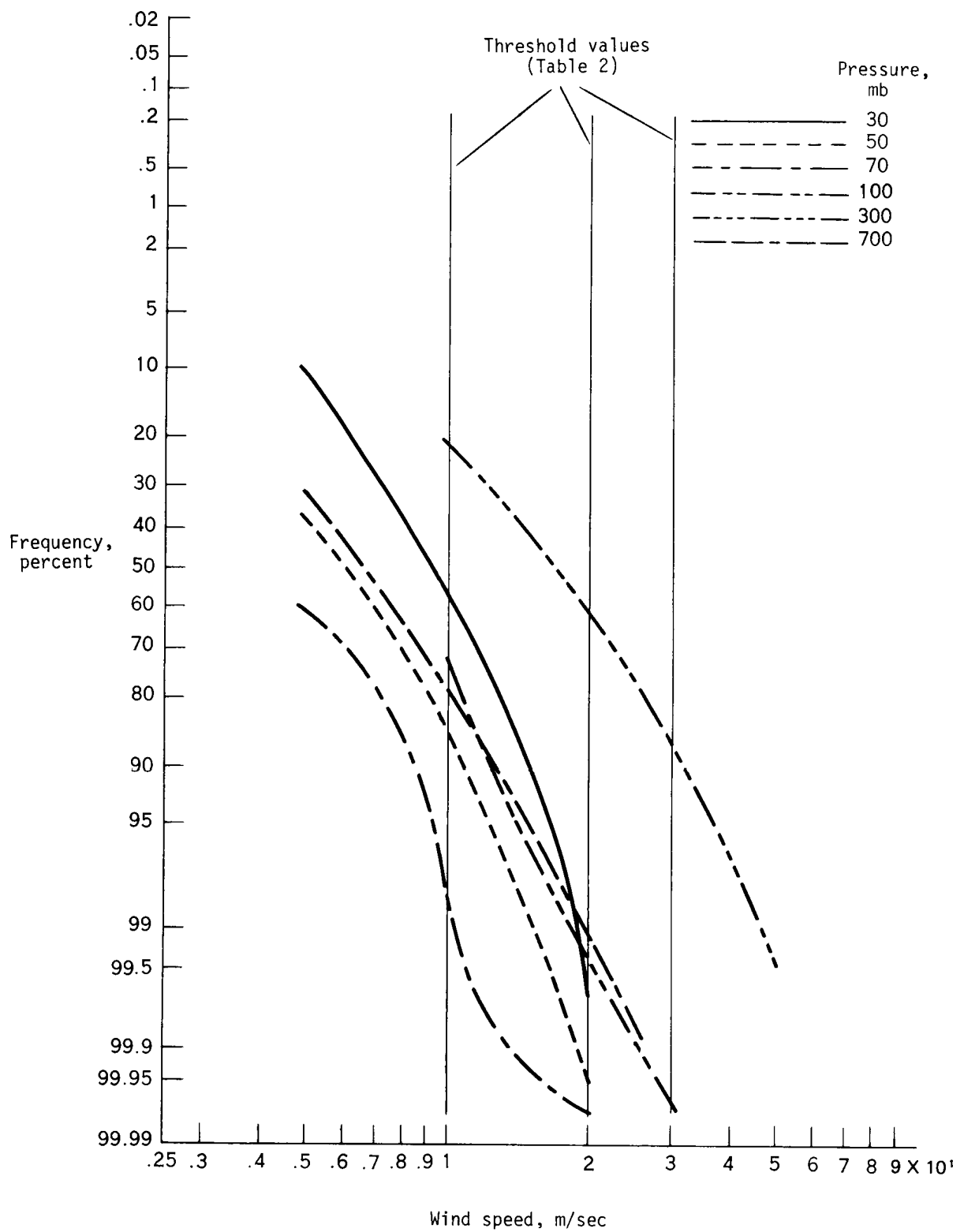
Figure 4. Summer cumulative distributions of wind speeds
for indicated pressure levels.
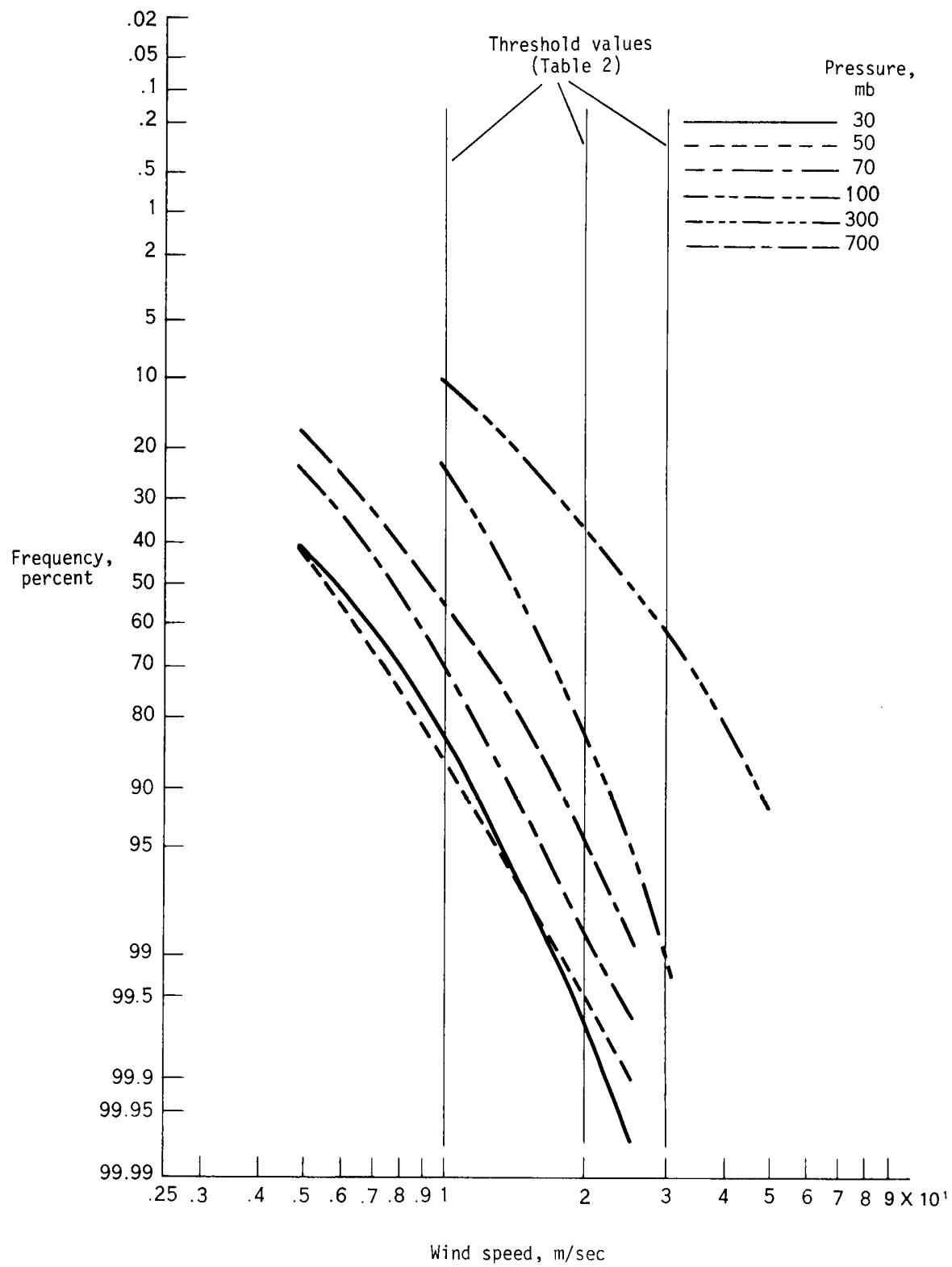
Figure 5. Fall cumulative distributions of wind speeds for indicated pressure levels.
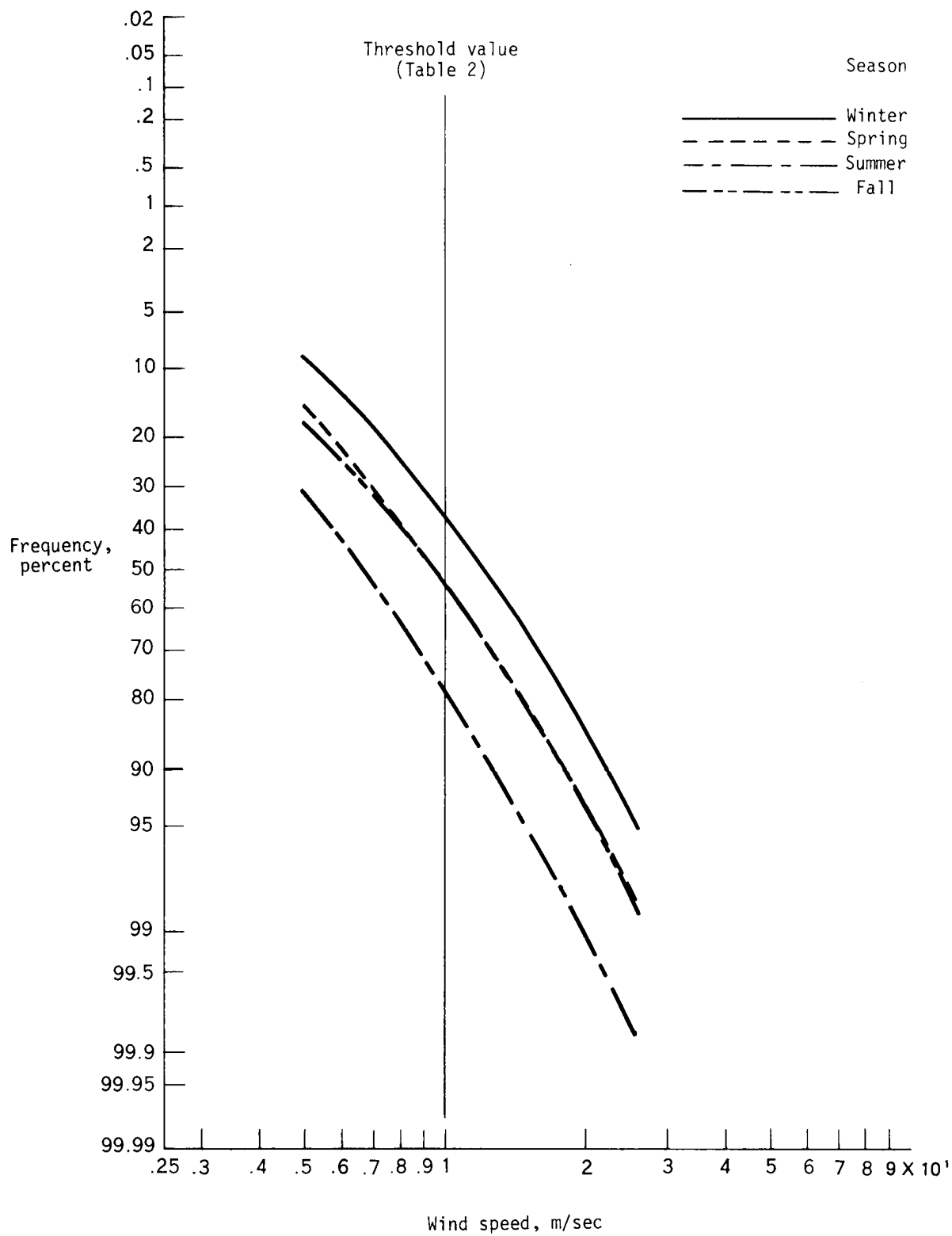
Figure 6.   Seasonal cumulative distributions of 700 mb wind speeds.
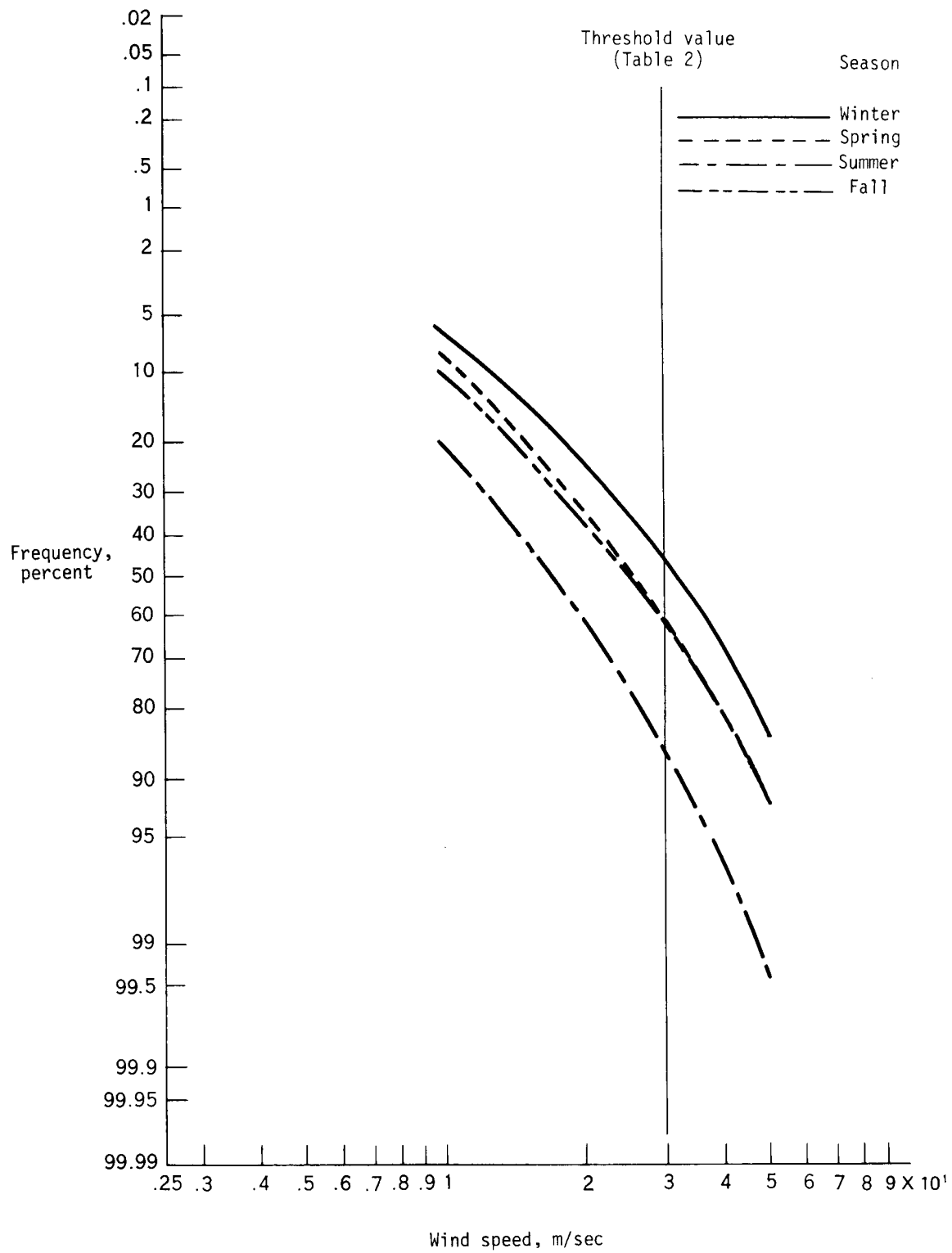
Figure 7. Seasonal cumulative distributions of 300 mb wind speeds.
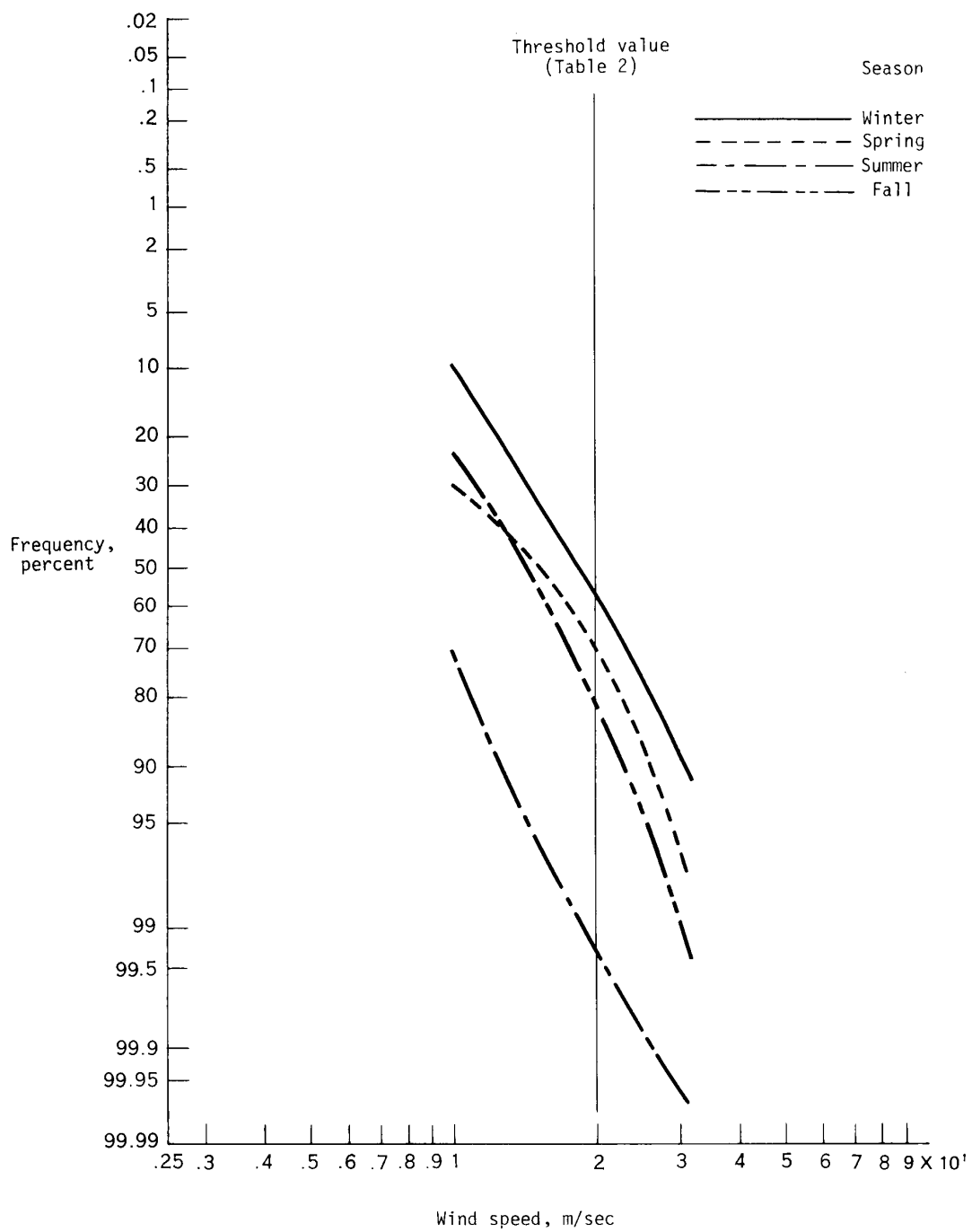
Figure 8. Seasonal cumulative distributions of 100 mb wind speeds.

.02
.05
.1
.2
.5
1
2

Threshold value
(Table 2)

Season

———————— Winter
— — — — — — Spring
— · — · — · — Summer
— ·· — ·· — ·· — Fall

5
10
20
30
40

Frequency,
percent

50
60
70
80
90
95

99
99.5

99.9
99.95

99.99

.25 .3   .4   .5 .6 .7 .8 .9 1   2   3   4   5   6 7 8 9 X 10¹
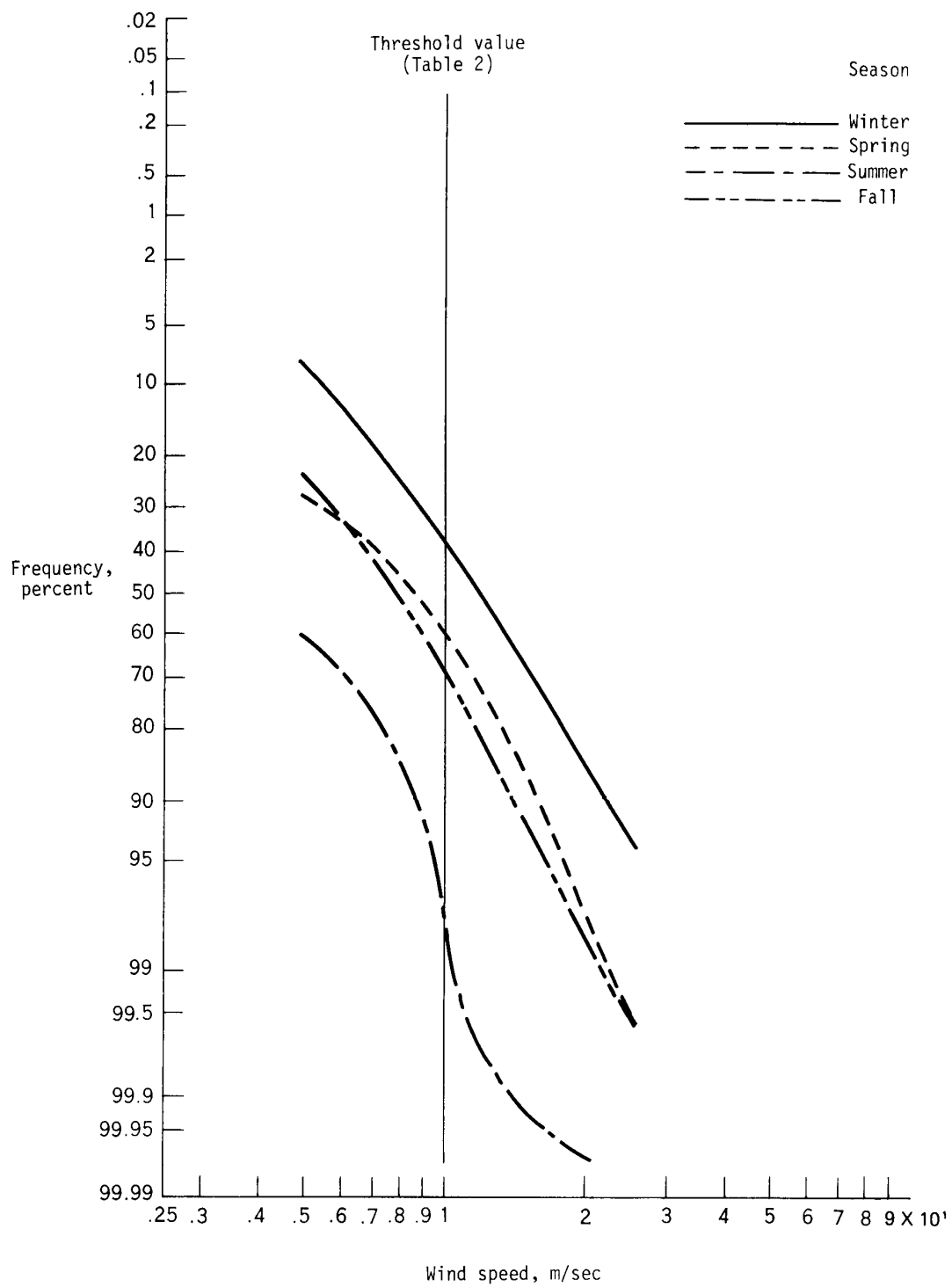
Wind speed, m/sec

Figure 9.   Seasonal cumulative distributions of 70 mb wind speeds.

38
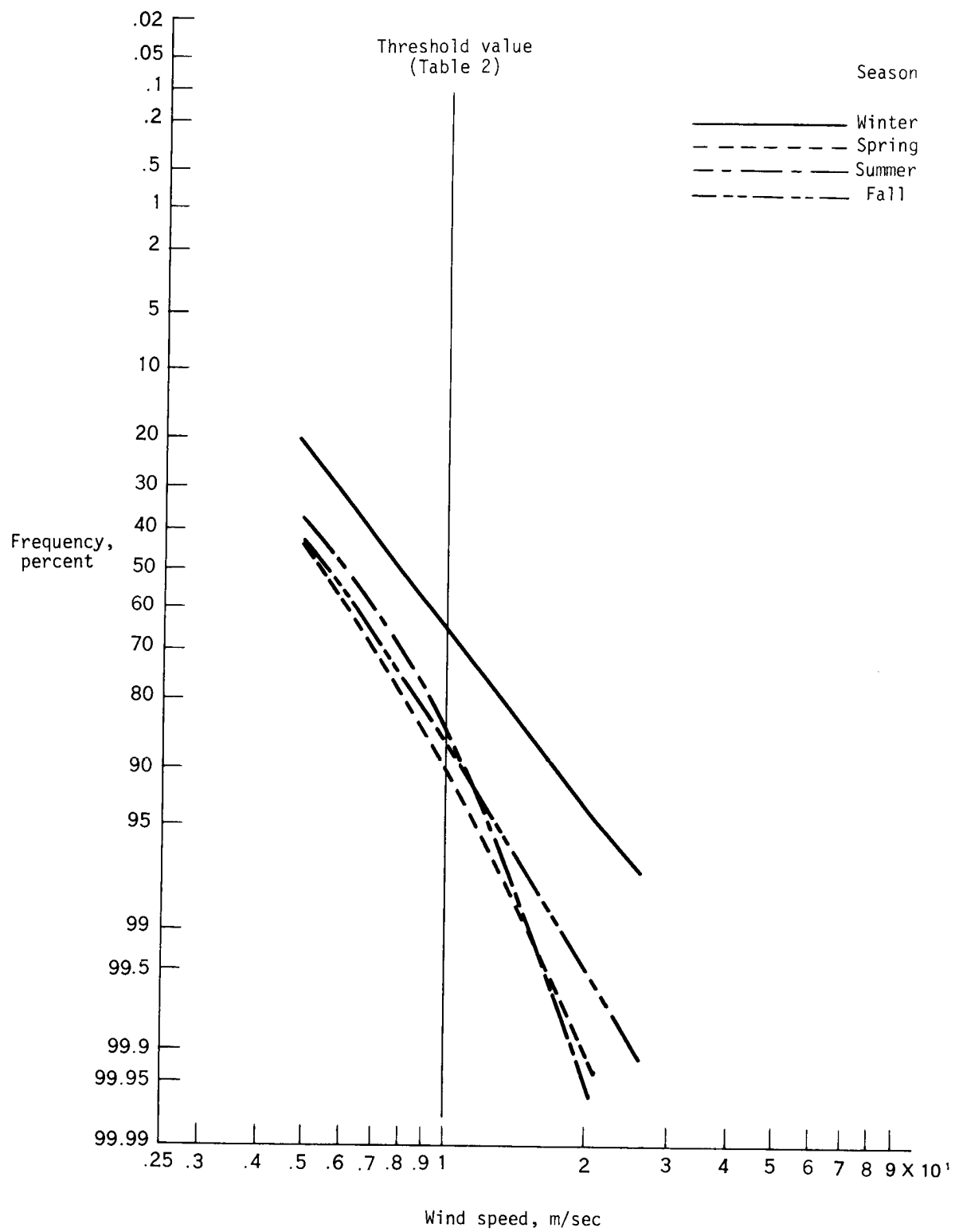
Figure 10. Seasonal cumulative distributions of 50 mb wind speeds.
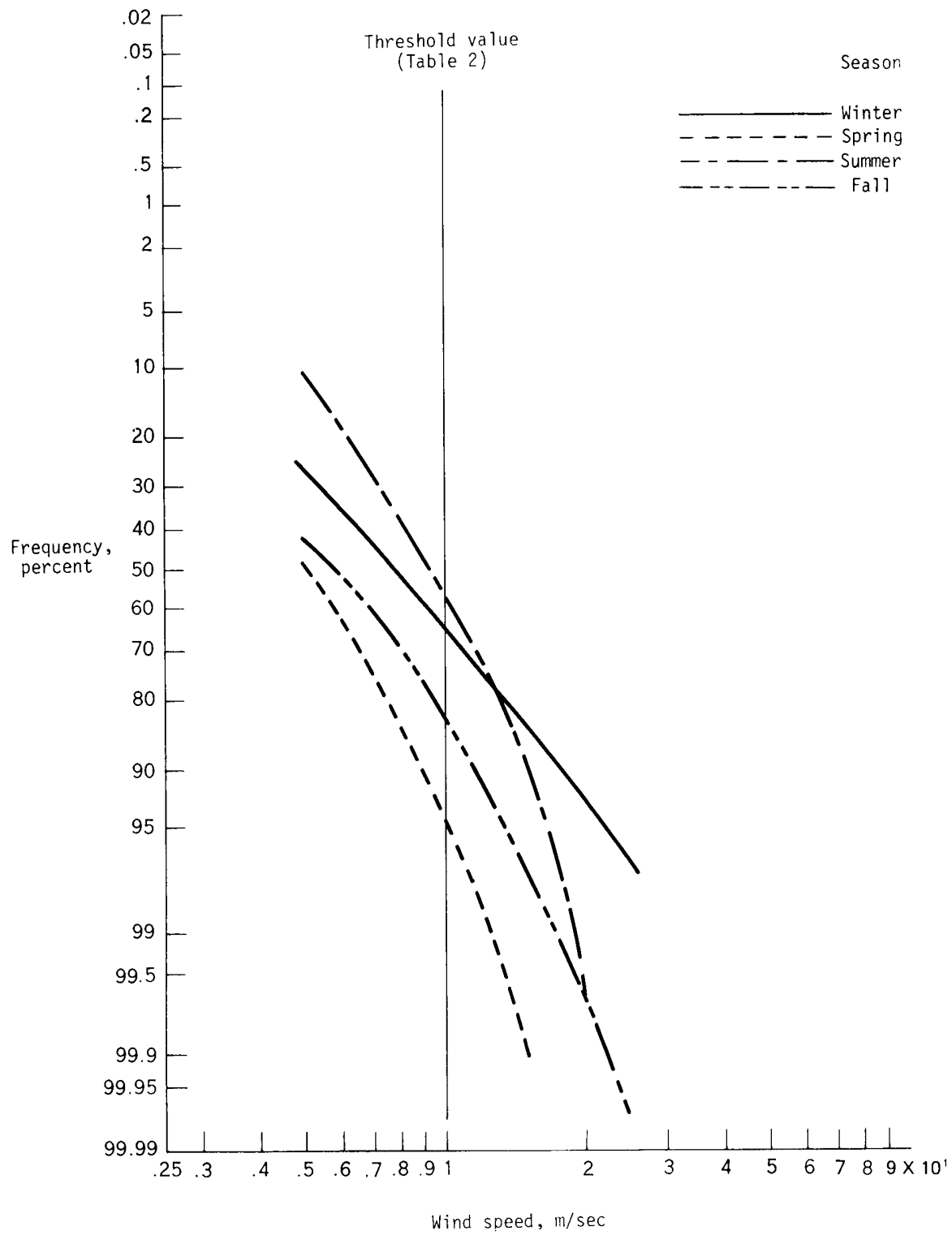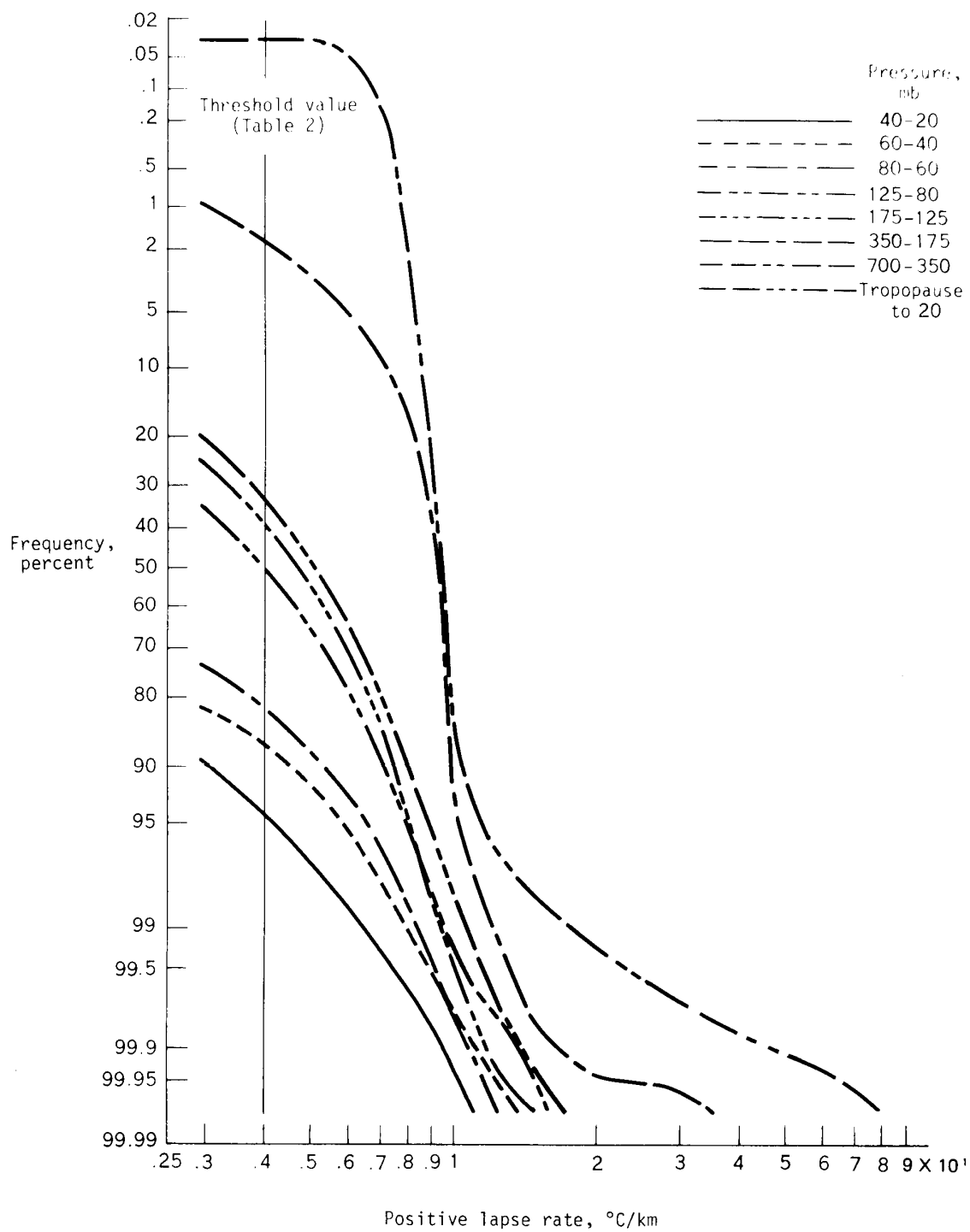
Figure 11. Seasonal cumulative distributions of 30 mb wind speeds.
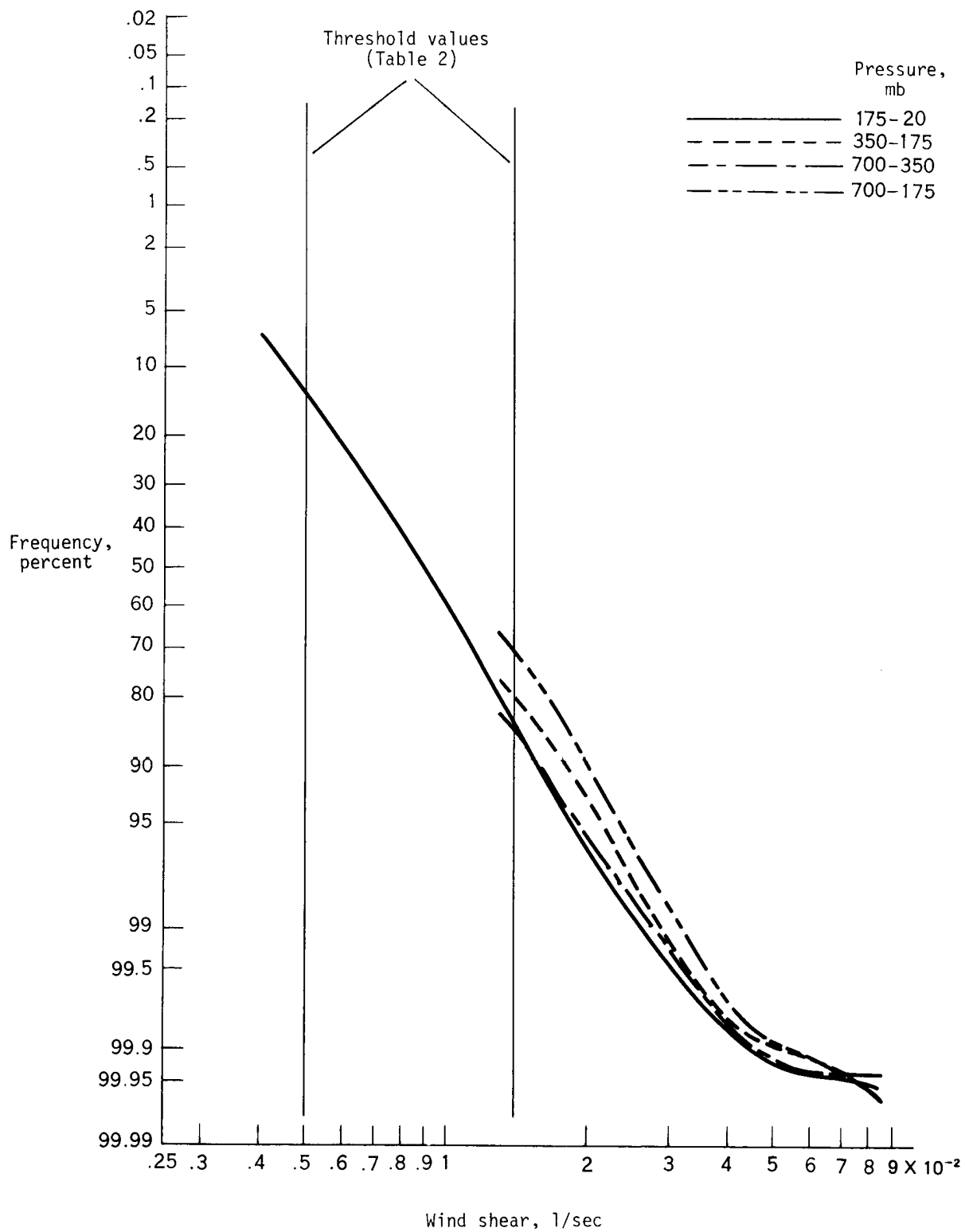
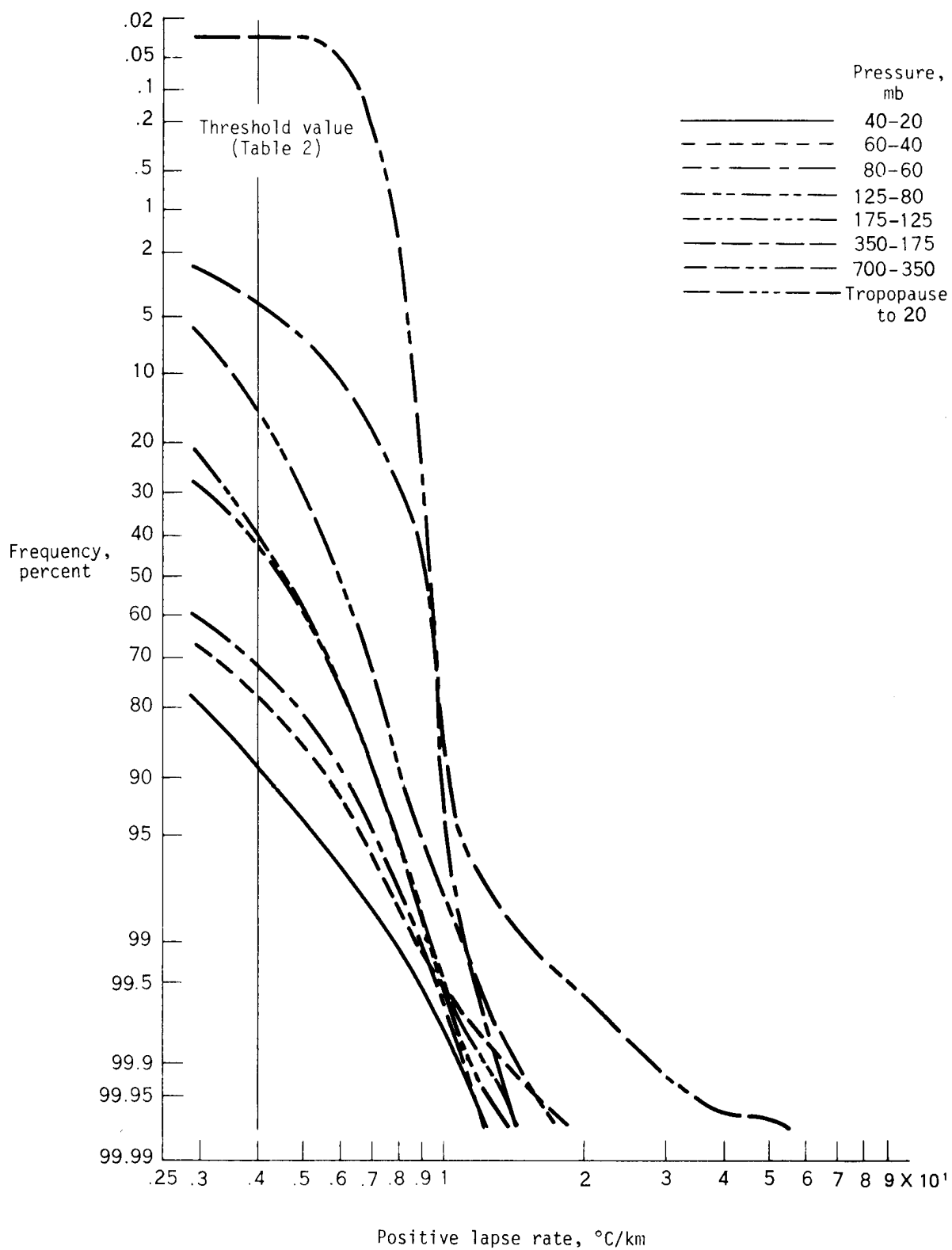Figure 12.   Annual cumulative distributions of wind shears
for indicated layers.
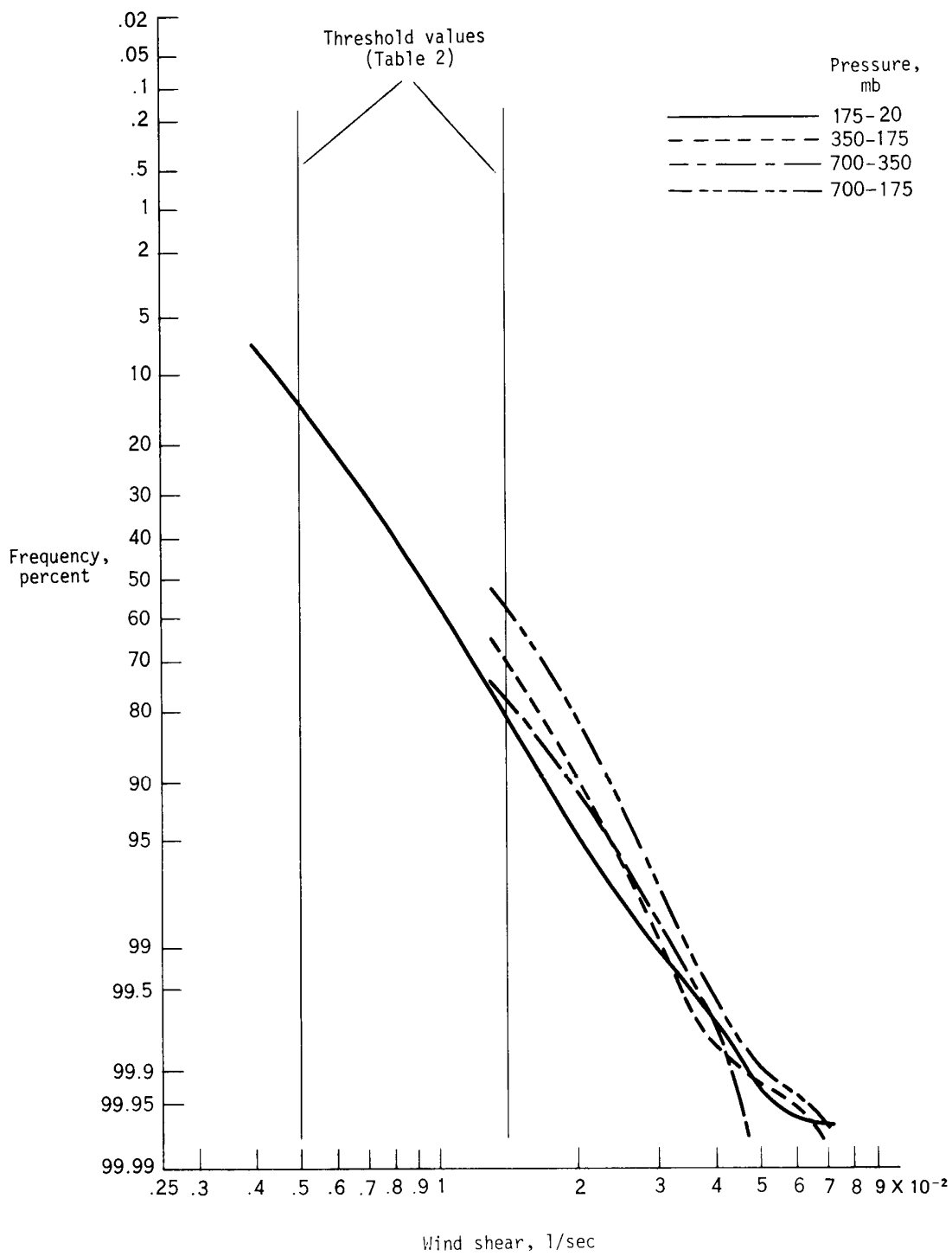
Figure 13. Winter cumulative distributions of wind shears
for indicated layers.
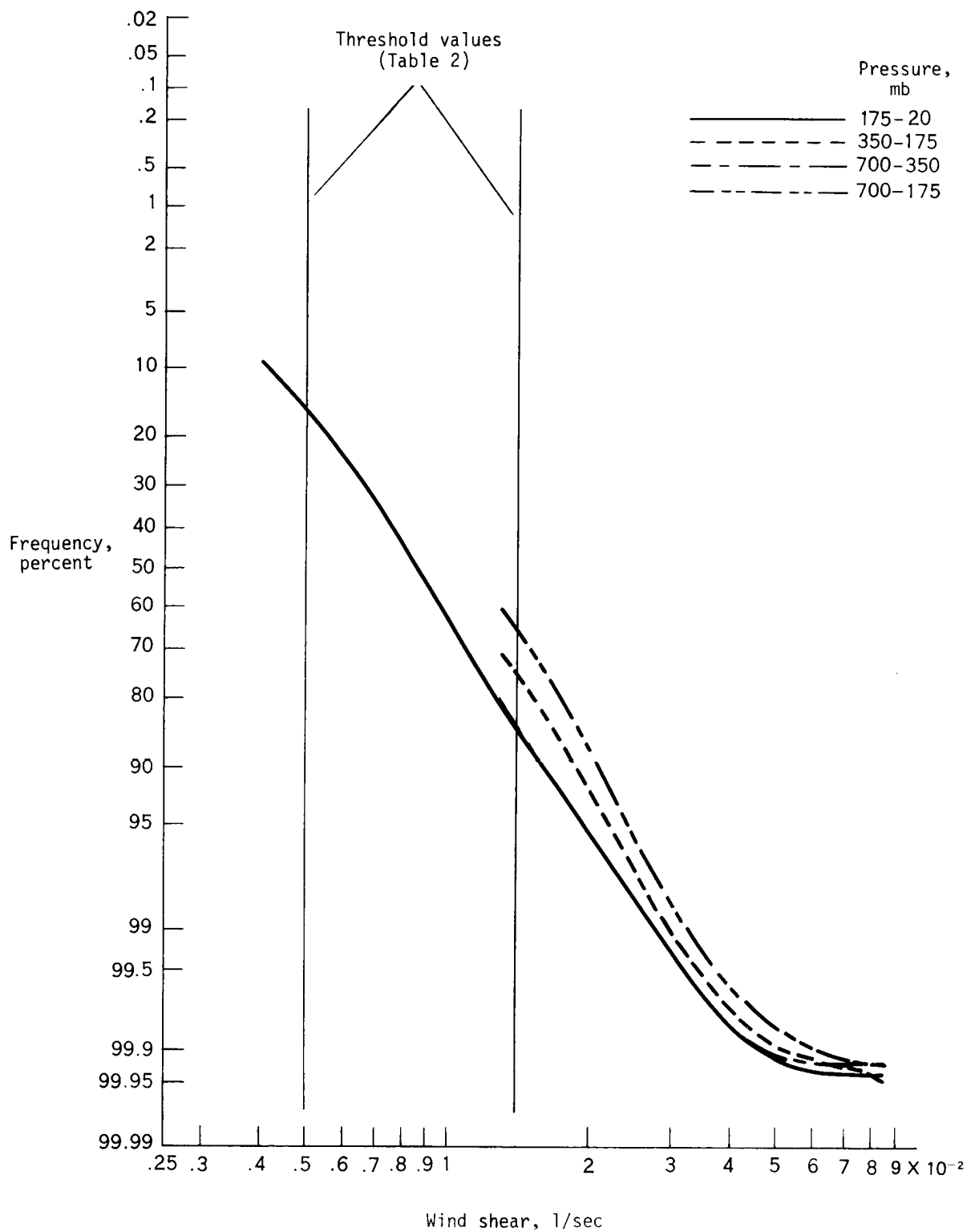
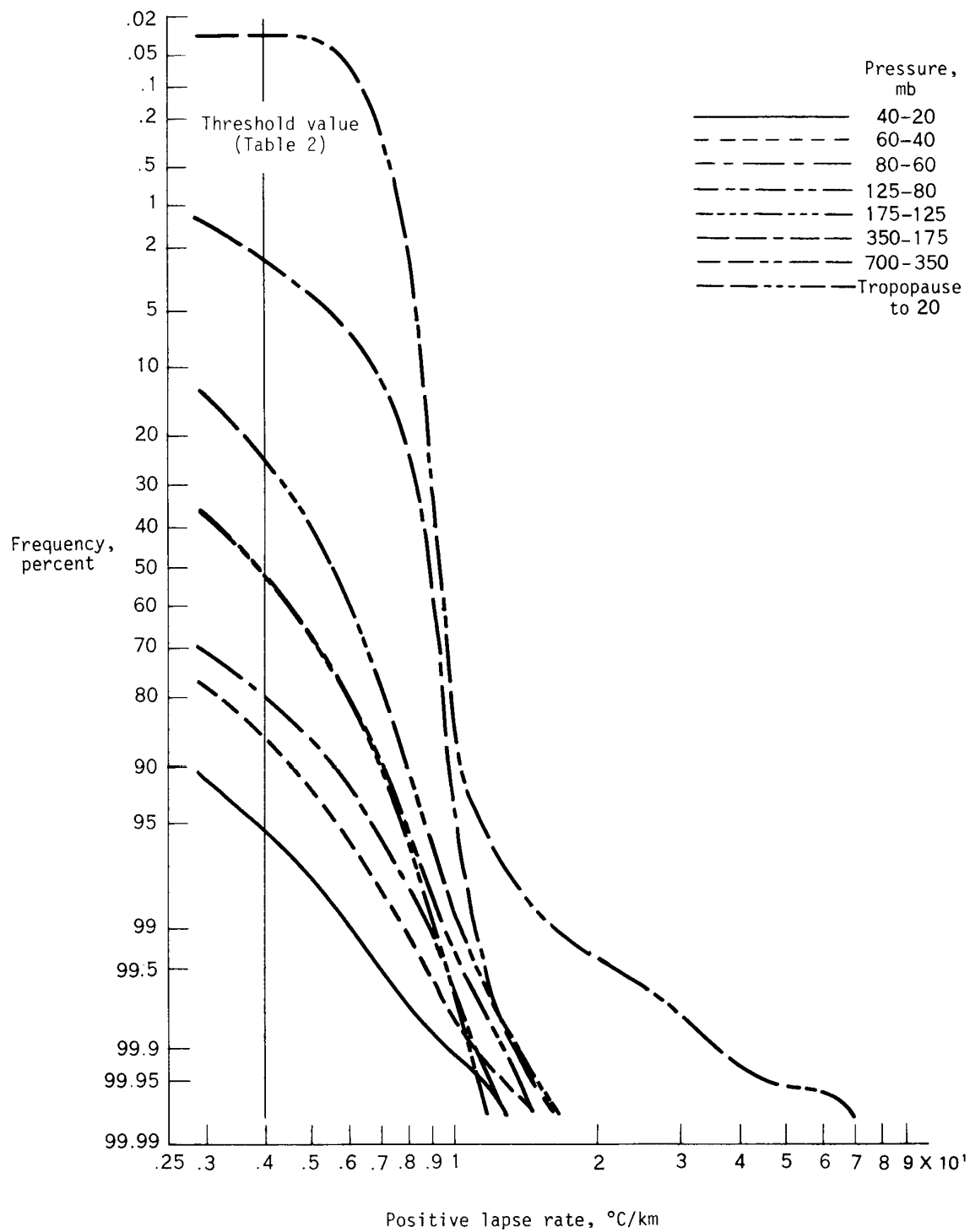Figure 14. Spring cumulative distributions of wind shears for indicated layers.
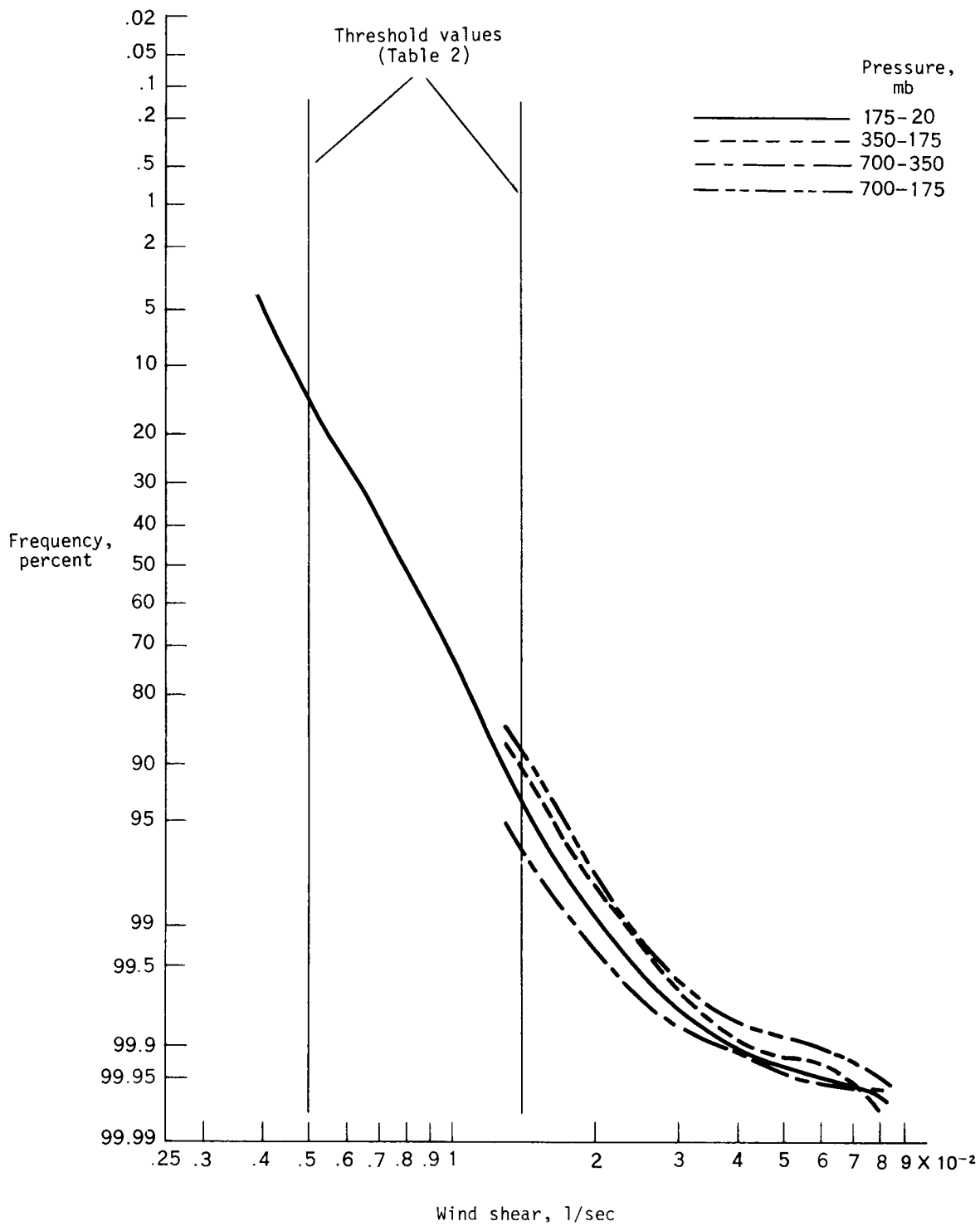
Figure 15. Summer cumulative distributions of wind shears
for indicated layers.

44
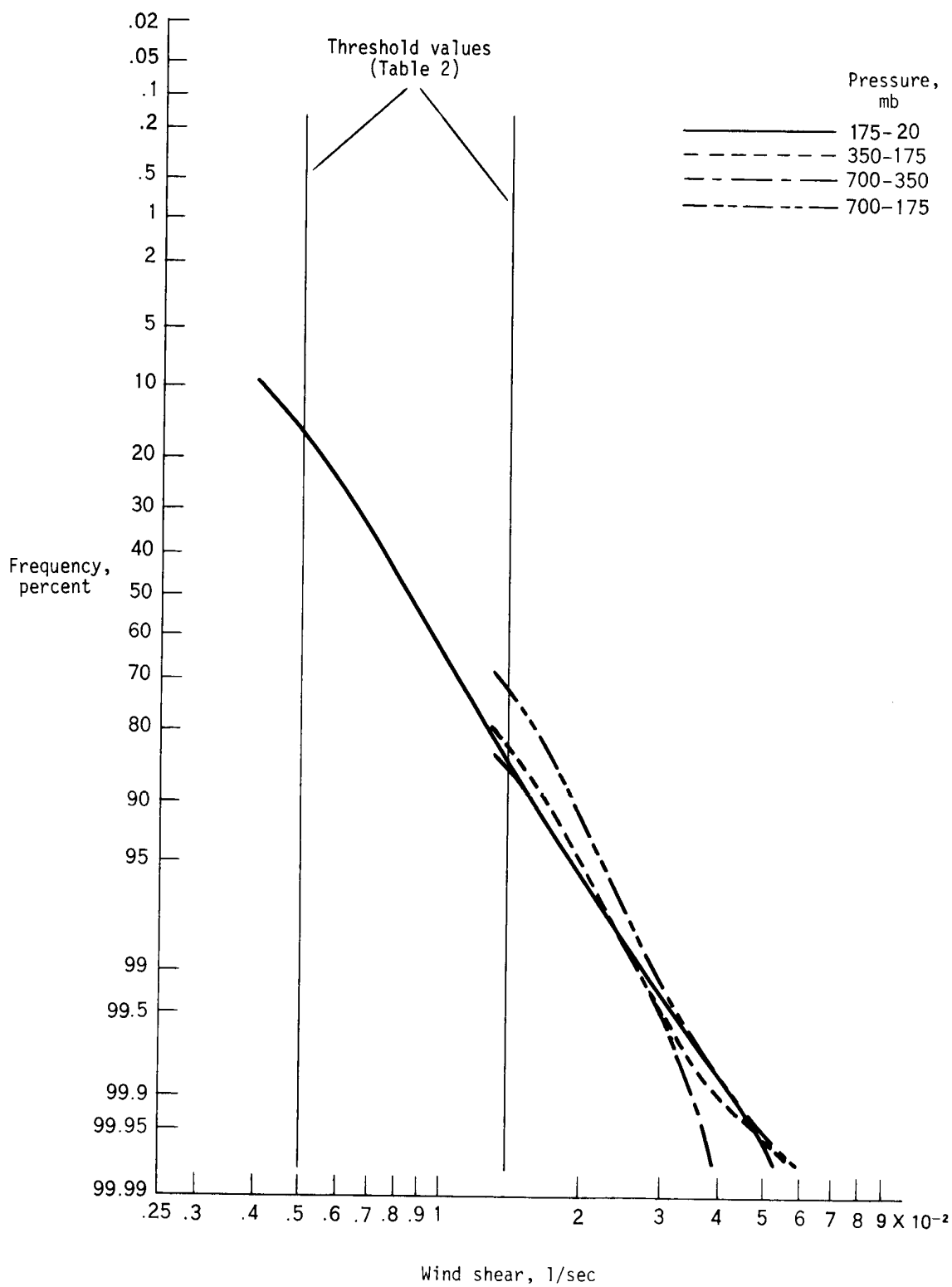
Figure 16. Fall cumulative distributions of wind shears for indicated layers.

45
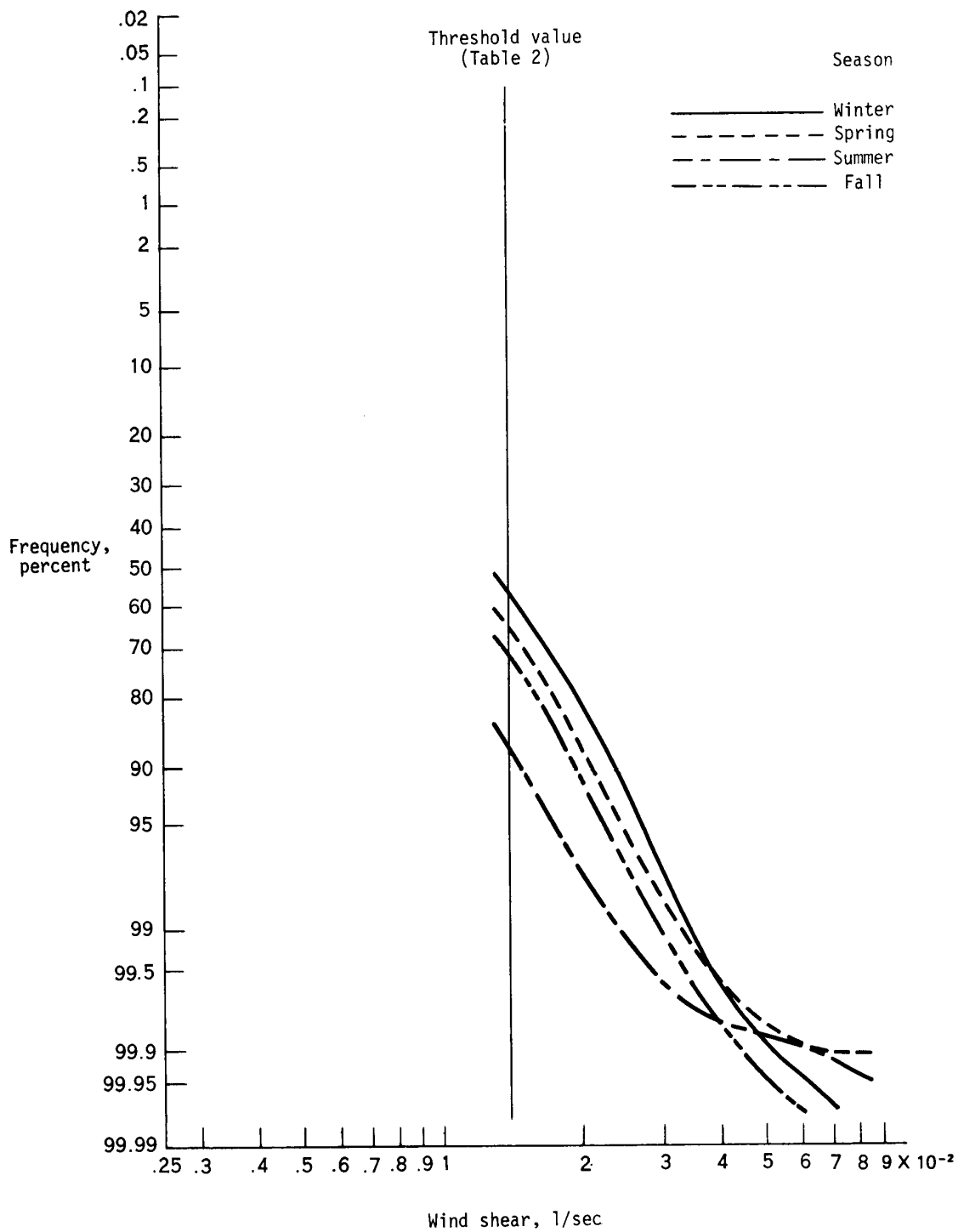
Figure 17. Seasonal cumulative distributions of wind shears
for the 700-175 mb layer.
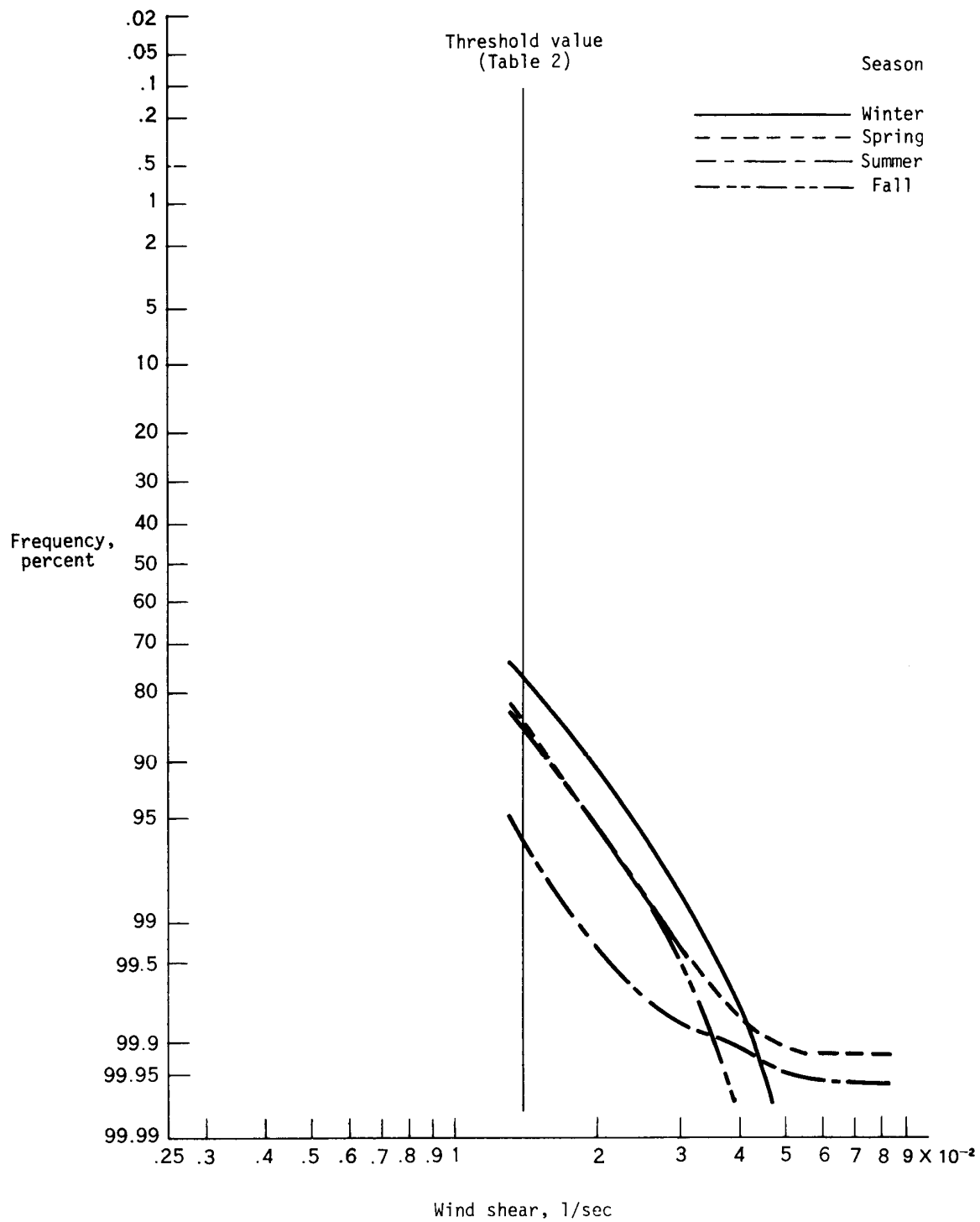
Figure 18. Seasonal cumulative distributions of wind shears
for the 700-350 mb layer.
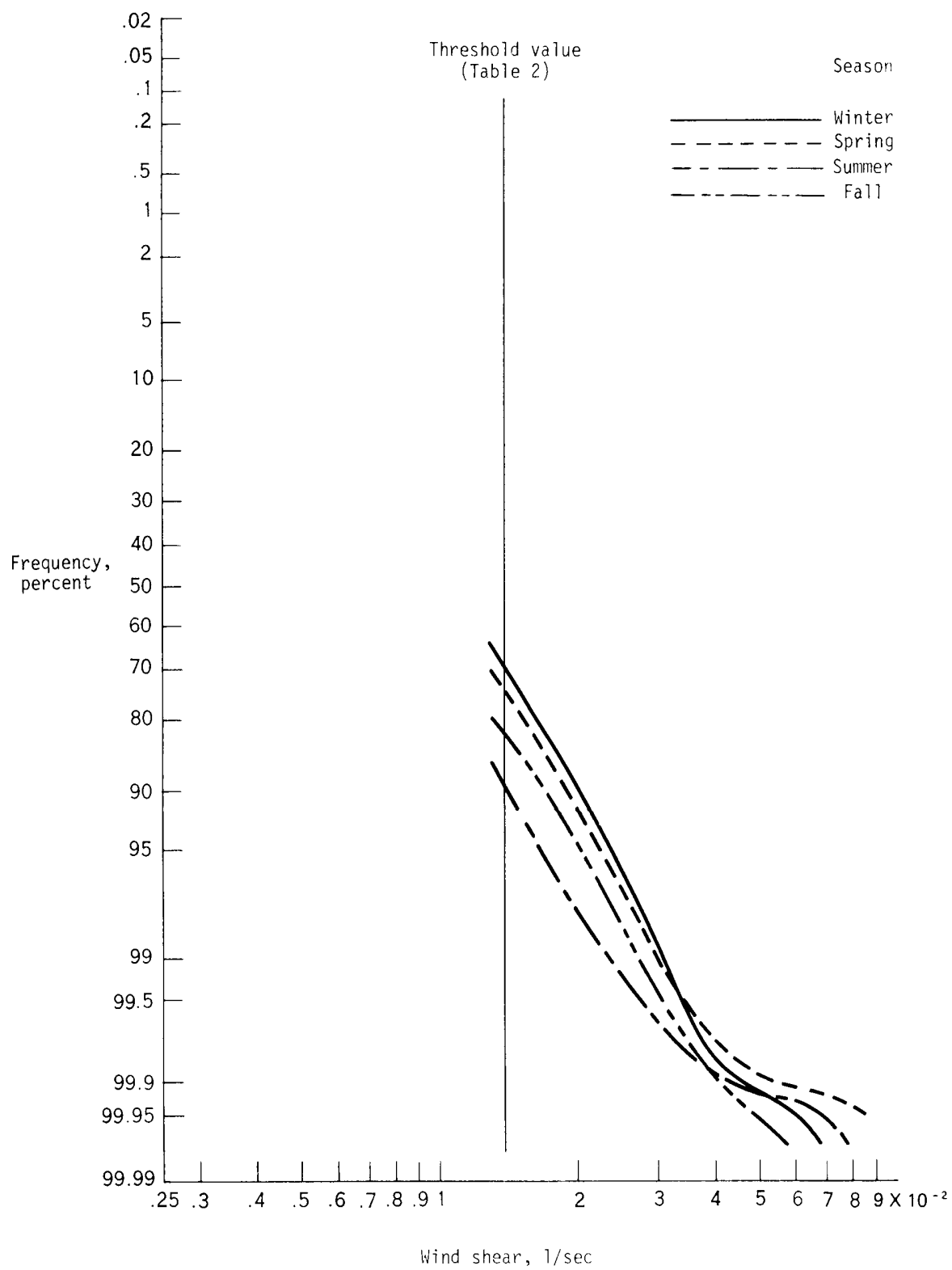
Figure 19. Seasonal cumulative distributions of wind shears for the 350-175 mb layer.
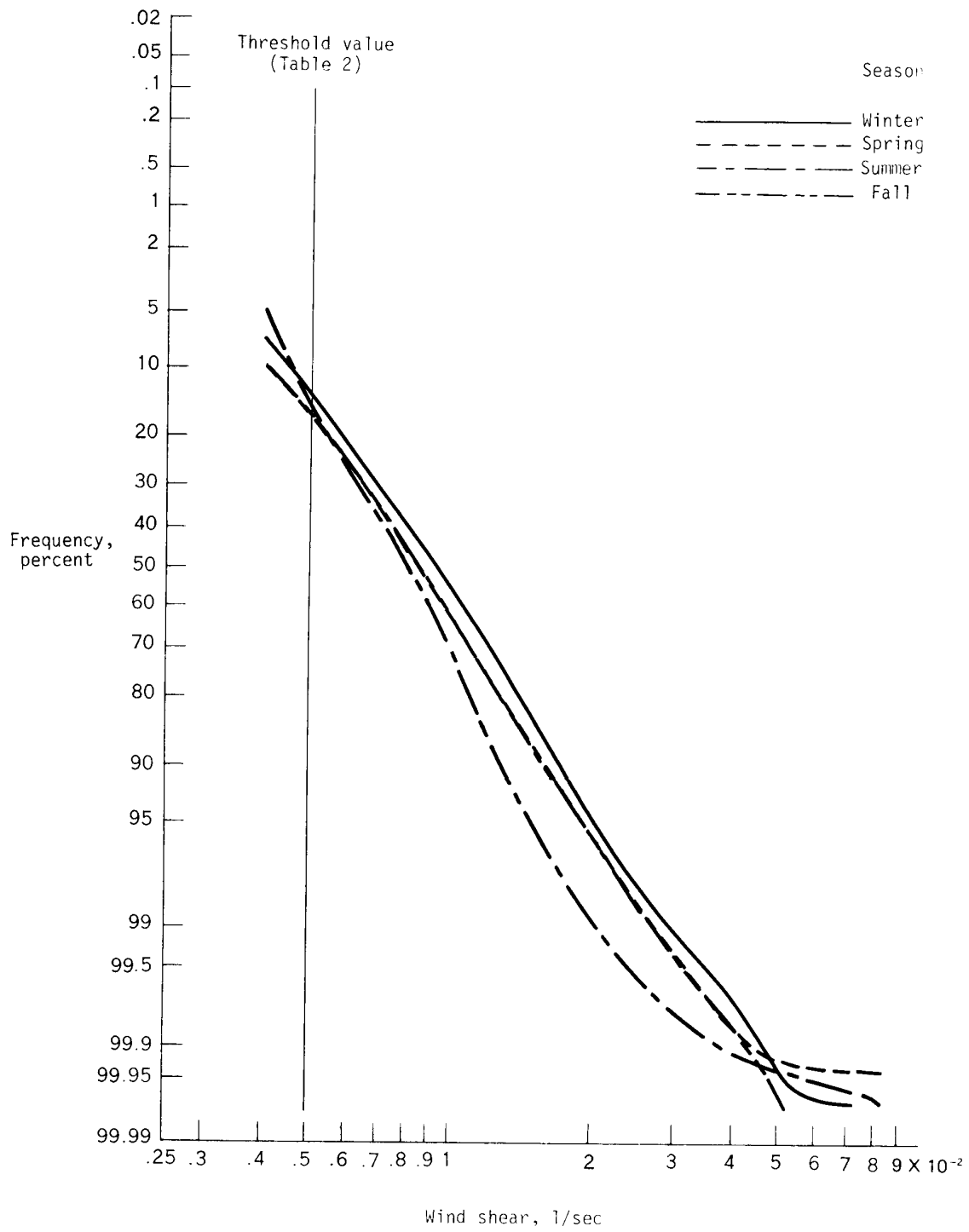
Figure 20. Seasonal cumulative distributions of wind shears
for the 175-20 mb layer.
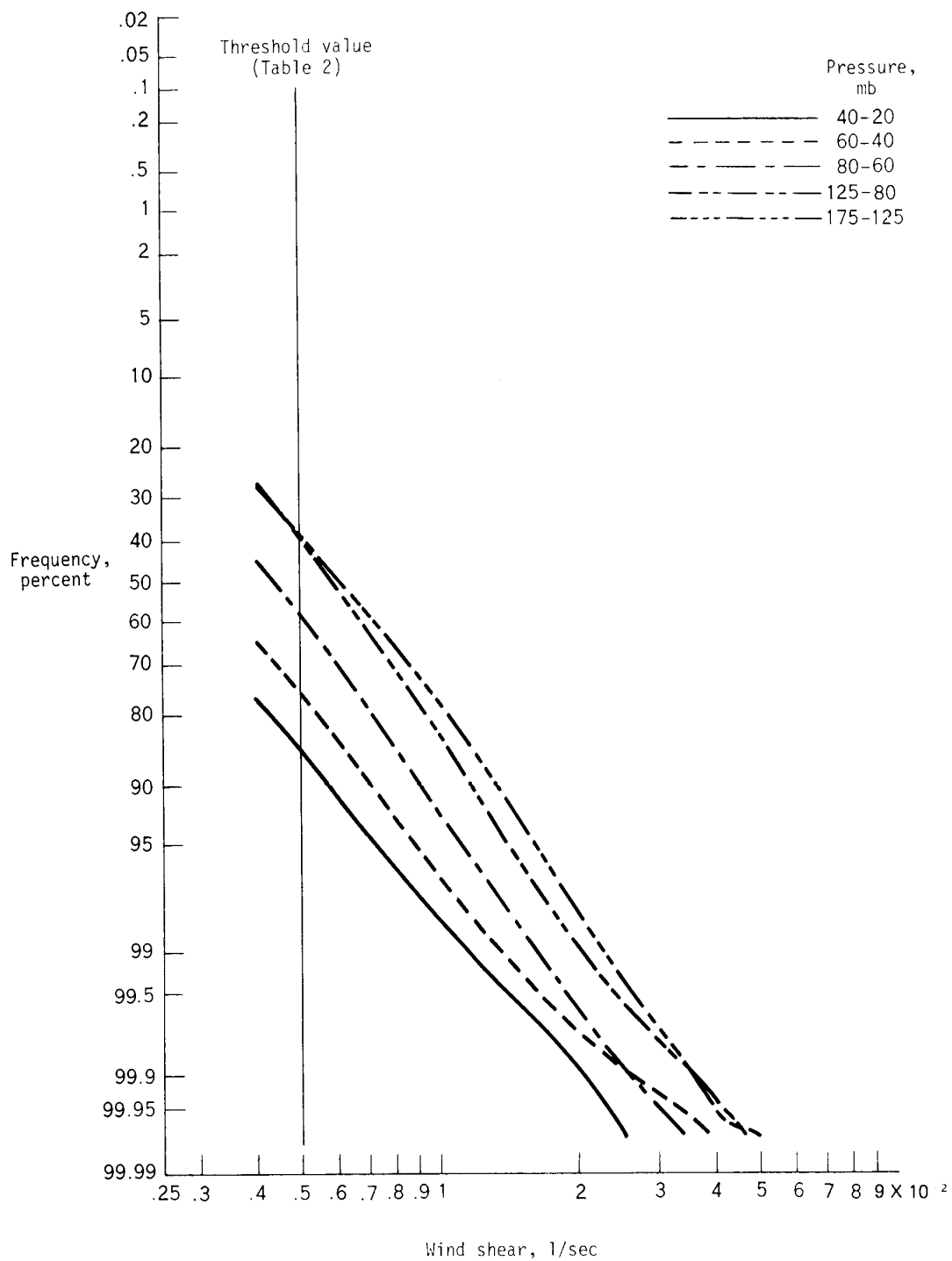
Figure 21. Annual cumulative distributions of wind shears
for indicated layers.

50
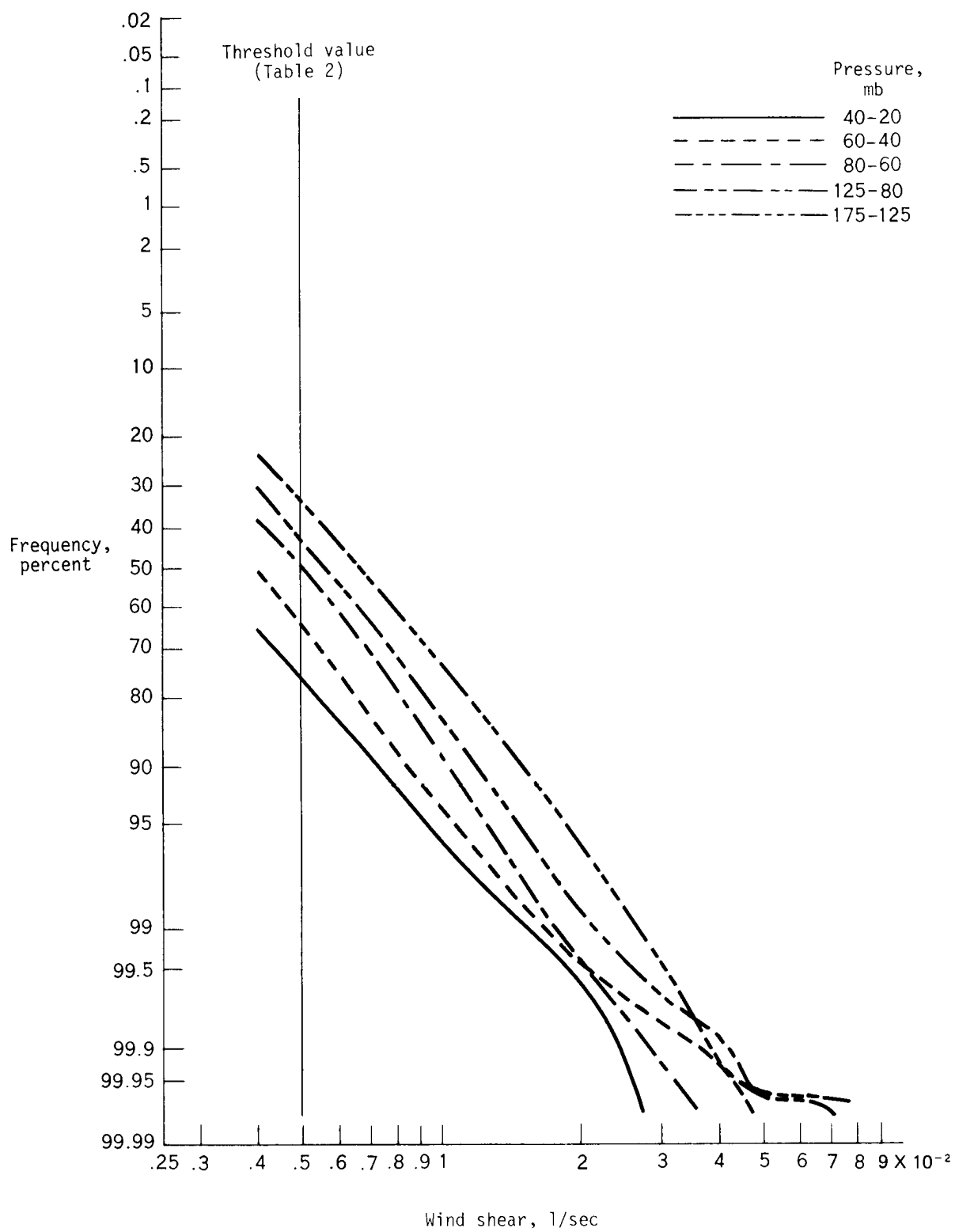
Figure 22.   Winter cumulative distributions of wind shears
for indicated layers.
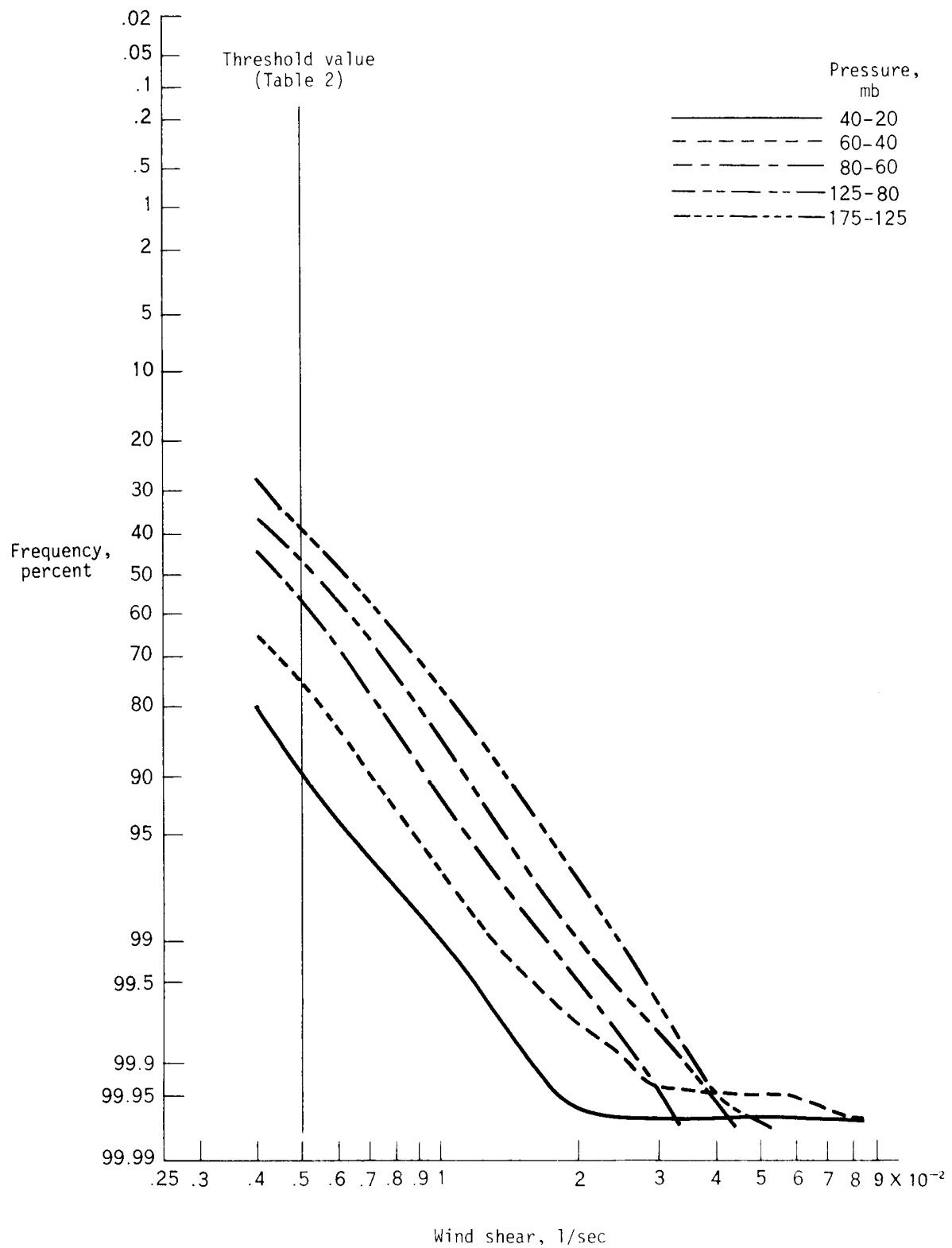
Figure 23. Spring cumulative distributions of wind shears
for indicated layers.
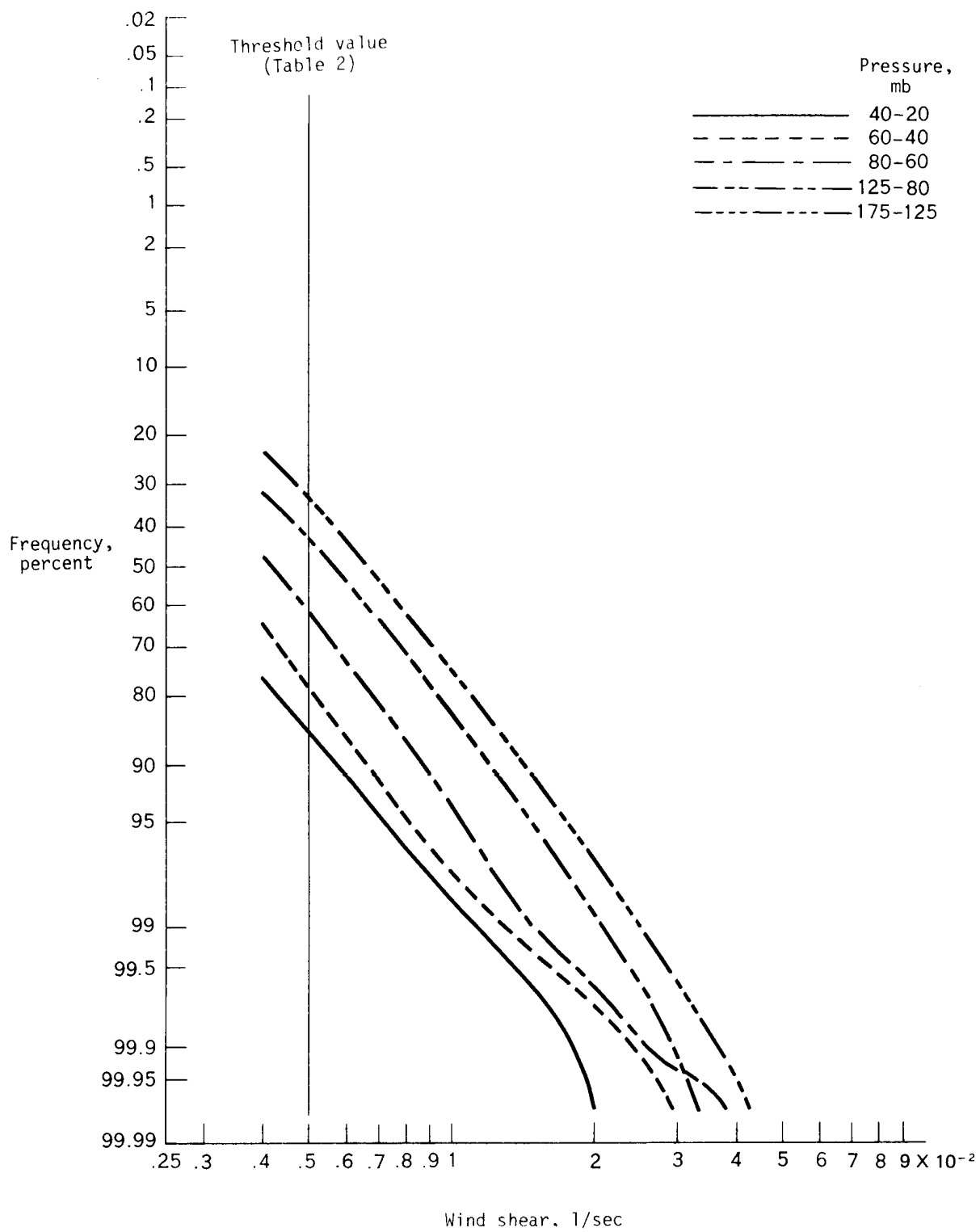
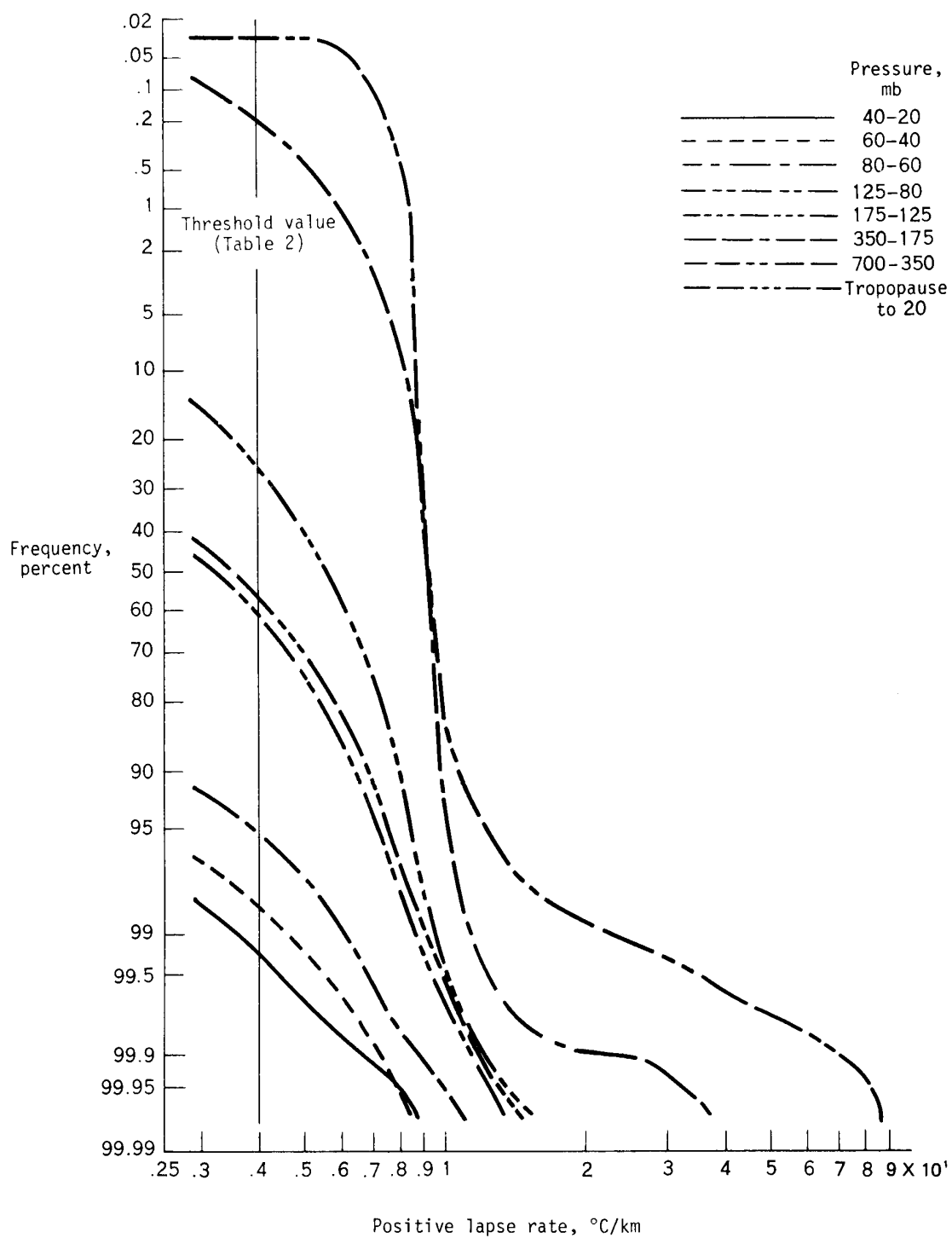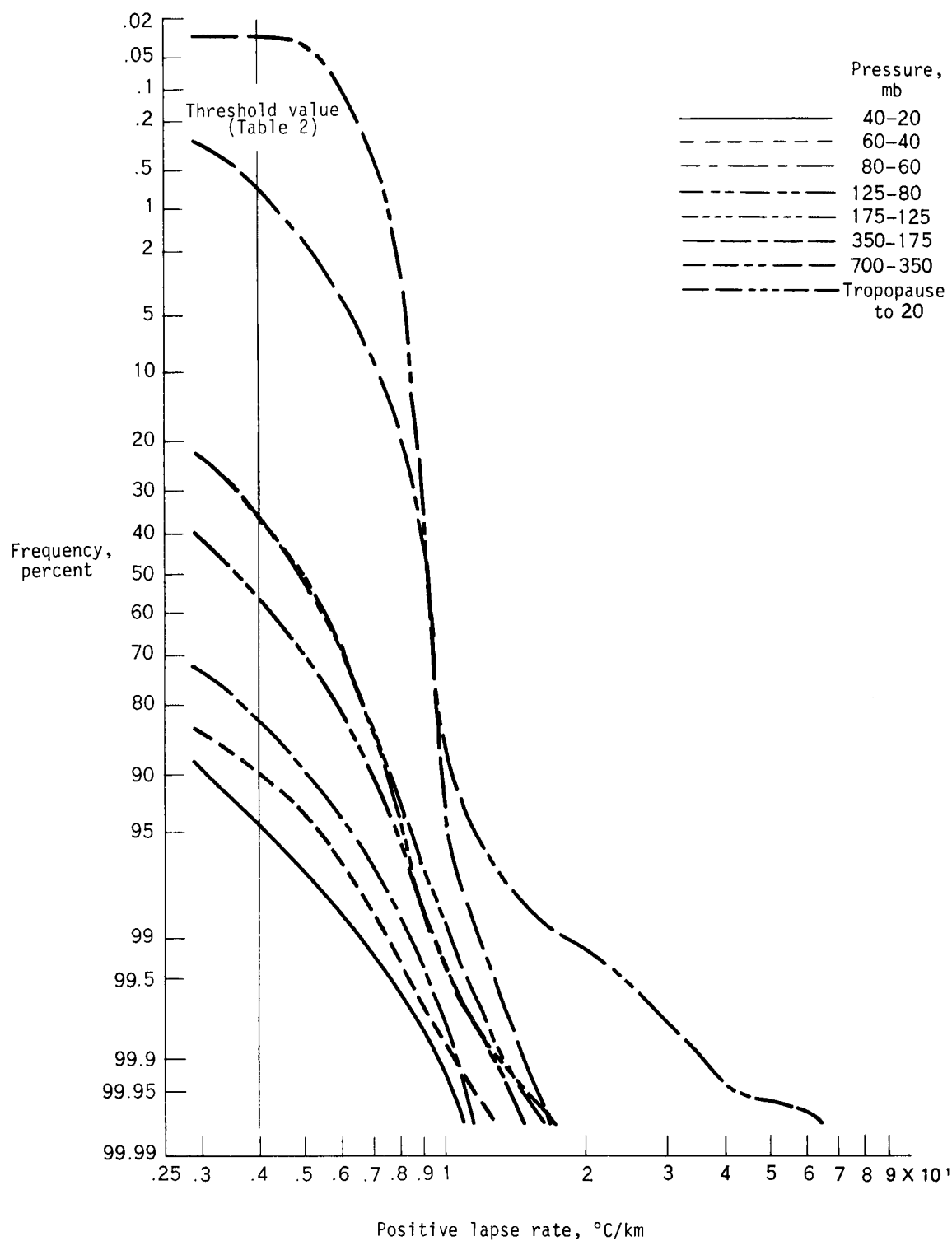Figure 25.   Fall cumulative distributions of wind shears
for indicated layers.
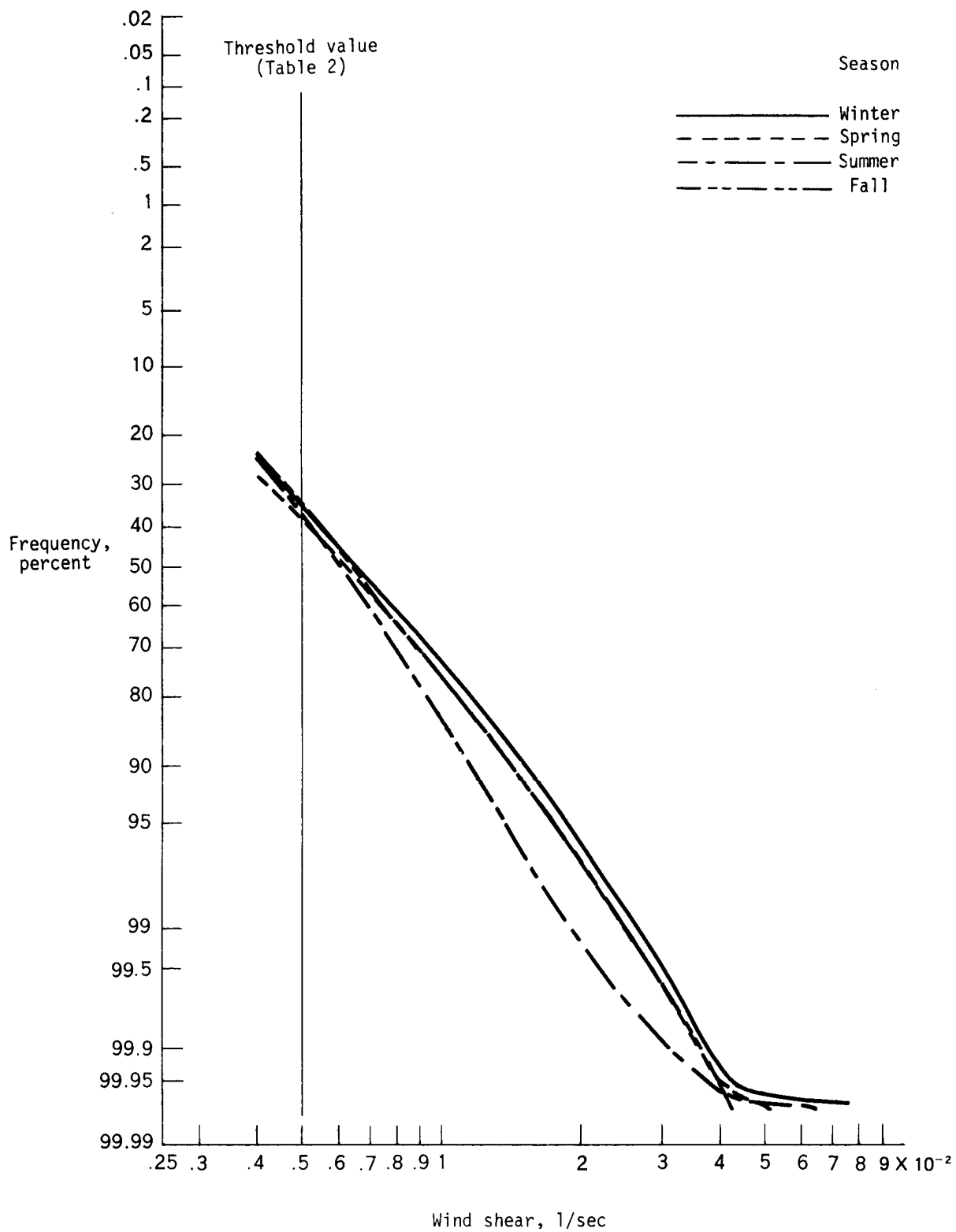
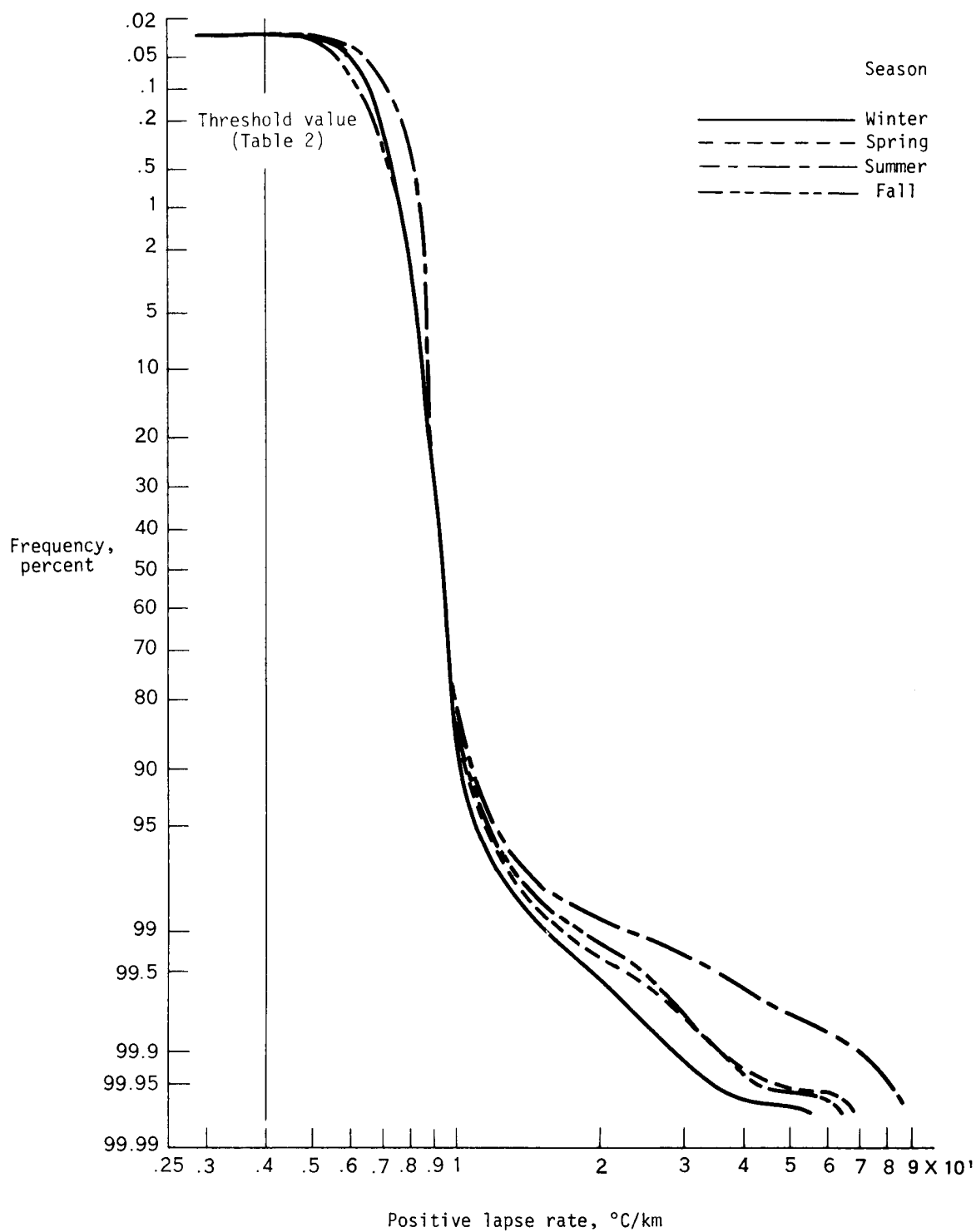Figure 26. Seasonal cumulative distributions of wind shears
for the 175-125 mb layer.
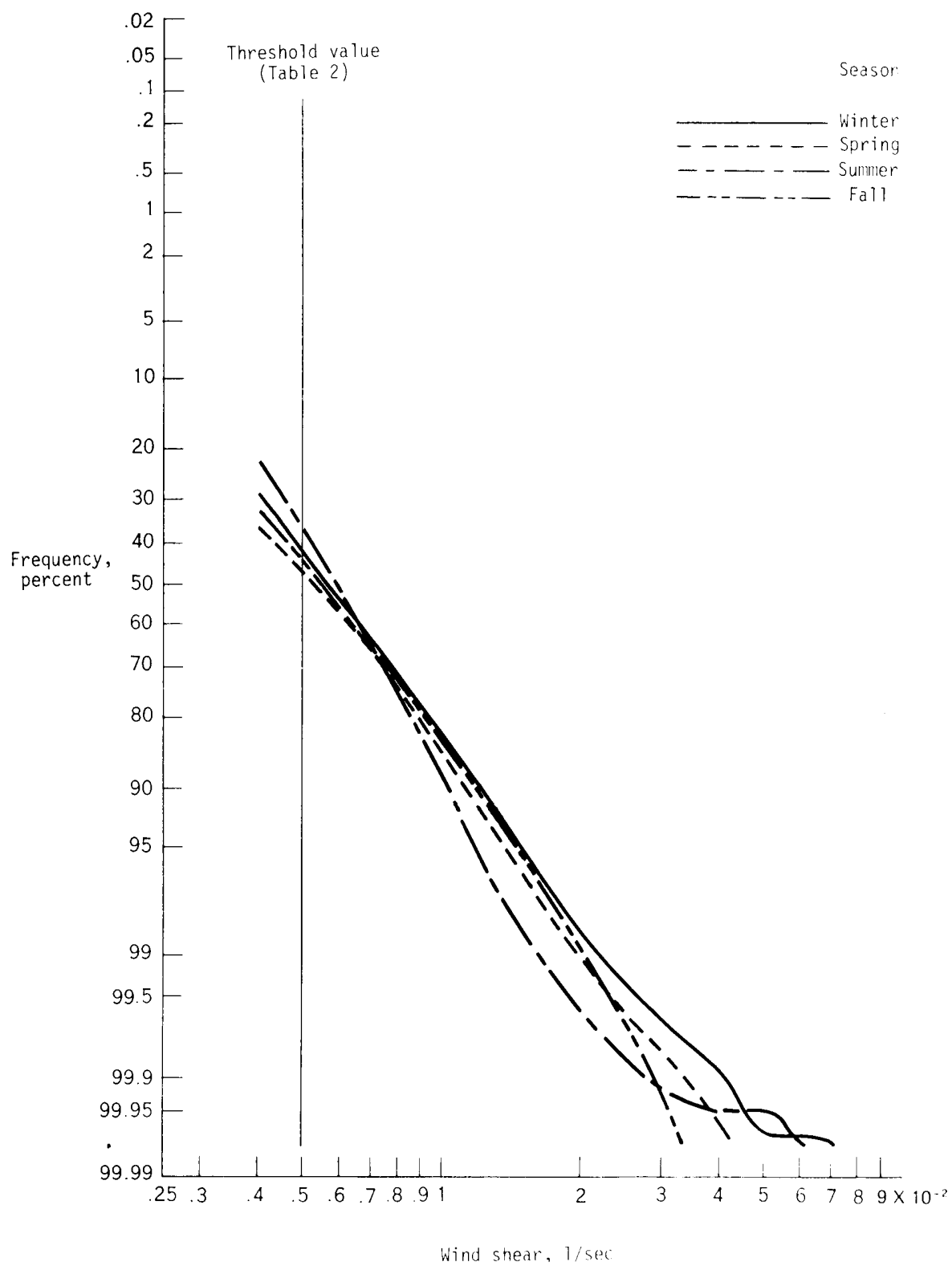
Figure 27.   Seasonal cumulative distributions of wind shears
for the 125-80 mb layer.
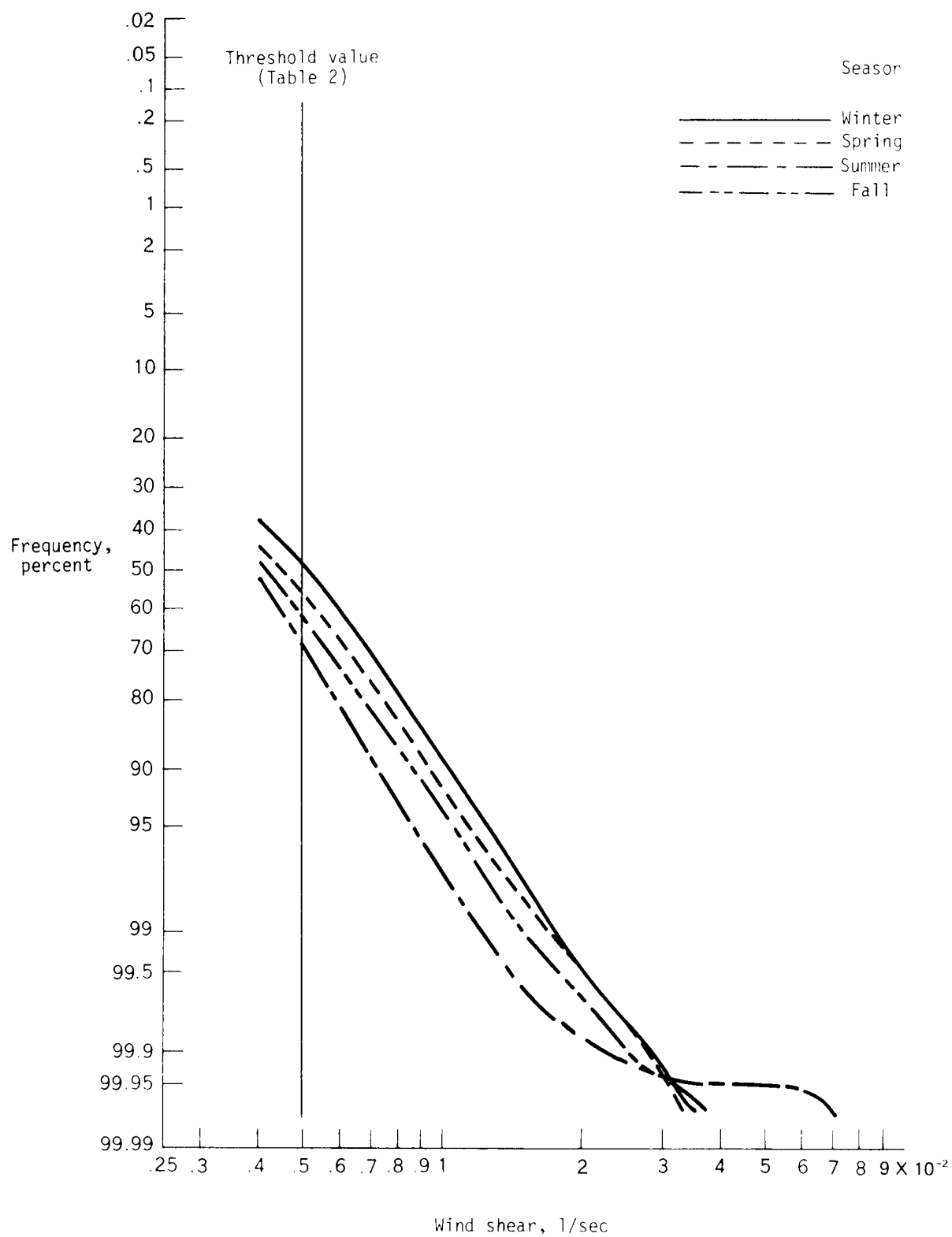
Figure 28. Seasonal cumulative distributions of wind shears
for the 80-60 mb layer.
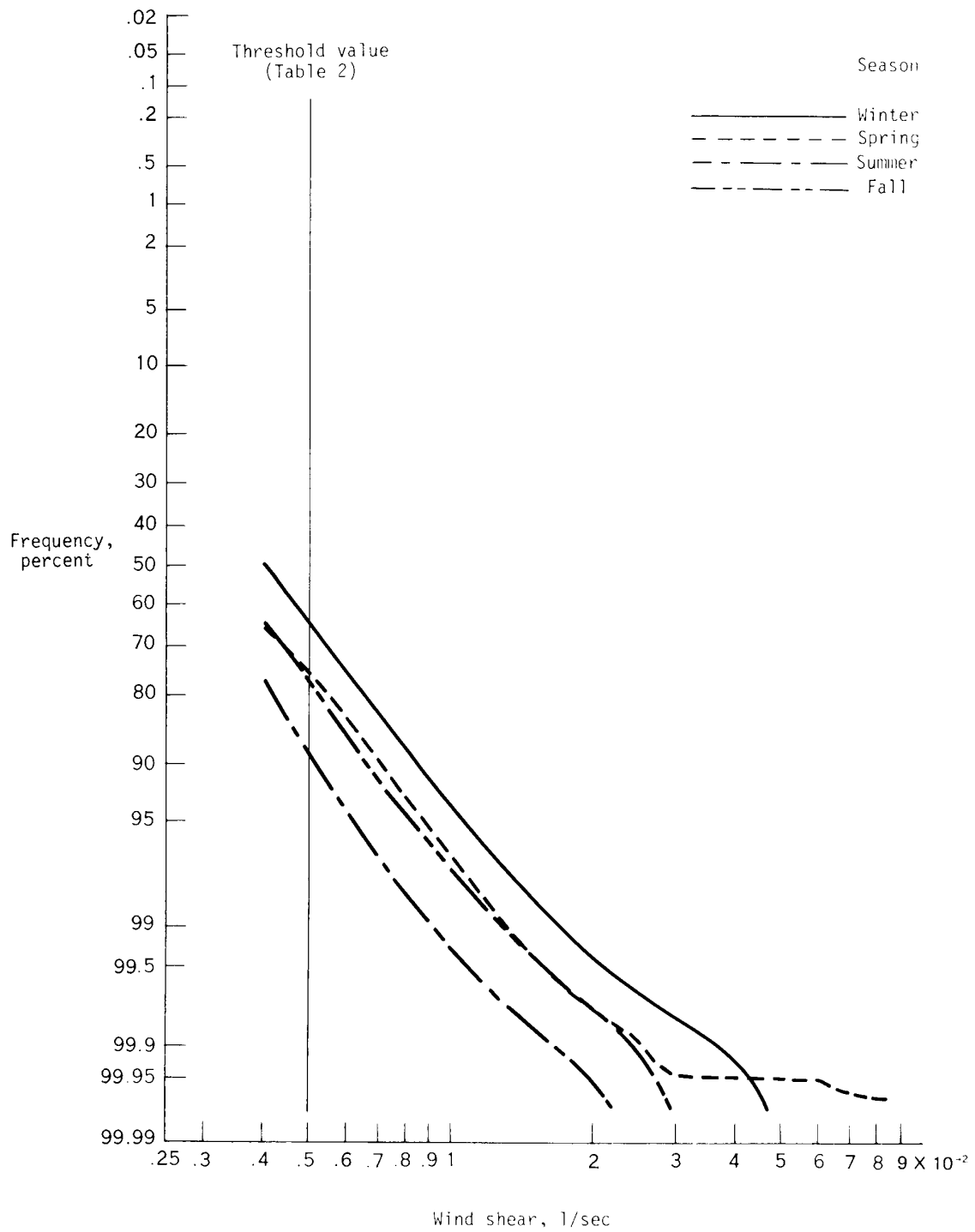
Figure 29. Seasonal cumulative distributions of wind shears
for the 60-40 mb layer.
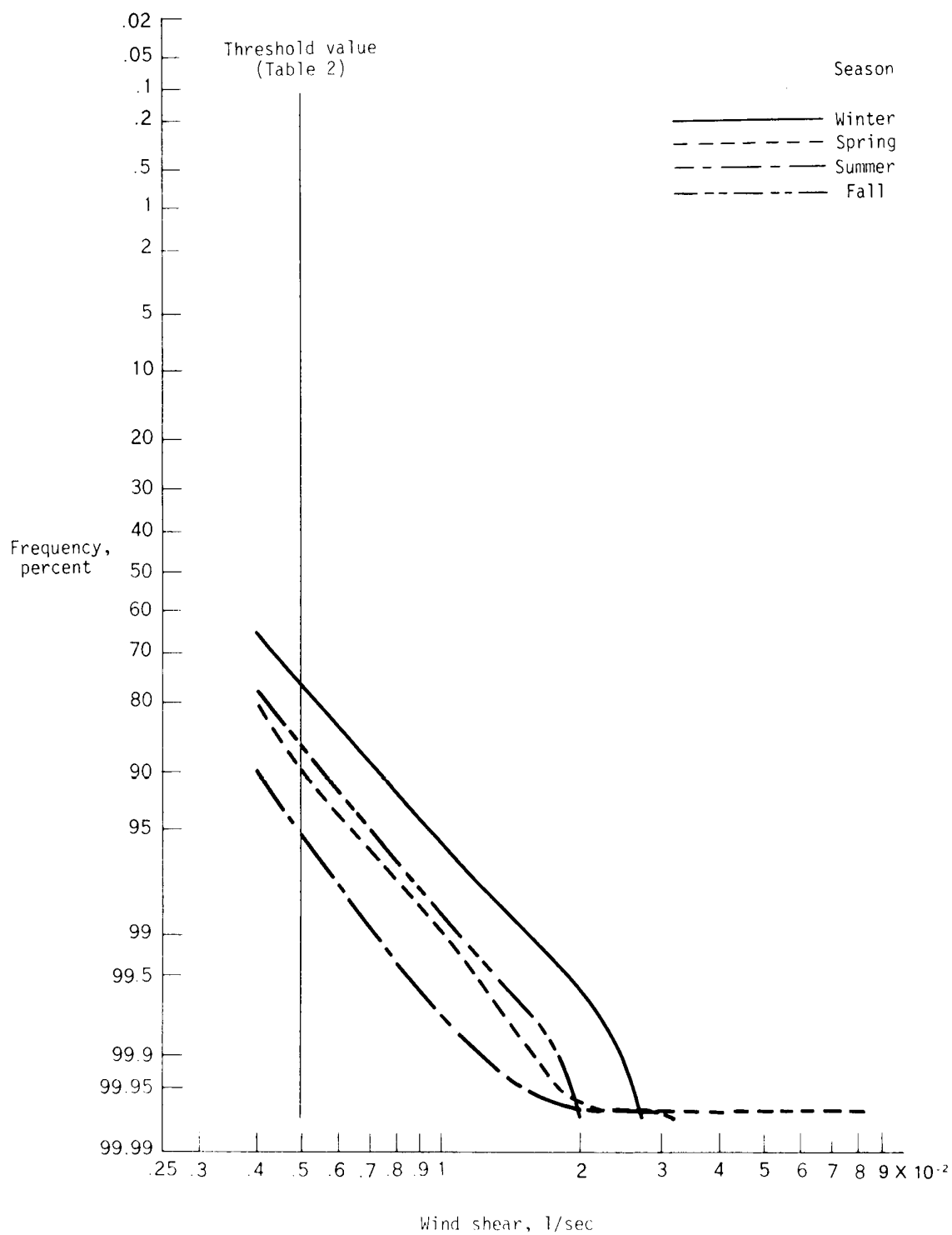
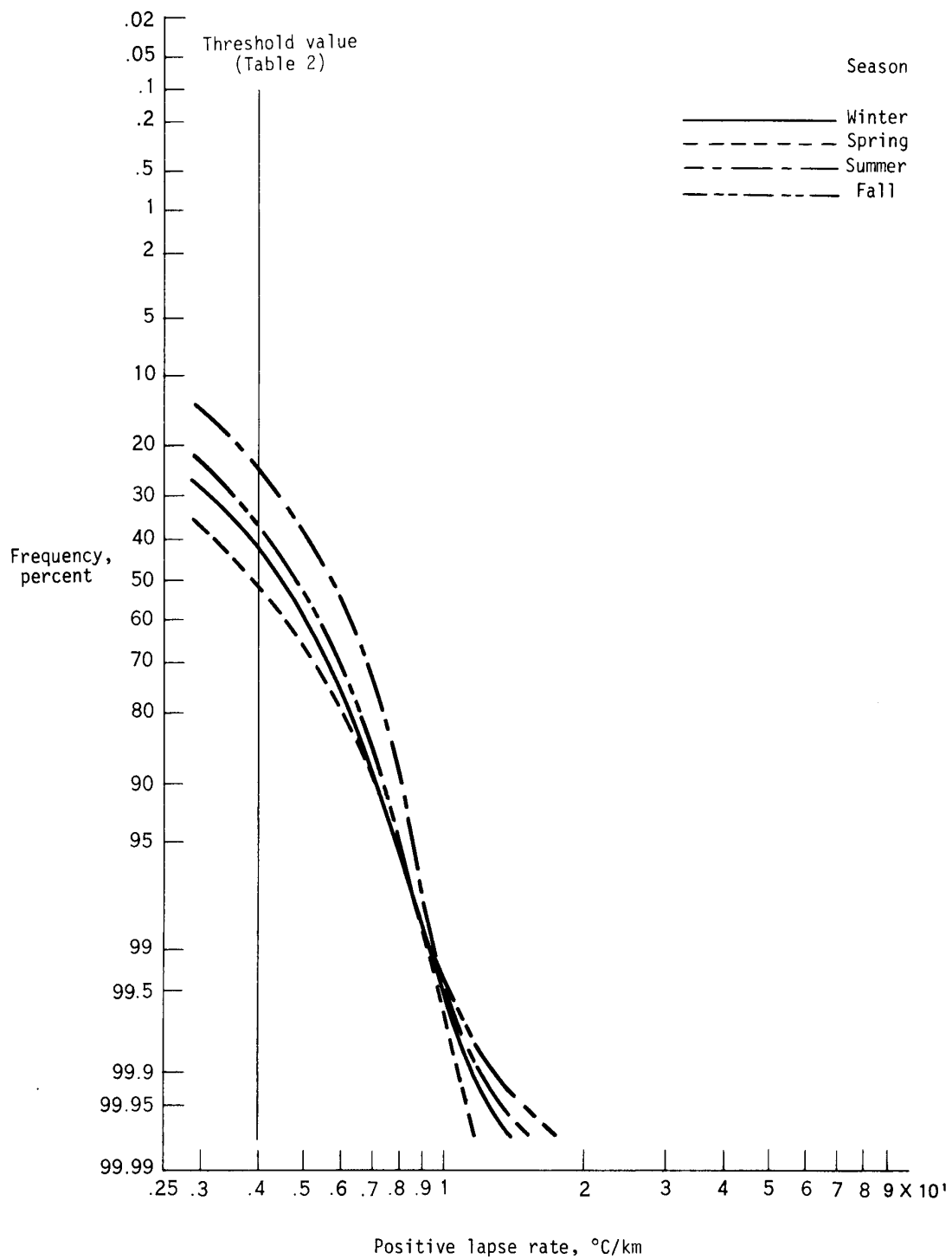Figure 30. Seasonal cumulative distributions of wind shears
for the 40-20 mb layer.
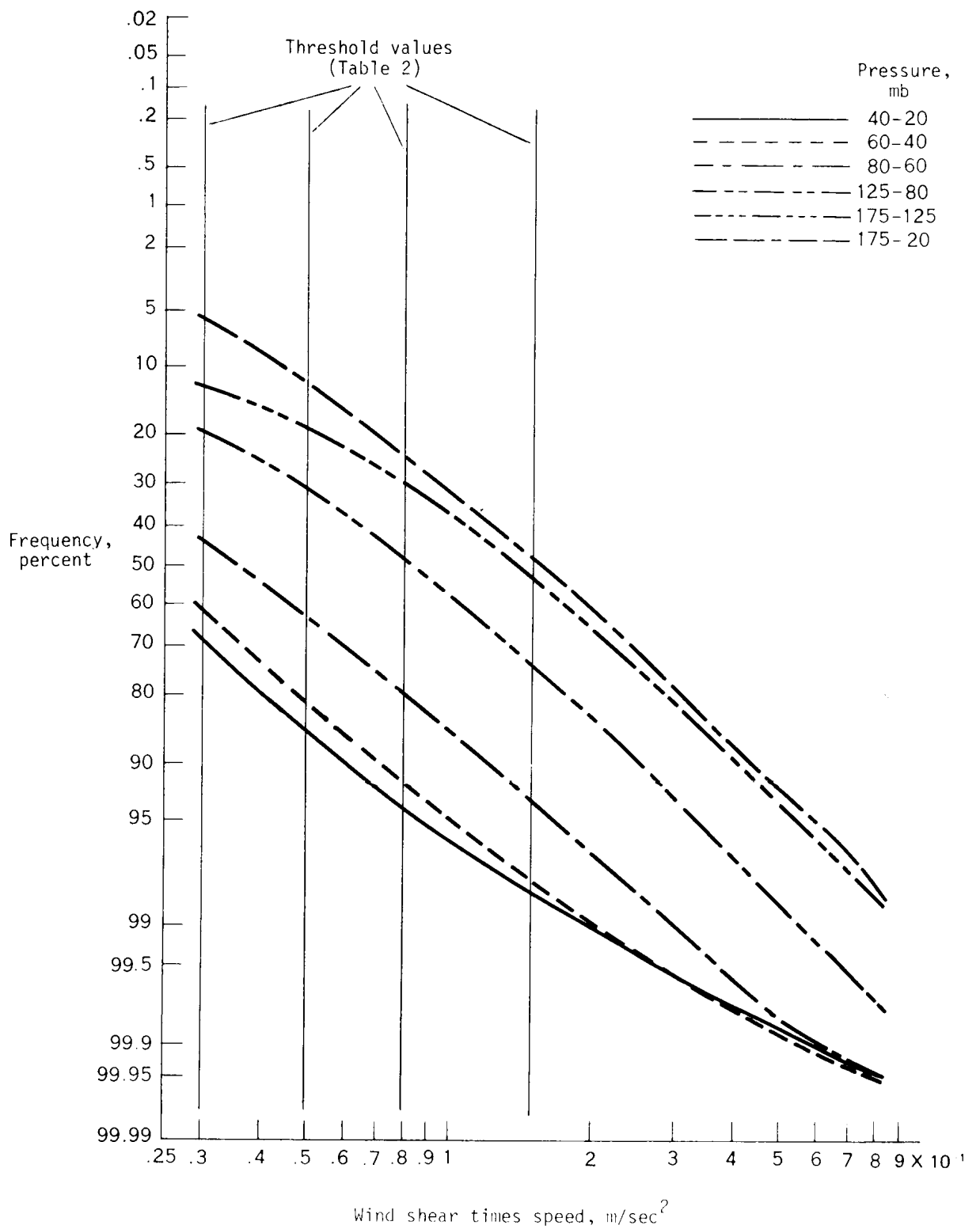
Figure 31. Annual cumulative distributions of wind shear times speed
for indicated layers.
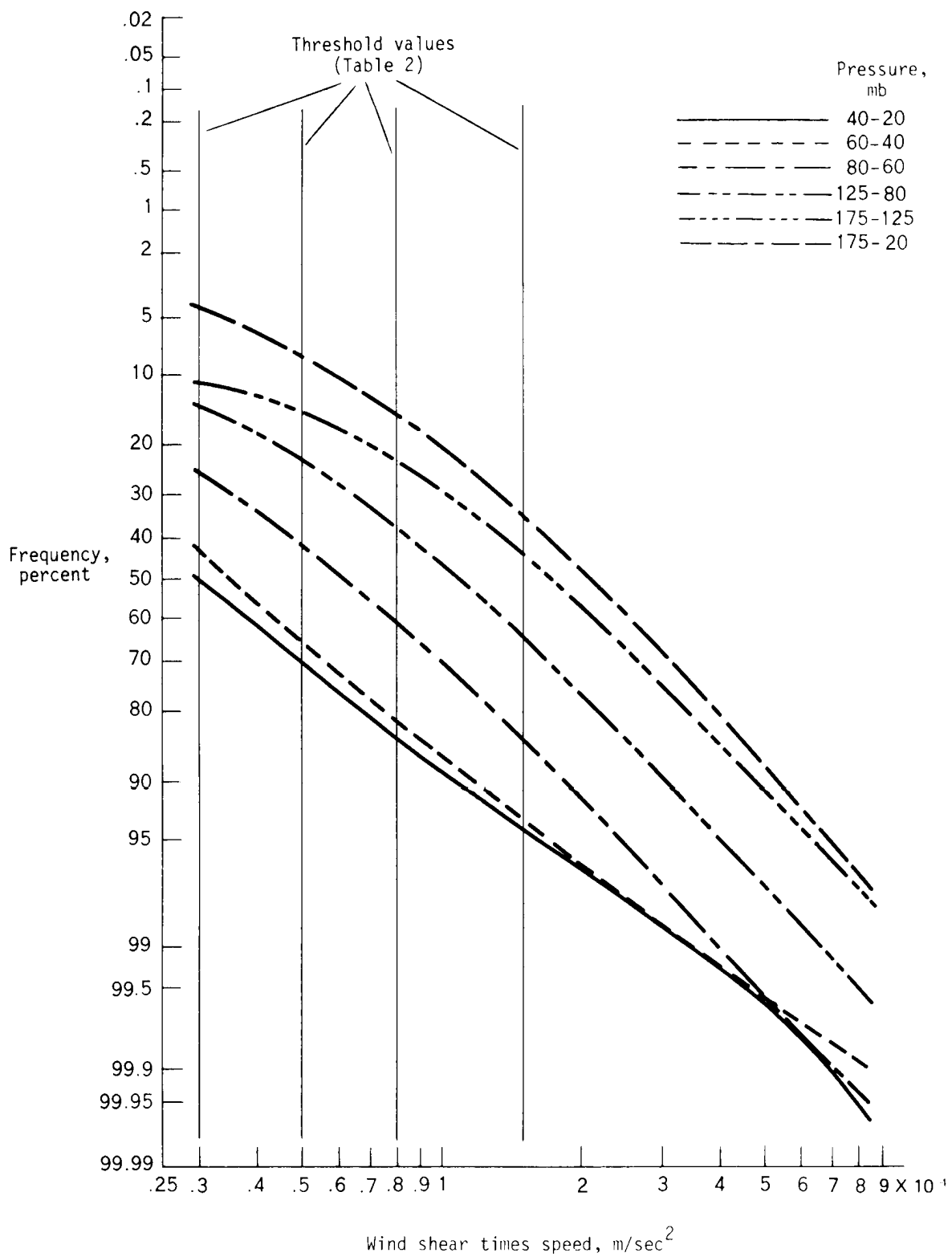
Figure 32. Winter cumulative distributions of wind shear times speed
for indicated layers.
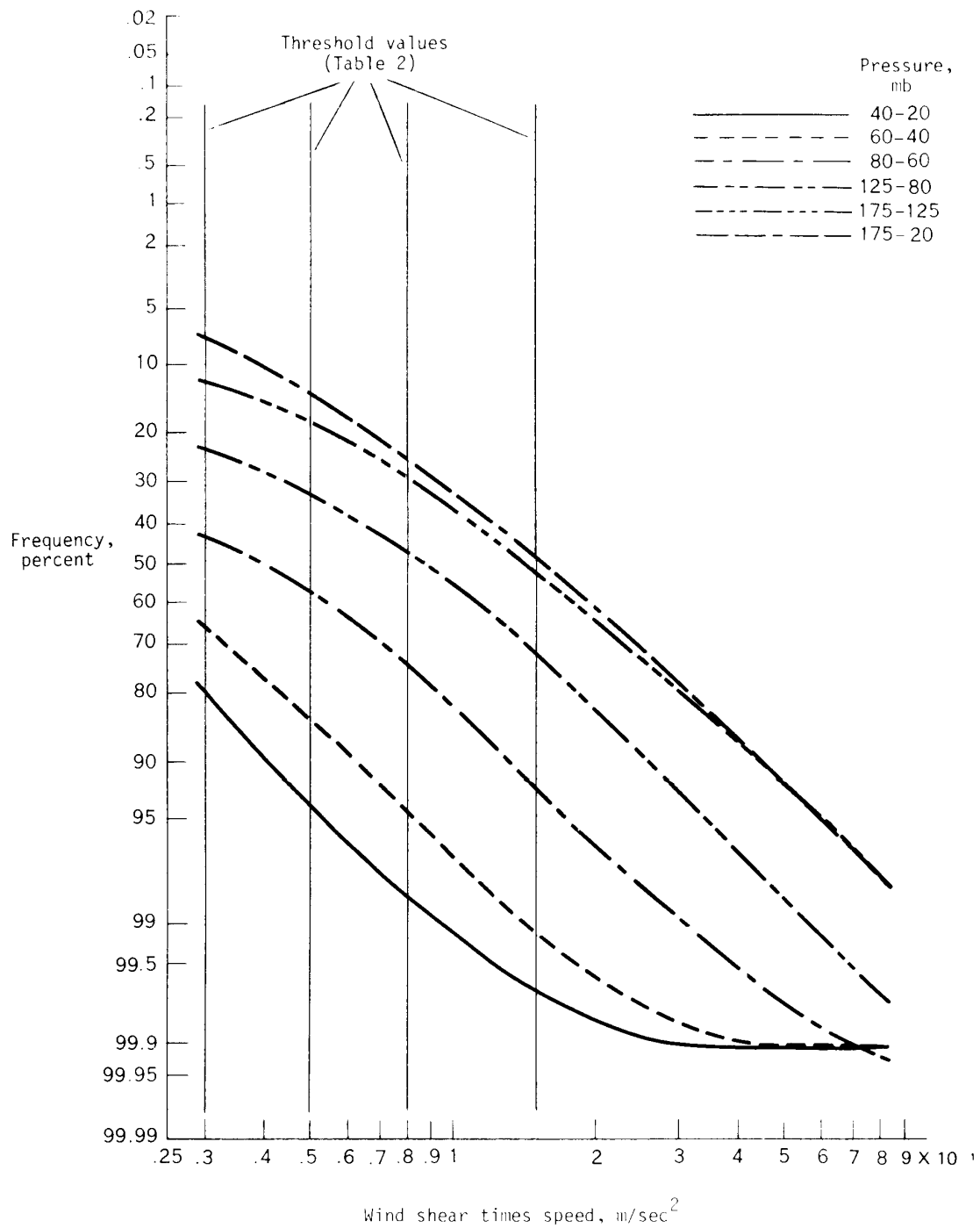
Figure 33.   Spring cumulative distributions of wind shear times speed
for indicated layers.

Figure 34. Summer cumulative distributions of wind shear times speed
for indicated layers.
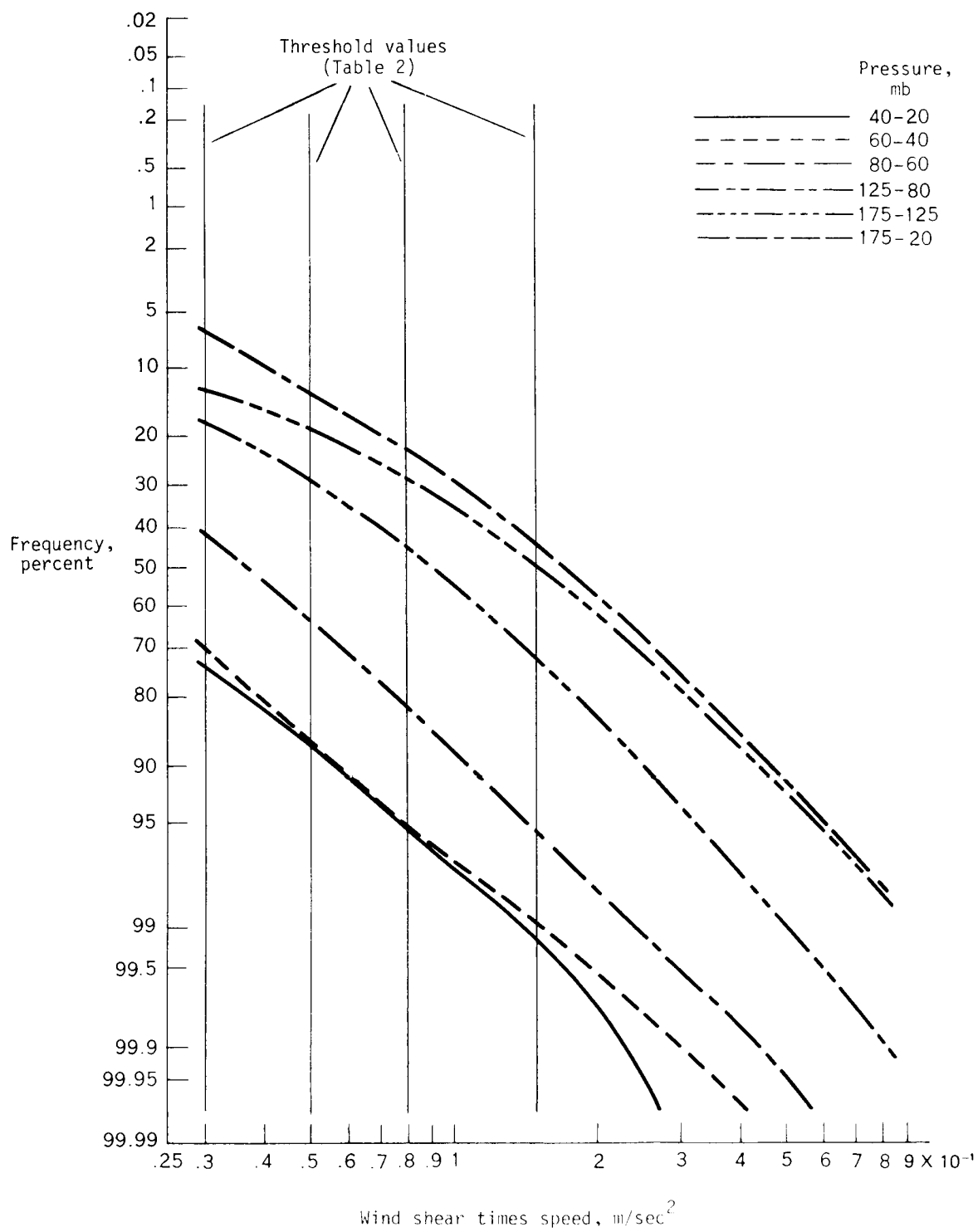
Figure 35. Fall cumulative distributions of wind shear times speed for indicated layers.
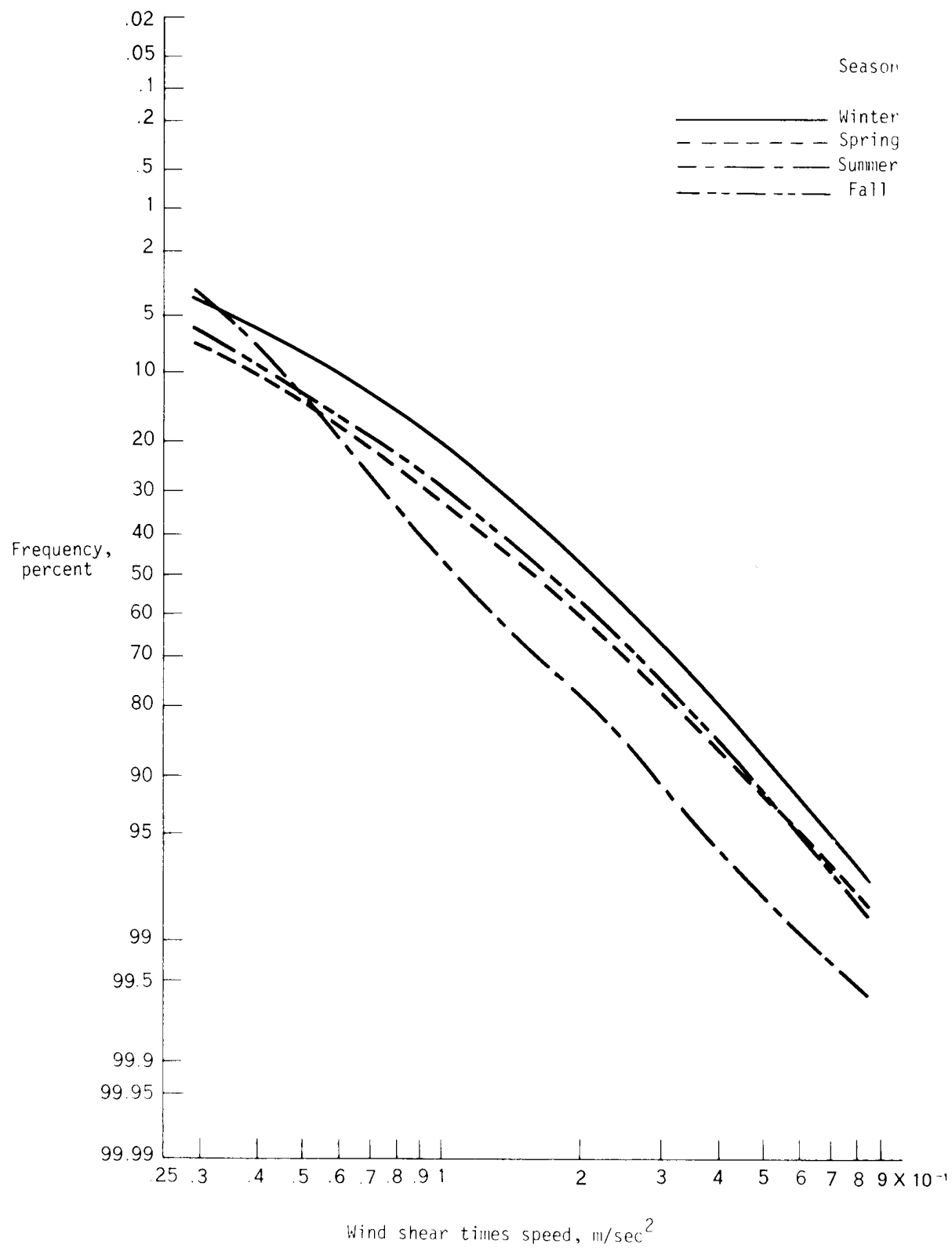
Figure 36. Seasonal cumulative distributions of wind shear times speed for the 175-20 mb layer.
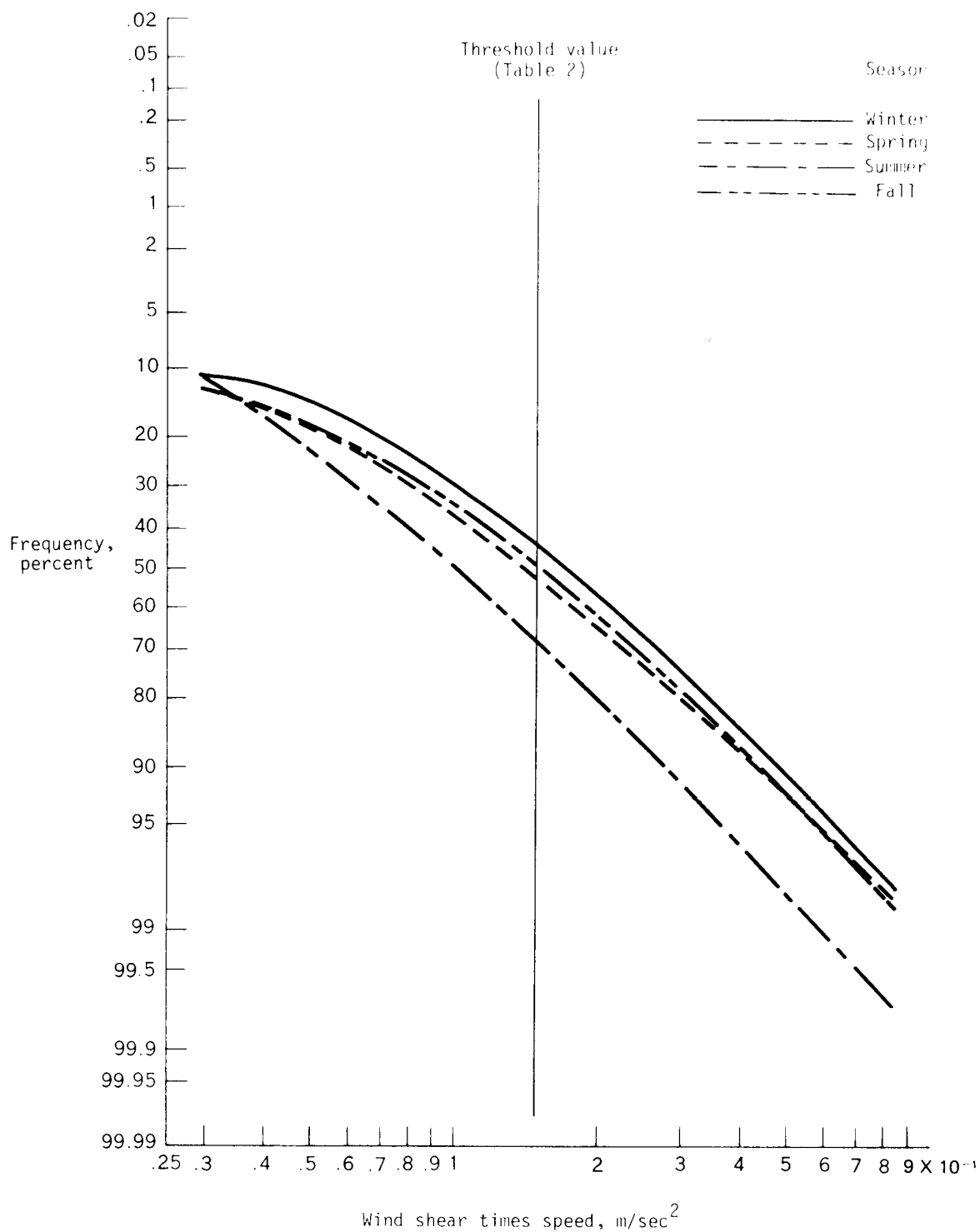
Figure 37.   Seasonal cumulative distributions of wind shear times speed
for the 175-125 mb layer.
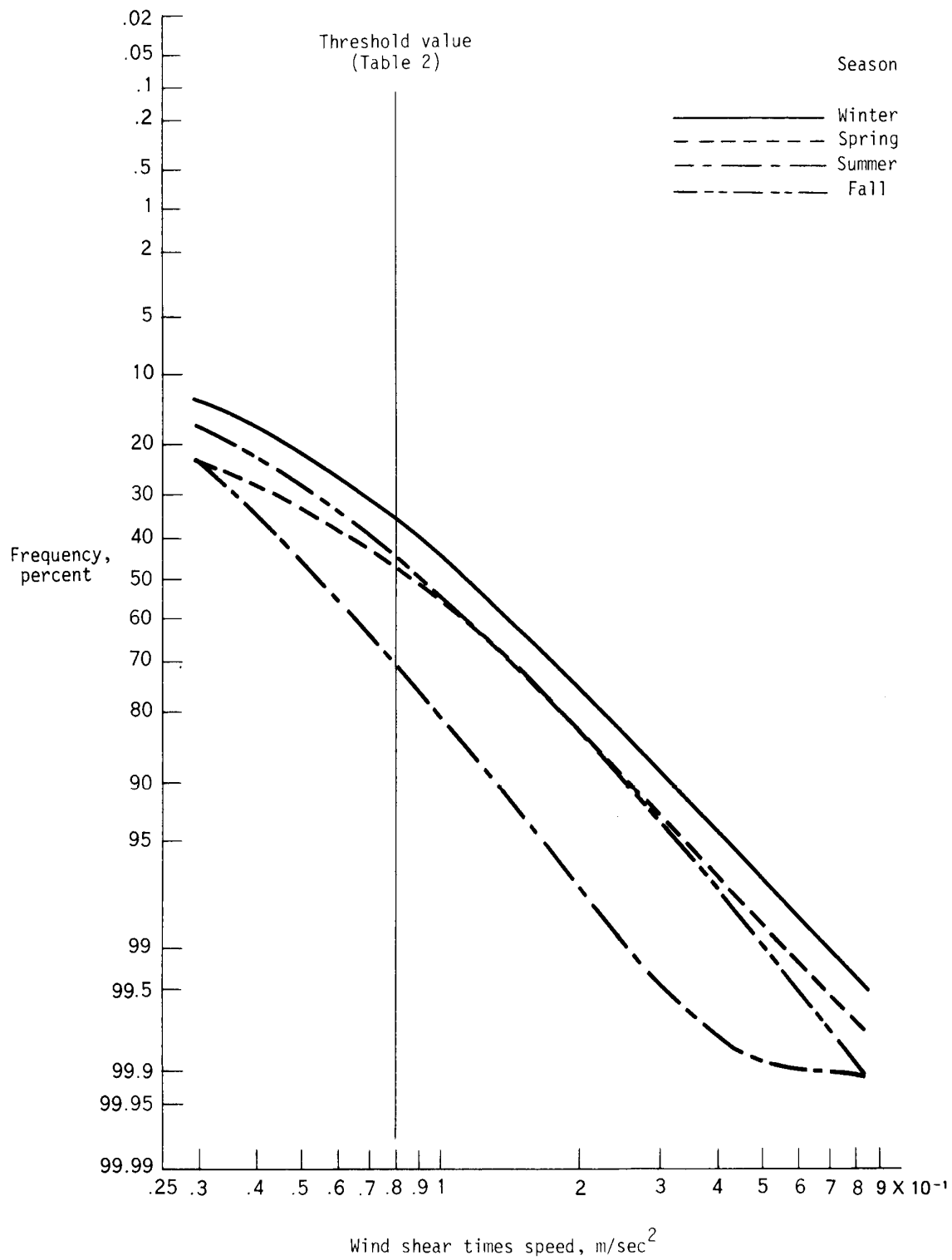
Figure 38. Seasonal cumulative distributions of wind shear times speed
for the 125-80 mb layer.
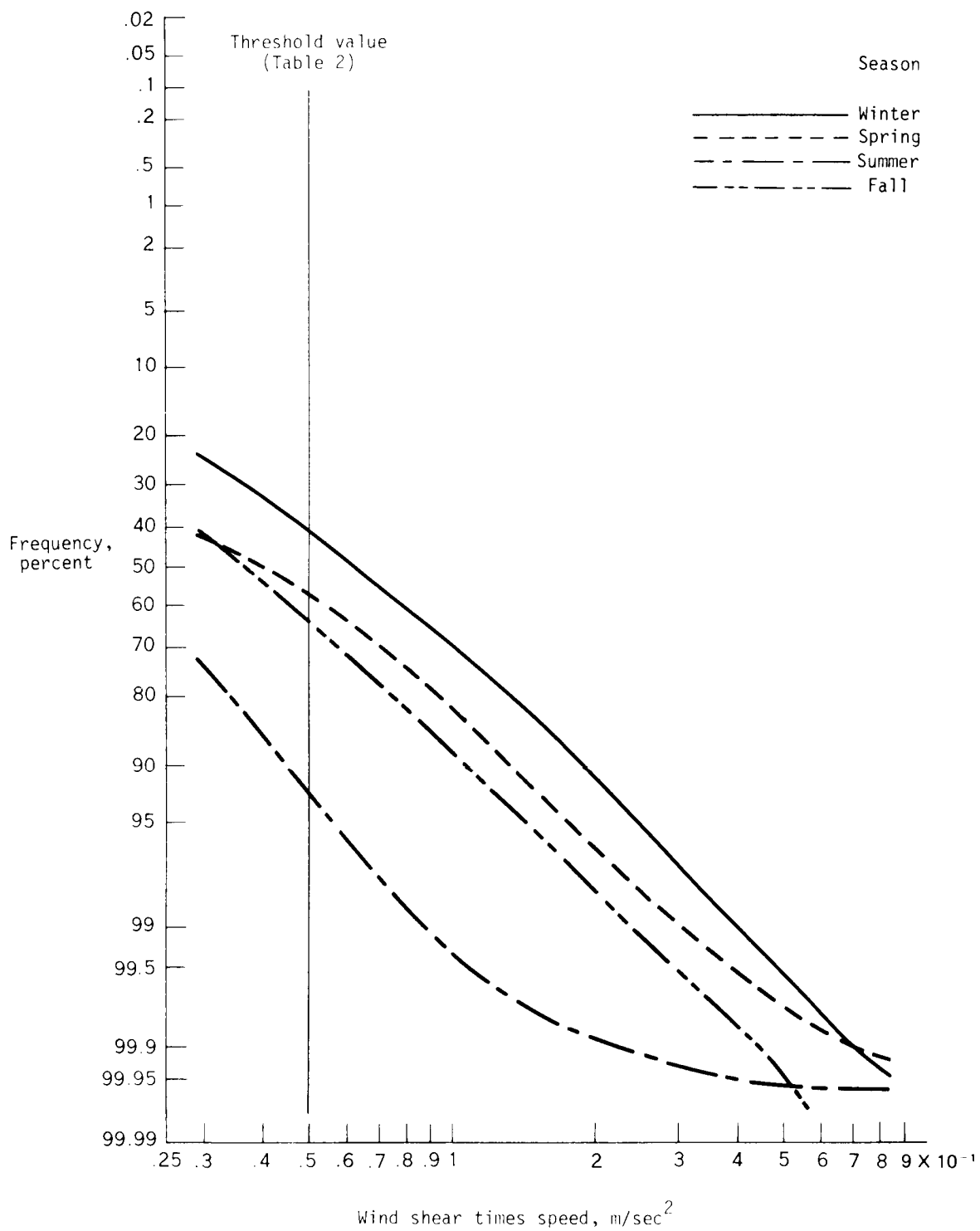
Figure 39.   Seasonal cumulative distributions of wind shear times speed
for the 80-60 mb layer.
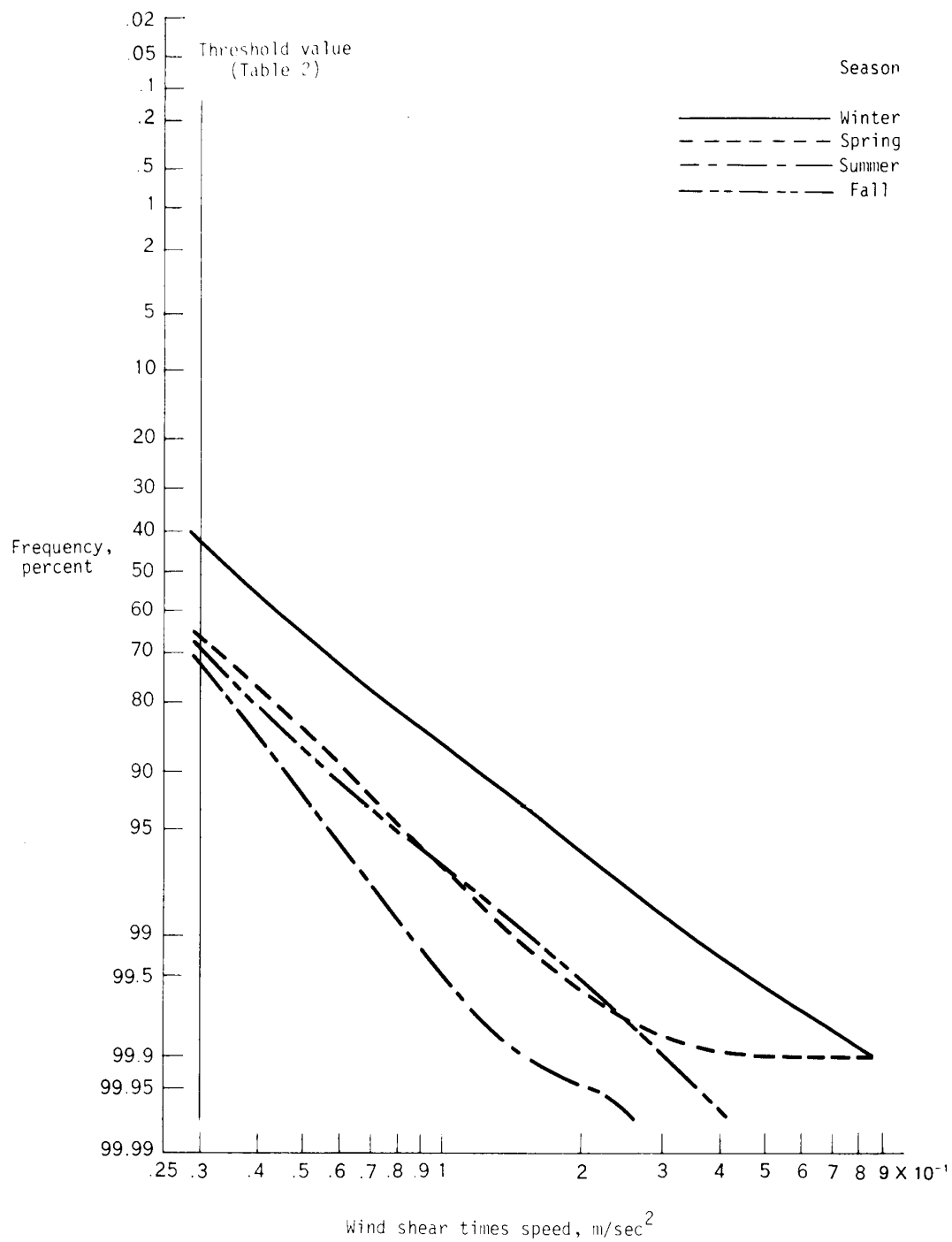
Figure 40. Seasonal cumulative distributions of wind shear times speed
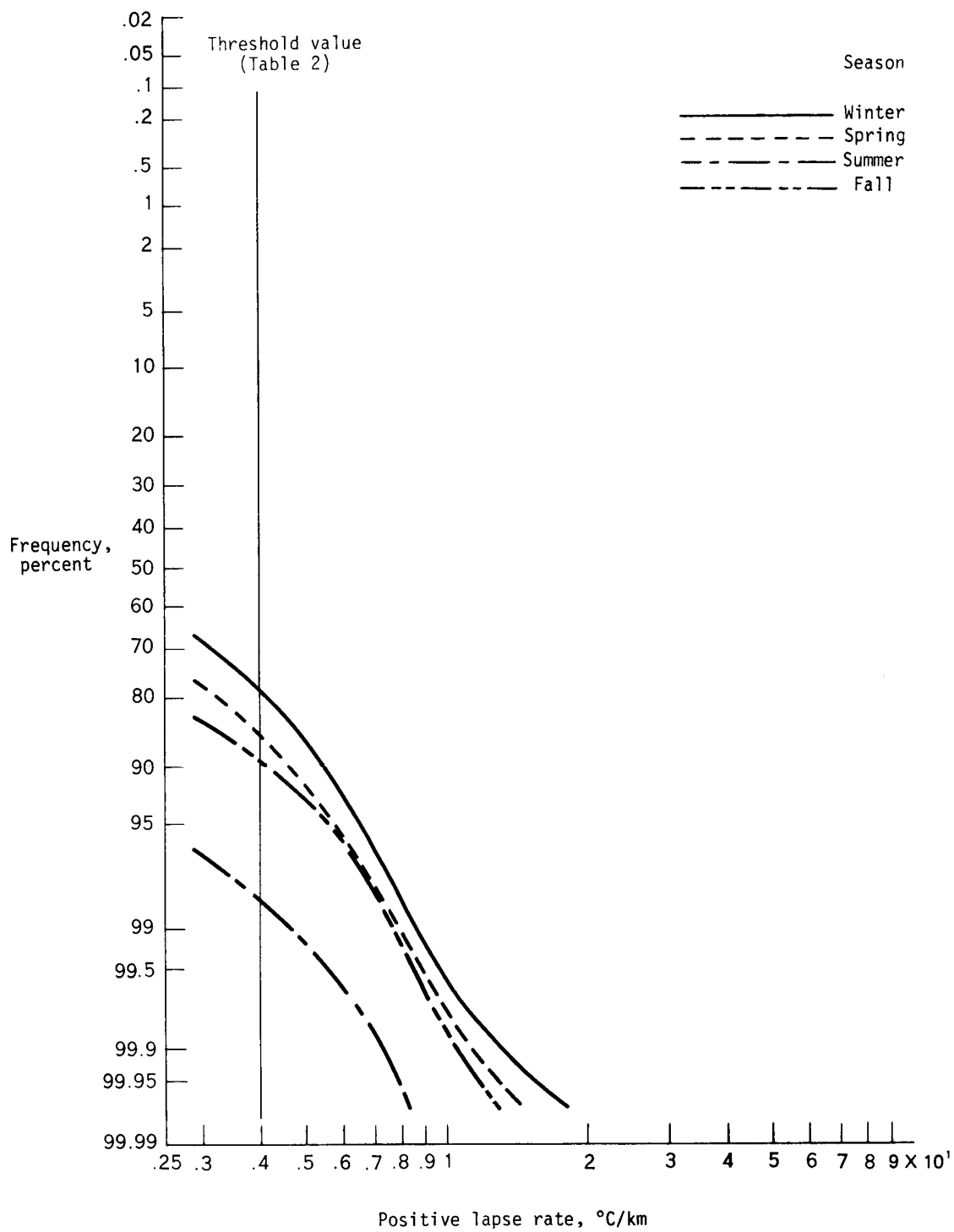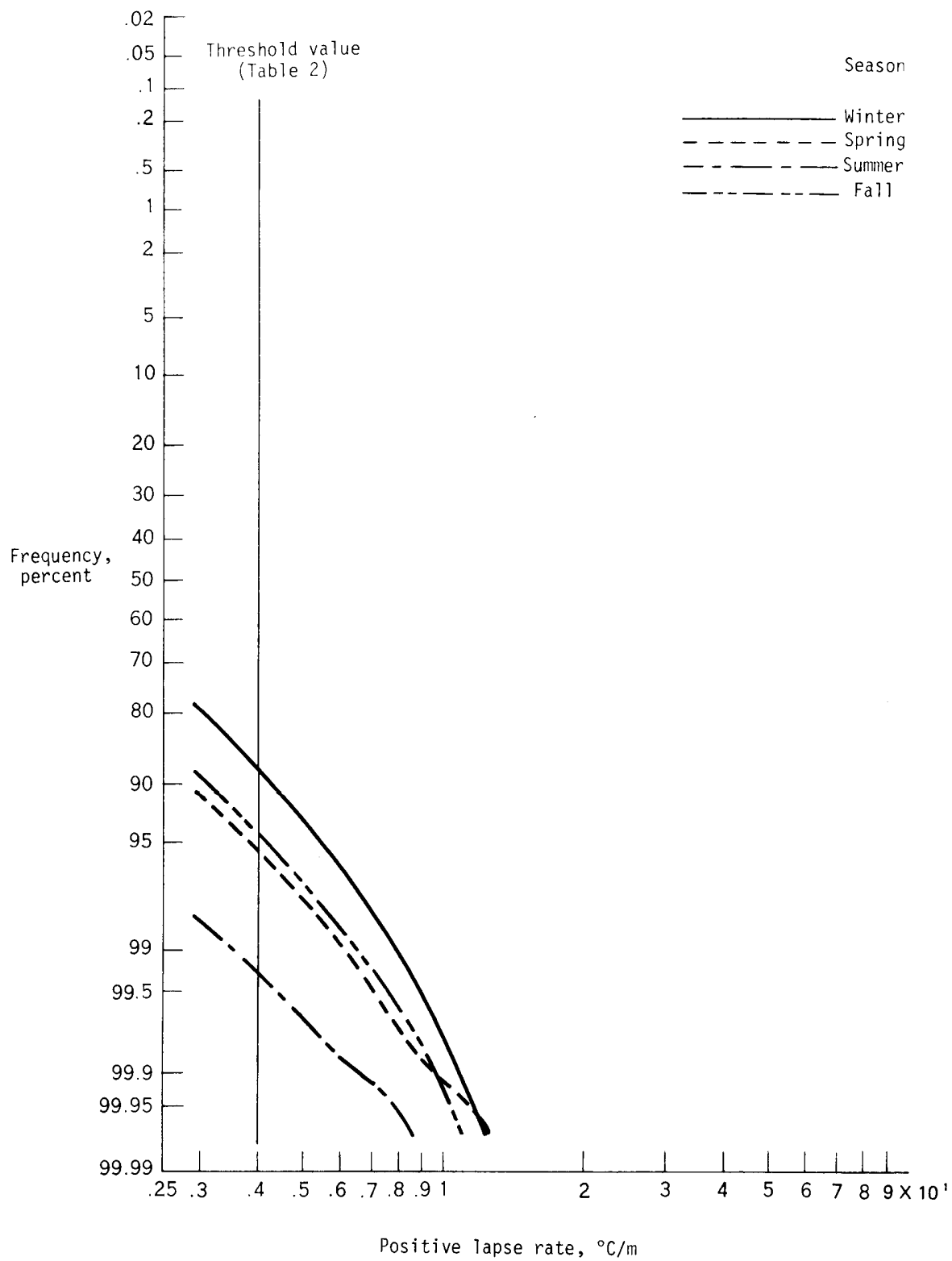for the 60-40 mb layer.
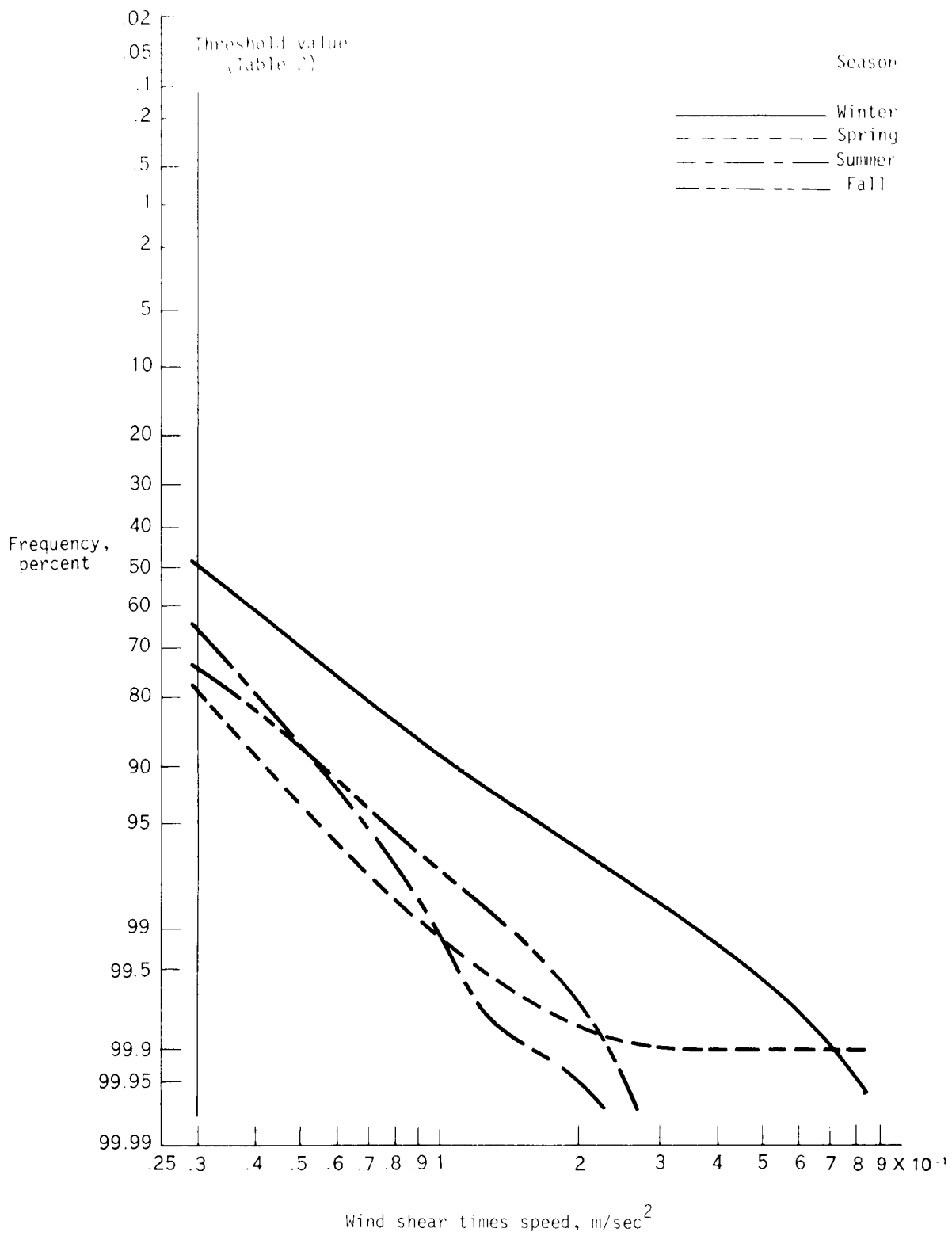
Figure 41.   Seasonal cumulative distributions of wind shear times speed
for the 40-20 mb layer.

Figure 42. Annual cumulative distributions of positive lapse rates
for indicated layers.

Figure 43. Winter cumulative distributions of positive lapse rates
for indicated layers.

Figure 44. Spring cumulative distributions of positive lapse rates
for indicated layers.

Figure 45. Summer cumulative distributions of positive lapse rates
for indicated layers.

74

Figure 46. Fall cumulative distributions of positive lapse rates
for indicated layers.

Figure 47.   Seasonal cumulative distributions of positive lapse rates
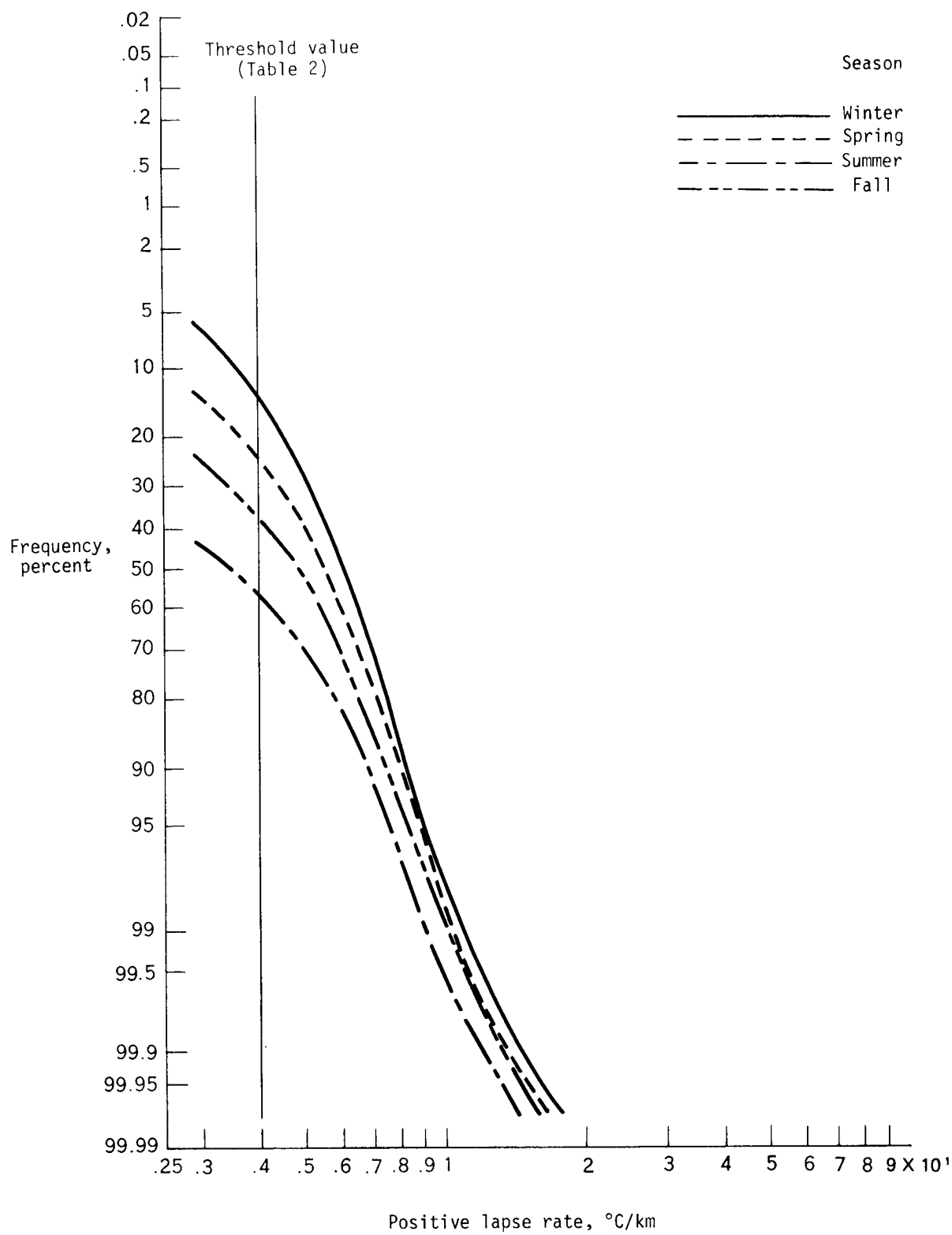for the 700-350 mb layer.
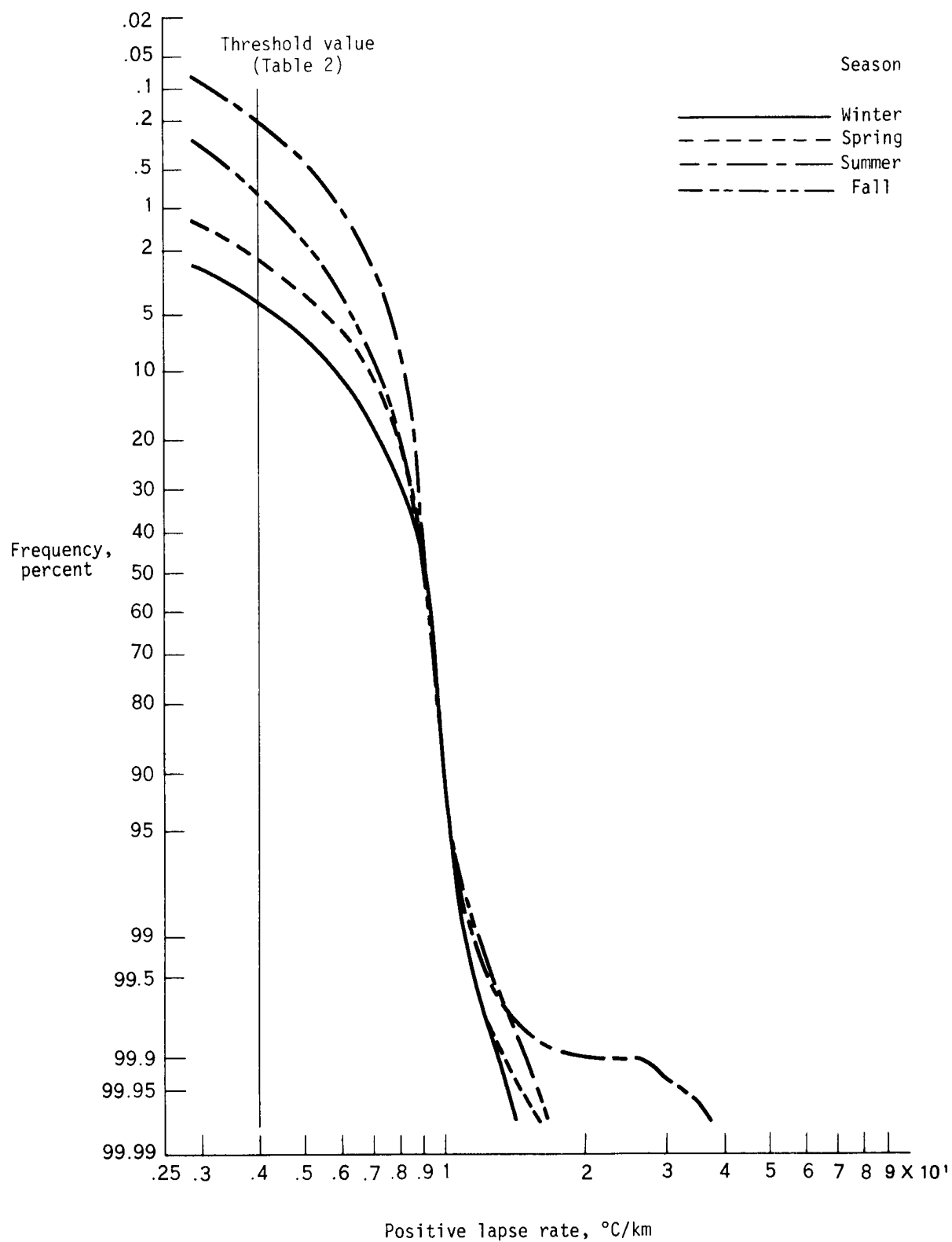
Figure 48. Seasonal cumulative distributions of positive lapse rates
for the 350-175 mb layer.

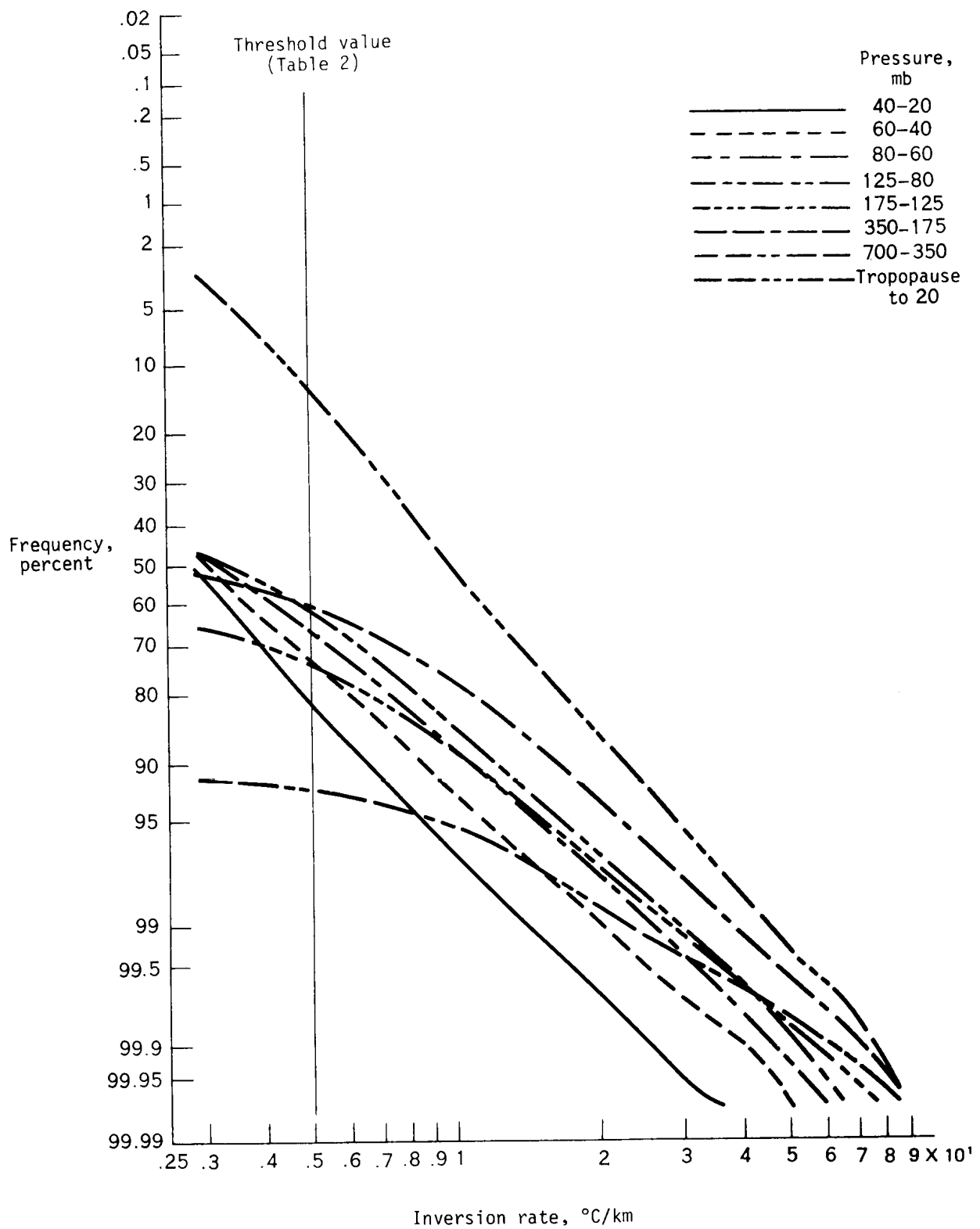Figure 49. Seasonal cumulative distributions of positive lapse rates
for the 175-125 mb layer.
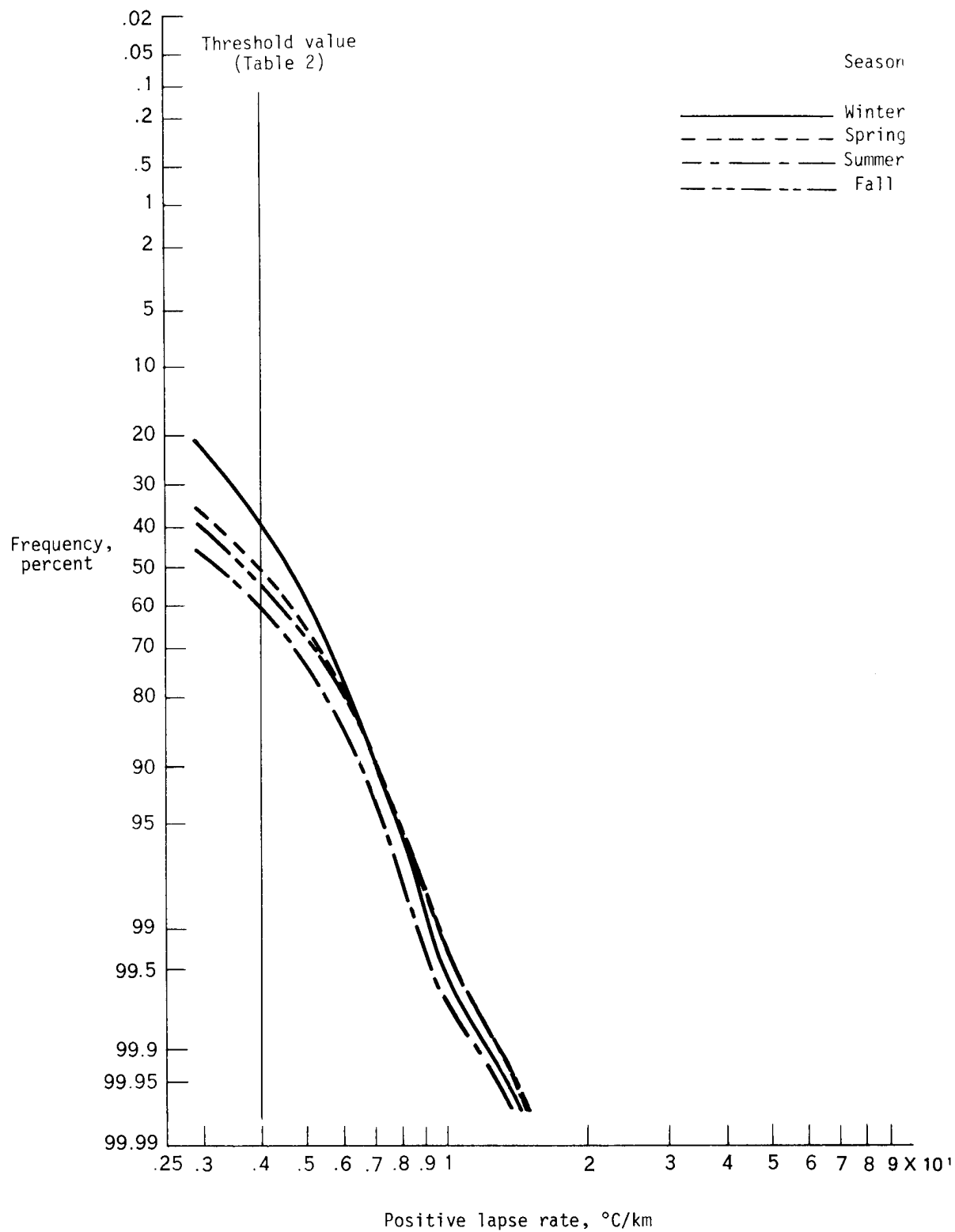
Figure 50.   Seasonal cumulative distributions of positive lapse rates
for the 125-80 mb layer.
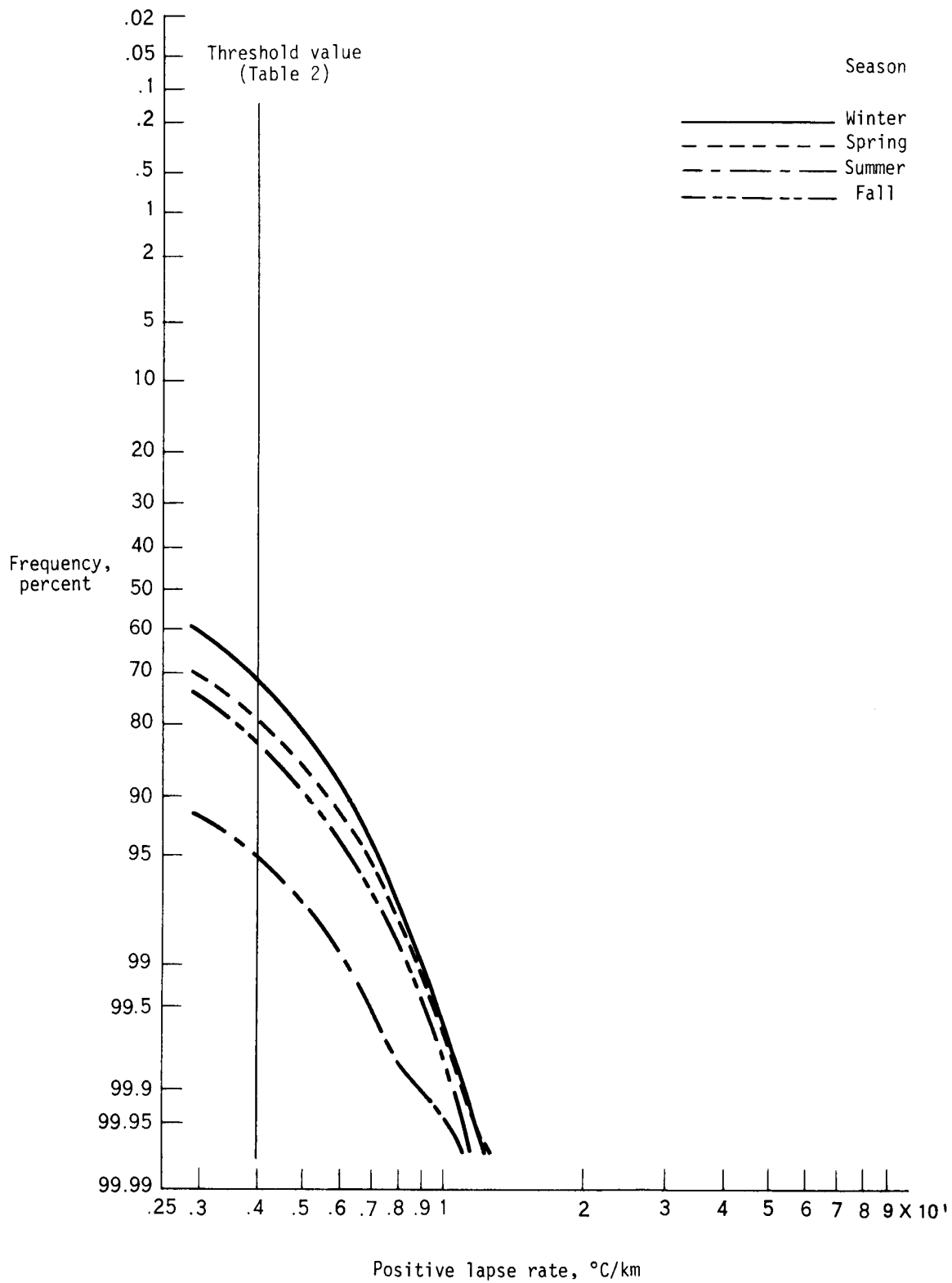
Figure 51. Seasonal cumulative distributions of positive lapse rates
for the 80-60 mb layer.

Figure 52. Seasonal cumulative distributions of positive lapse rates
for the 60-40 mb layer.

Figure 53. Seasonal cumulative distributions of positive lapse rates
for the 40-20 mb layer.

Figure 54. Seasonal cumulative distributions of positive lapse rates for the tropopause-20 mb layer

Figure 55. Annual cumulative distributions of inversion rates
(negative lapse rates) for indicated layers
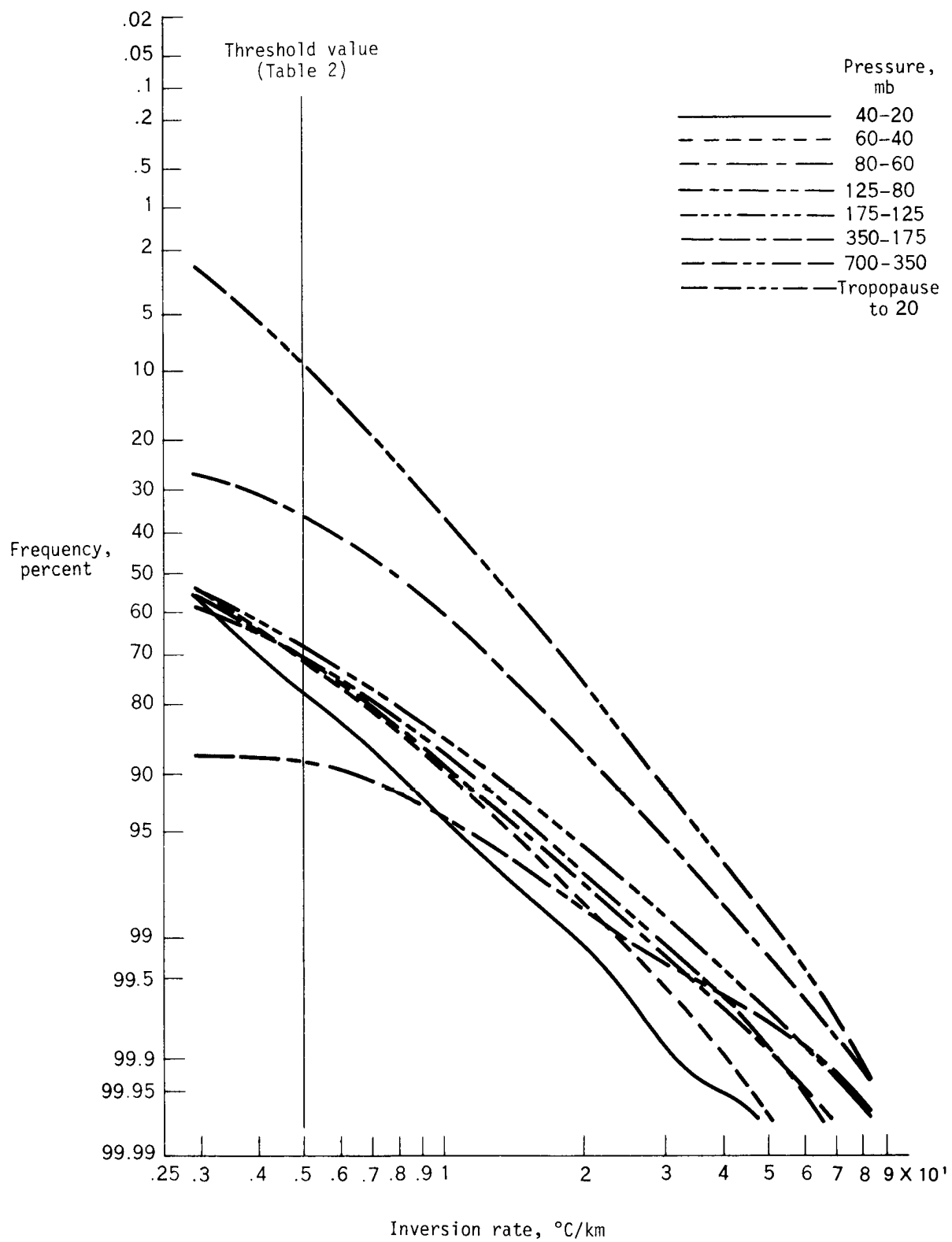
Figure 56. Winter cumulative distributions of inversion rates (negative lapse rates) for indicated layers.
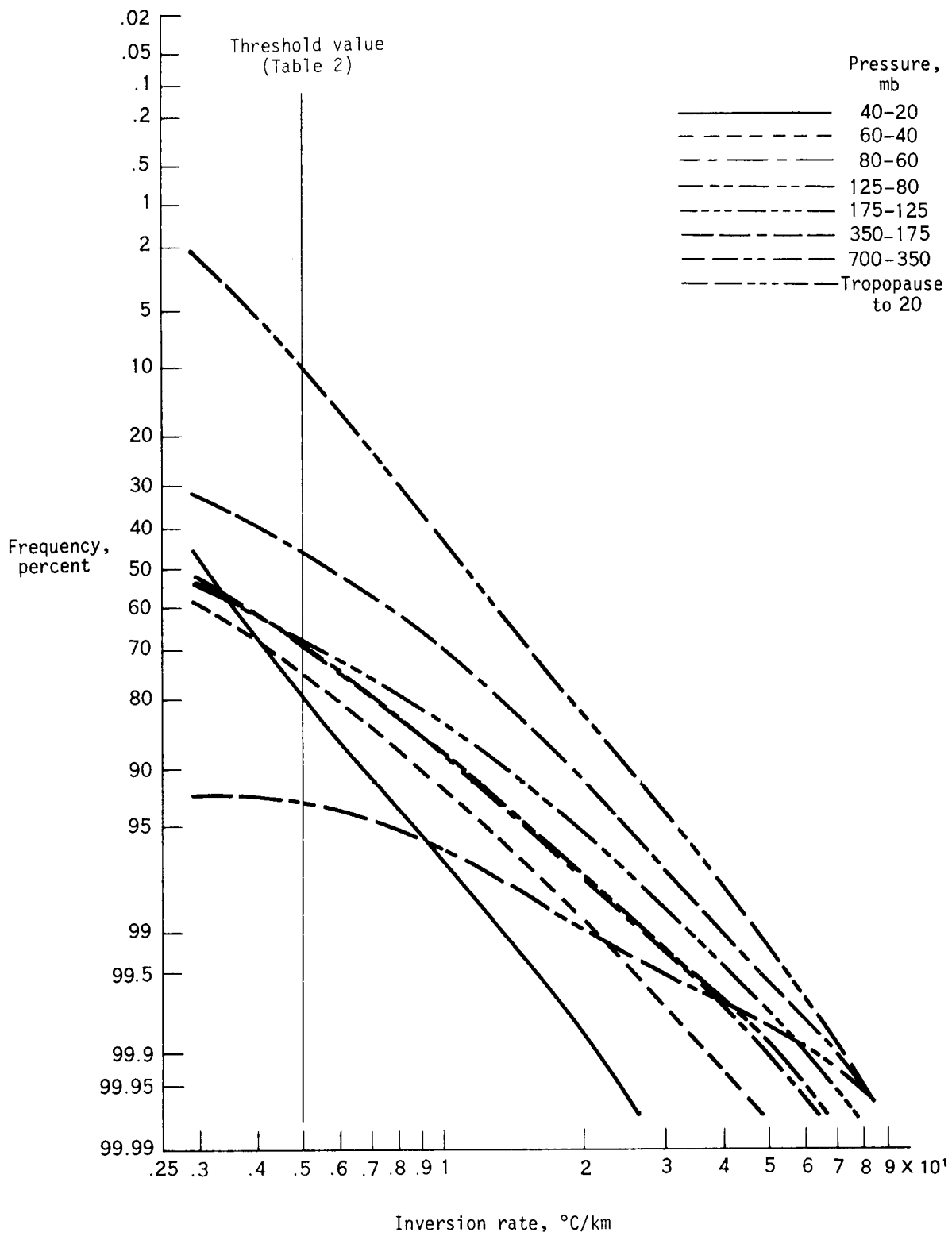
Figure 57. Spring cumulative distributions of inversion rates
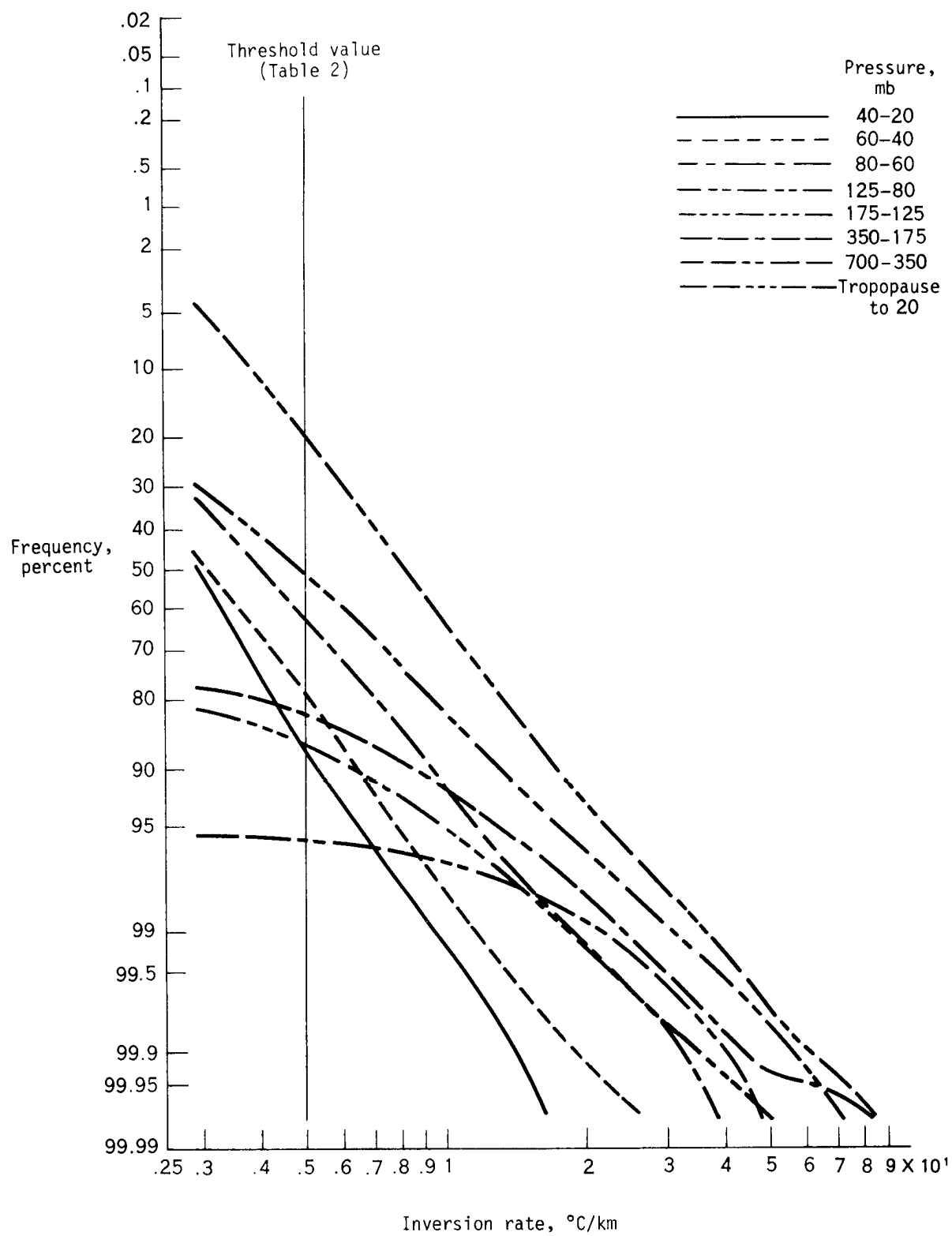(negative lapse rates) for indicated layers.

Figure 58. Summer cumulative distributions of inversion rates (negative lapse rates) for indicated layers.
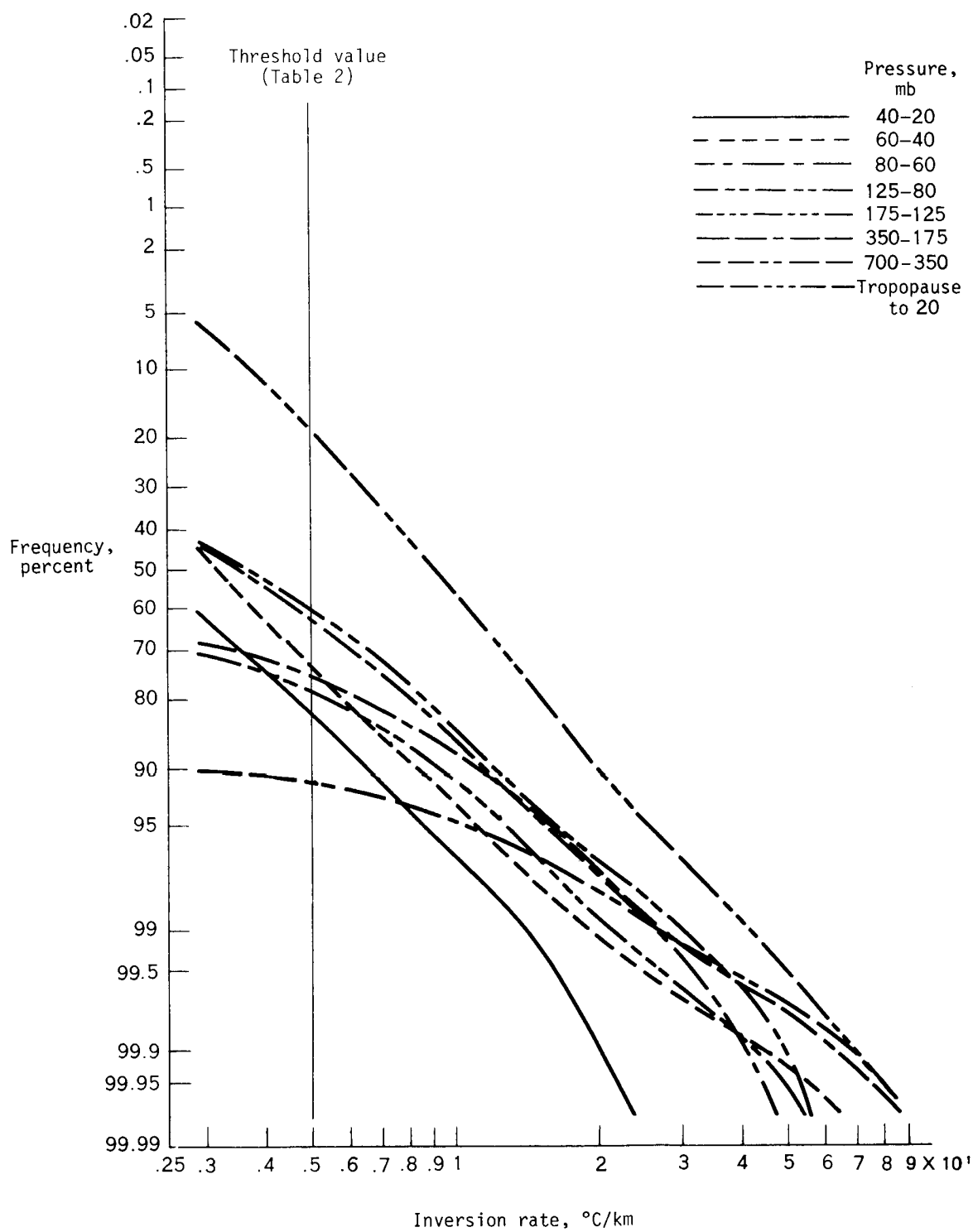
Figure 59. Fall cumulative distributions of inversion rates
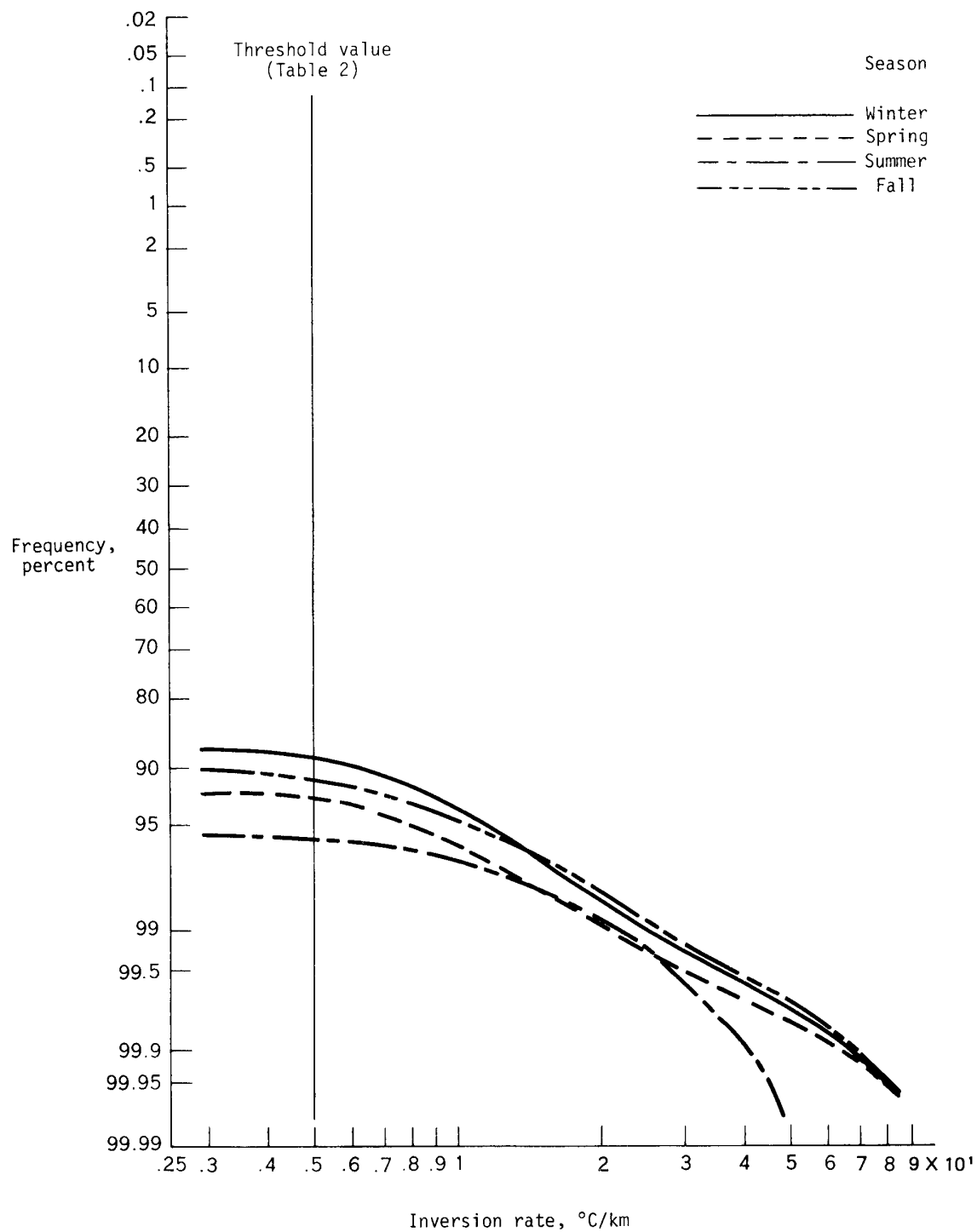(negative lapse rates) for indicated layers.

88

.02
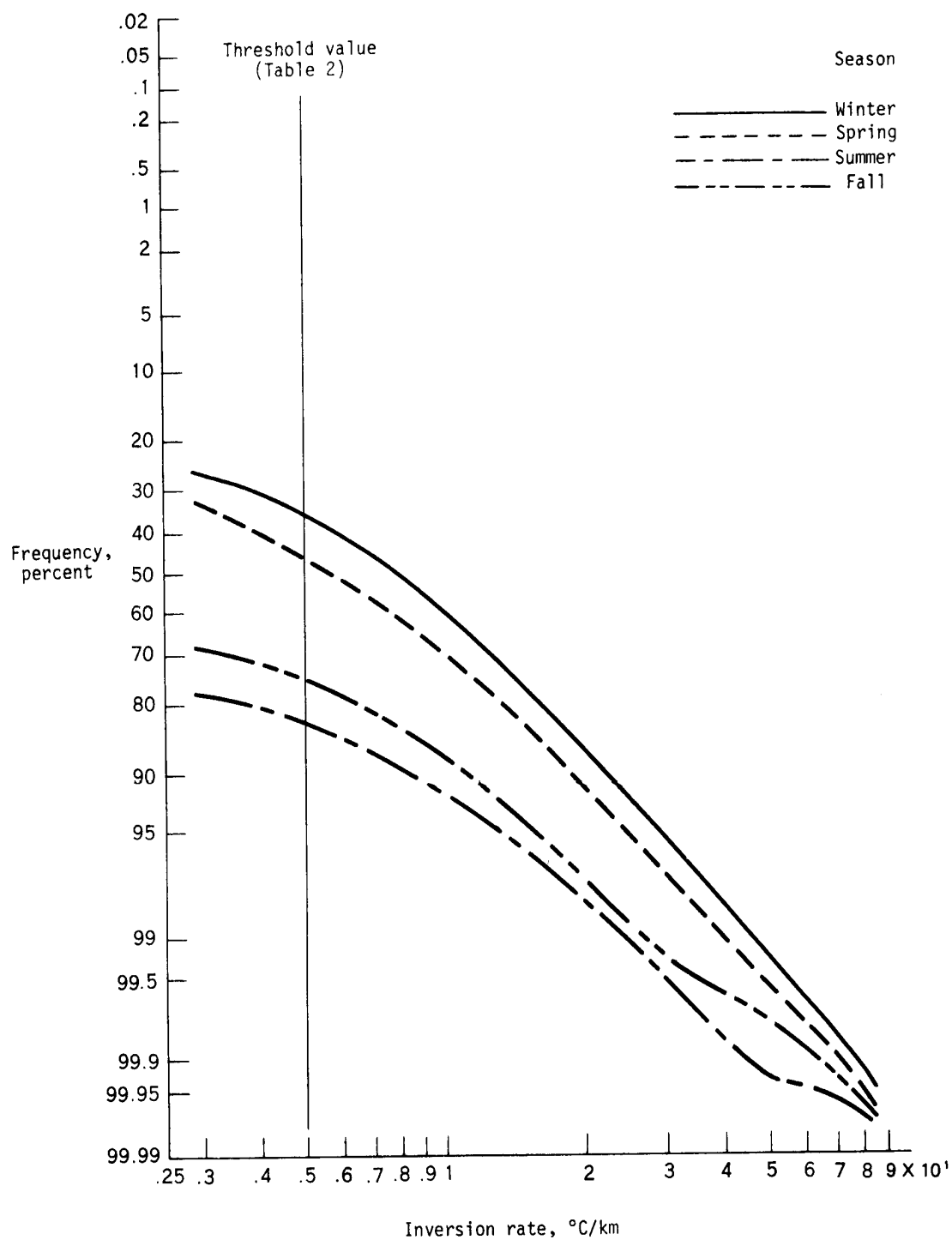
.05

.1

.2

.5

1

2

5

10

20

30

40

Frequency,
percent 50

60

70

80

90

95

99

99.5

99.9

99.95

99.99

Threshold value
(Table 2)

Season

———————— Winter

— — — — — — Spring

— — ——— — — Summer

—— · ·— —— · ·—— Fall

.25 .3   .4   .5 .6 .7 .8 .9 1   2   3   4   5   6 7 8 9 X 10¹

Inversion rate, °C/km

Figure 60.   Seasonal cumulative distributions of inversion rates
(negative lapse rates) for the 700-350 mb layer.

89

Figure 61. Seasonal cumulative distributions of inversion rates
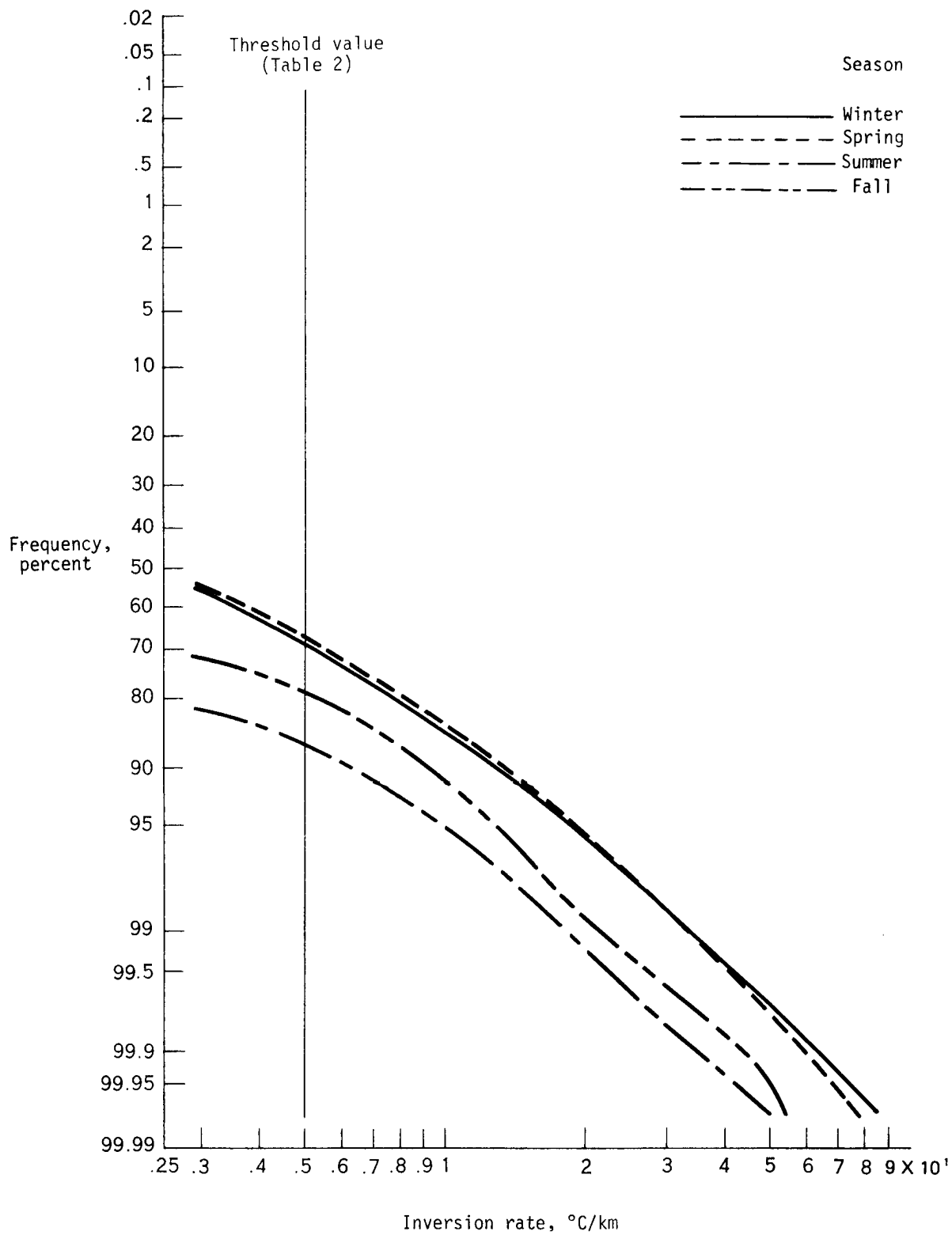(negative lapse rates) for the 350-175 mb layer.

Figure 62. Seasonal cumulative distributions of inversion rates
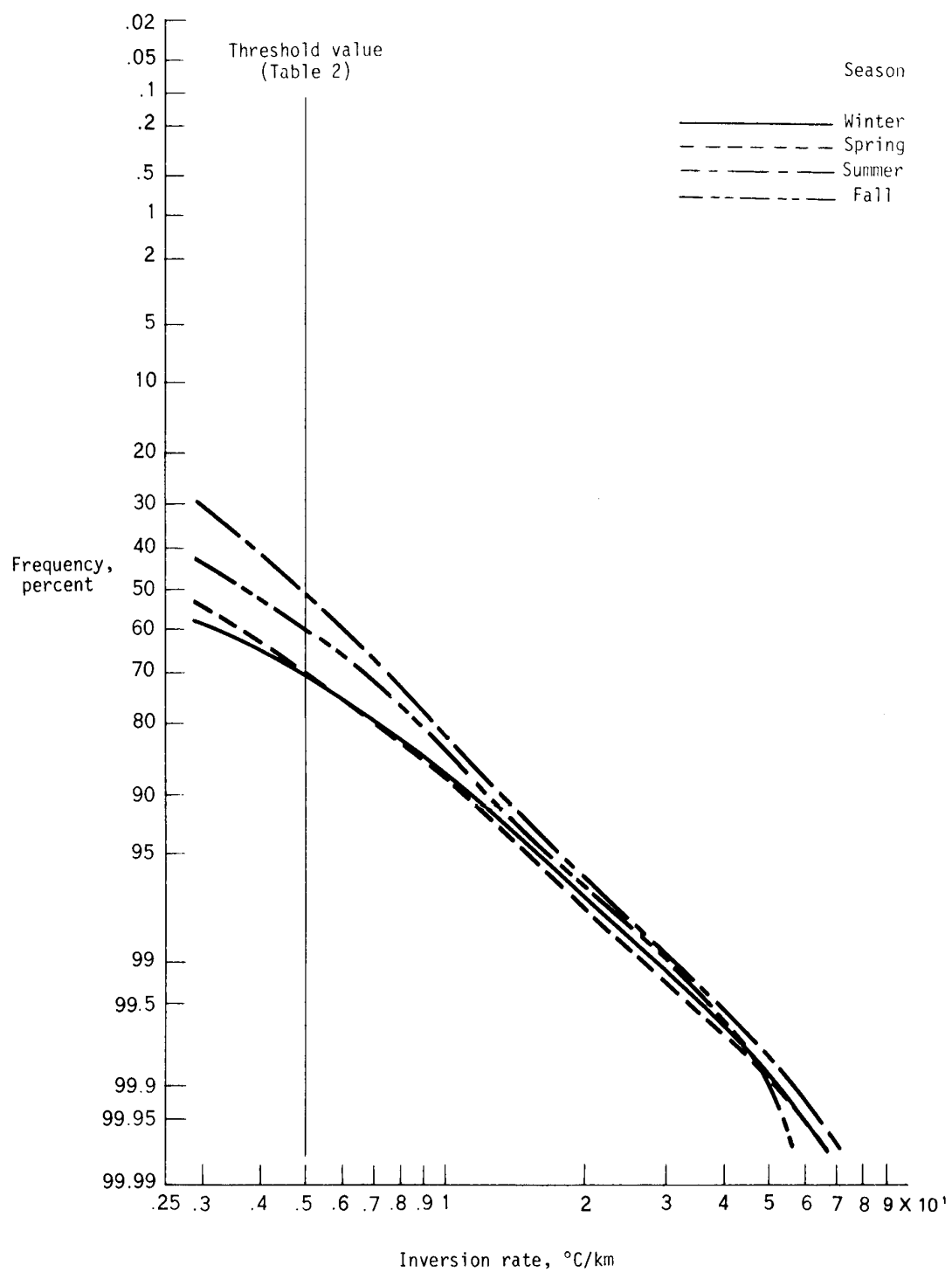(negative lapse rates) for the 175-125 mb layer.

Figure 63. Seasonal cumulative distributions of inversion rates
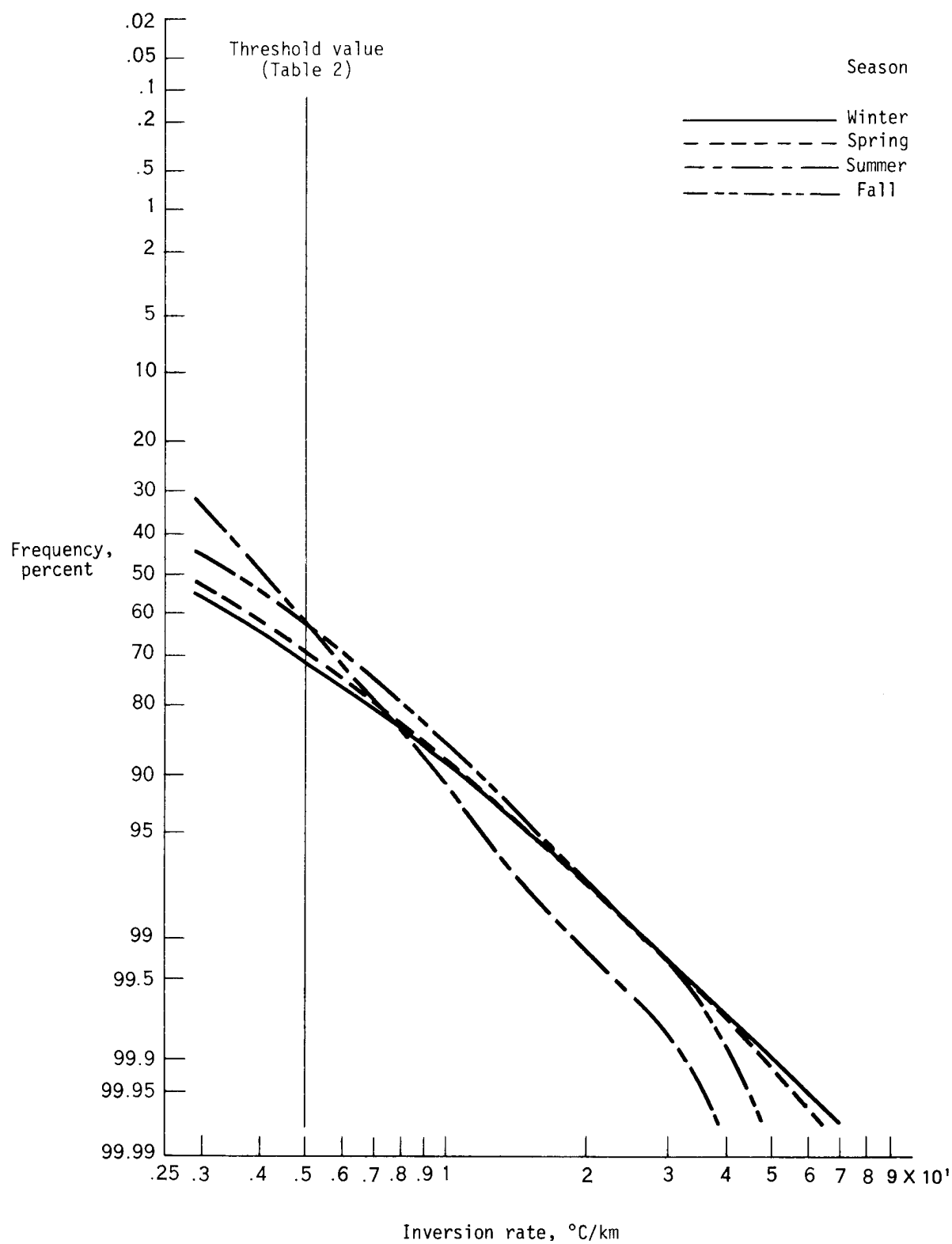(negative lapse rates) for the 125-80 mb layer.

Figure 64.   Seasonal cumulative distributions of inversion rates
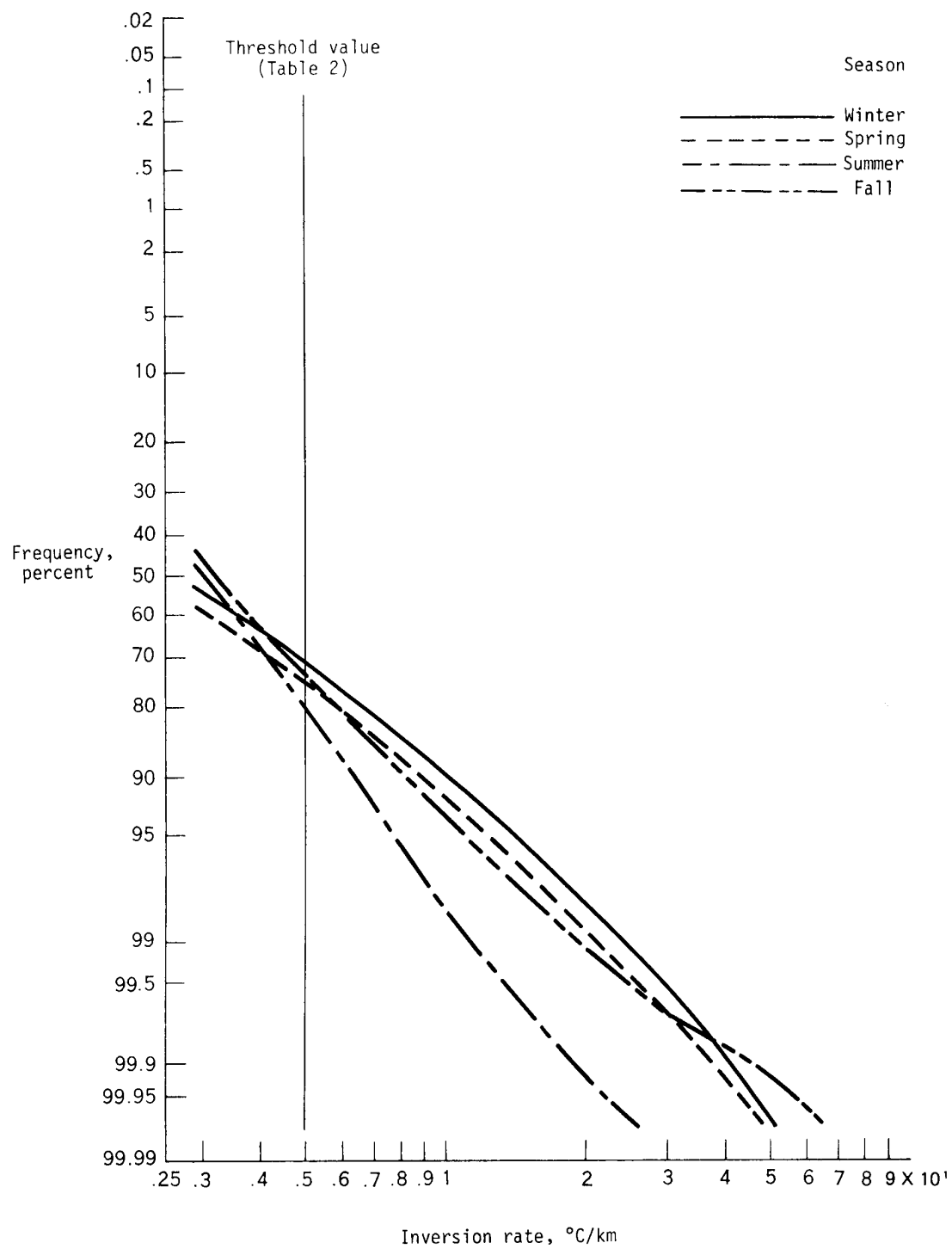(negative lapse rates) for the 80-60 mb layer.

93

Figure 65. Seasonal cumulative distributions of inversion rates
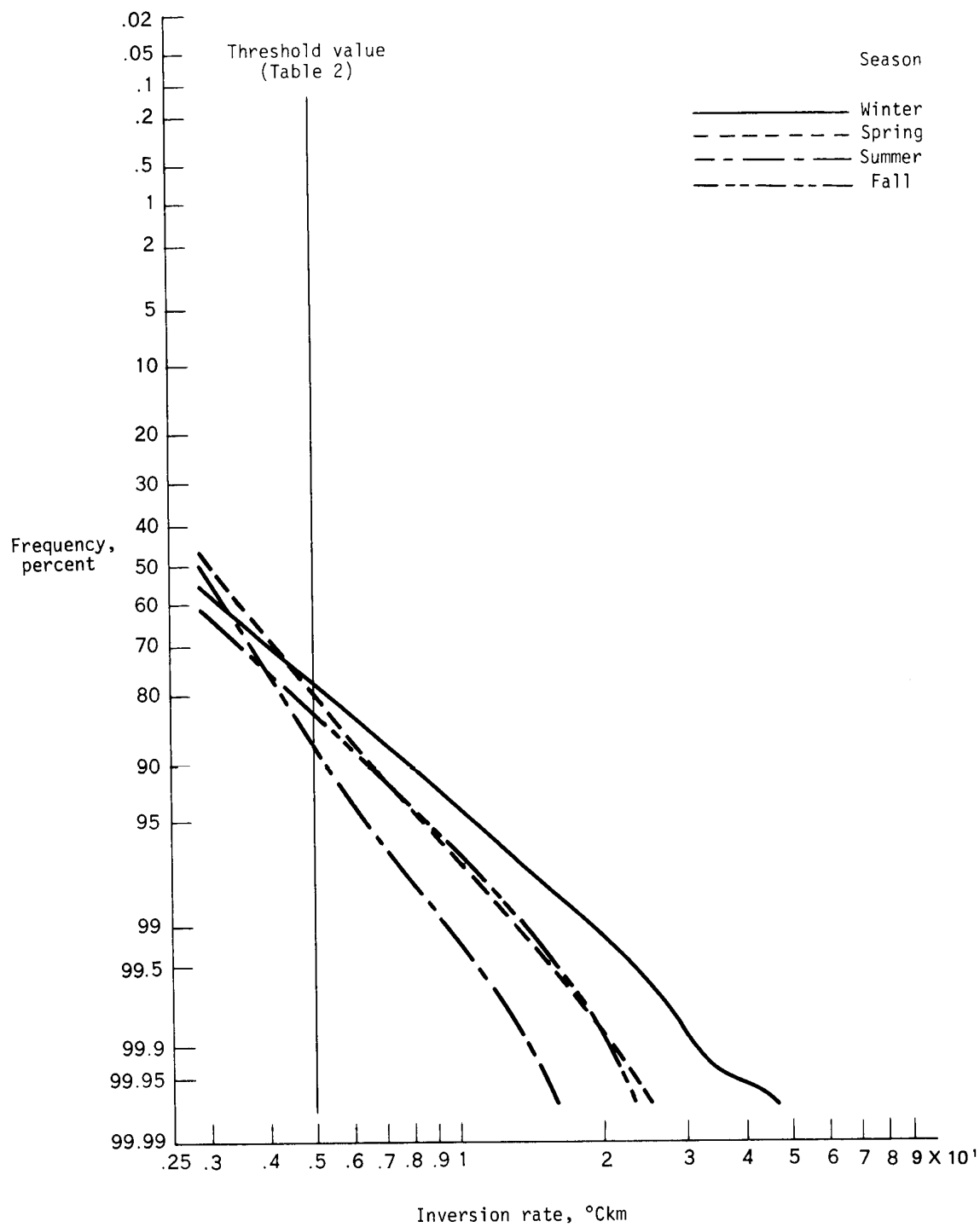(negative lapse rates) for the 60-40 mb layer.

Figure 66. Seasonal cumulative distributions of inversion rates
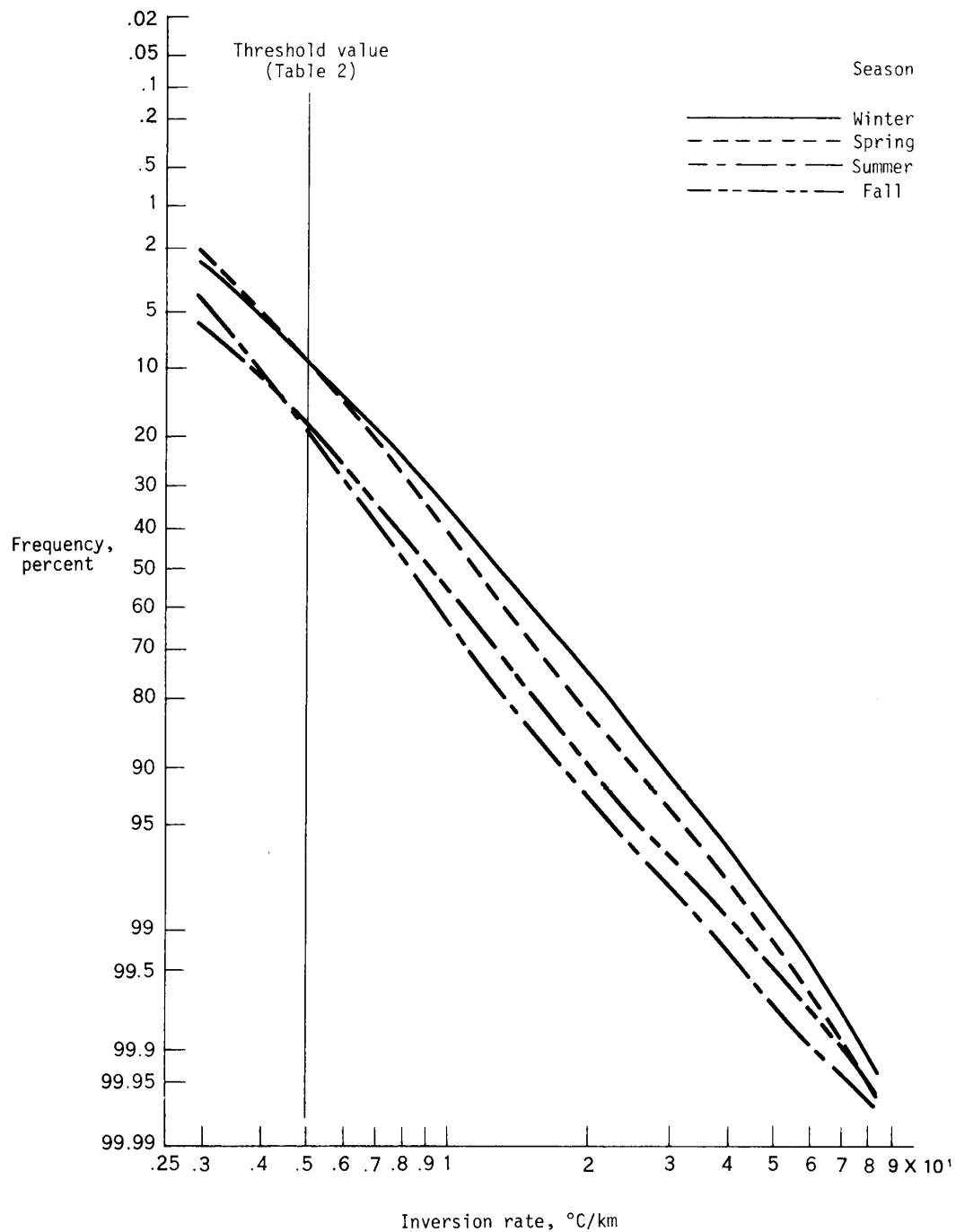(negative lapse rates) for the 40-20 mb layer.

Figure 67. Seasonal cumulative distributions of inversion rates
(negative lapse rates) for the tropopause-20 mb layer.

1. Report No. NASA TM-81353	2. Government Accession No.	3. Recipient's Catalog No.
4. Title and Subtitle CLIMATOLOGICAL CHARACTERISTICS OF HIGH ALTITUDE WIND SHEAR AND LAPSE RATE LAYERS		5. Report Date February 1981
		6. Performing Organization Code RTOP 505-44-14
7. Author(s) L. J. Ehernberger and Nathaniel B. Guttman		8. Performing Organization Report No. H-1132
		10. Work Unit No.
9. Performing Organization Name and Address NASA Dryden Flight Research Center P.O. Box 273 Edwards, California 93523		11. Contract or Grant No.
		13. Type of Report and Period Covered Technical Memorandum
12. Sponsoring Agency Name and Address National Aeronautics and Space Administration Washington, D.C. 20546		14. Sponsoring Agency Code

15. Supplementary Notes

16. Abstract

Previous studies of clear air turbulence in the upper troposphere and stratosphere have noted its association with strong winds, vertical wind shear, temperature lapse rate, and inversion layers. The present pilot study was initiated to obtain indications of the climatological distribution of wind shear and temperature lapse and inversion rates as observed by rawinsonde measurements over the western United States. Frequencies of the strongest shear, lapse rates, and inversion layer strengths were observed for a 1 year period of record and were tabulated for the lower troposphere, the upper troposphere, and five altitude intervals in the lower stratosphere. Selected bivariate frequencies were also tabulated.

Results indicate that strong wind shears, lapse rates, and inversions are generally observed less frequently as altitude increases from 175 millibars to 20 millibars. On a seasonal basis the frequencies were higher in winter than in summer except for minor influences due to increased tropopause altitude in summer and the stratospheric wind reversal in the spring and fall. Example applications are presented and recommendations for future studies are discussed.

17. Key Words (Suggested by Author(s)) Climatology Temperature inversions Stratosphere	18. Distribution Statement Unclassified—Unlimited STAR category: 47

19. Security Classif. (of this report) Unclassified	20. Security Classif. (of this page) Unclassified	21. No. of Pages 101	22. Price* A06

*For sale by the National Technical Information Service, Springfield, Virginia 22161